5-5-2017

Kinetic Analysis of Rat Blood and Tissue and Human Blood Acetylcholinesterase and Butyrylcholinesterase after Inhibition with Novel Nerve Agent Surrogates and Reactivation with Novel Oximes

Steven Archie Dezell

Kinetic analysis of rat blood and tissue and human blood acetylcholinesterase and butyrylcholinesterase after inhibition with novel nerve agent surrogates and reactivation with novel oximes

By

Steven Archie Dezell

A Dissertation
Submitted to the Faculty of
Mississippi State University
in Partial Fulfillment of the Requirements
for the Degree of Doctor of Philosophy
in Environmental Toxicology
in the College of Veterinary Medicine

Mississippi State, Mississippi

May 2017

Kinetic analysis of rat blood and tissue and human blood acetylcholinesterase and butyrylcholinesterase after inhibition with novel nerve agent surrogates and reactivation with novel oximes

By

Steven Archie Dezell

Approved:

Janice E. Chambers
(Major Professor)

John Allen Crow
(Committee Member)

Kenneth O. Willeford
(Committee Member)

Xueyan Shan
(Committee Member)

Russell L. Carr
(Committee Member / Graduate Coordinator)

Mark L. Lawrence
Associate Dean
College of Veterinary Medicine

Name: Steven Archie Dezell

Date of Degree: May 5, 2017

Institution: Mississippi State University

Major Field: Environmental Toxicology

Major Professor: Dr. Janice E. Chambers

Title of Study: Kinetic analysis of rat blood and tissue and human blood acetylcholinesterase and butyrylcholinesterase after inhibition with novel nerve agent surrogates and reactivation with novel oximes

Pages in Study 131

Candidate for Degree of Doctor of Philosophy

Organophosphates (OPs) are used in agriculture via pesticides, and warfare and terrorism via nerve agents. OPs can inhibit acetylcholinesterase (AChE) activity in the nervous system, leading to the buildup of acetylcholine (ACh), and overstimulation of the nervous system and eventual asphyxiation and death. The development of novel blood-brain barrier (BBB) penetrating pyridinium oxime reactivators have previously demonstrated efficacy towards treatment of OP poisoning after exposure of rats to a sarin or a VX surrogate, nitrophenyl isopropyl methylphosphonate (NIMP) and nitrophenyl ethyl methylphosphonate (NEMP), respectively. An effective oxime antidote capable of penetrating the BBB and restoring nervous system activity after exposure to a cyclosarin surrogate, nitrophenyl cyclohexyl methylphosphonate (NCMP), has yet to be determined. In Chapter 2, *in vitro* testing of the efficacy of 17 total novel oxime candidates to utilize against NCMP was conducted with a modified Ellman's AChE assay. Pools of naïve adult male rat brains were utilized as the AChE source. The first variable investigated was the measurement of AChE activity after inhibition with NCMP and subsequent reactivation with one of the oximes. The second variable investigated restoration of

AChE activity after simultaneous oxime and NCMP incubation. The final variable investigated the restoration of AChE activity after simultaneous 2-PAM, oxime and NCMP incubation. A thorough kinetic analysis of our best oximes has yet to be accomplished. In Chapter 3, the best oxime antidotes for NEMP and NIMP were used for kinetic analysis with a modified 96-well plate Ellman's AChE assay. Protein concentrations were analyzed with a modified Lowry protein tube assay to ensure consistent analytical concentrations. The sources of AChE included pooled rat brain and skeletal muscle, and rat and human erythrocytes and plasma. Butyrylcholinesterase (BChE) activity was also measured in the rat and human plasma samples. The results of these studies strengthen the argument that our oxime antidotes can be used as potential therapeutic drugs for OP poisoning. The kinetic data provided critical information to help propose, for Chapter 4, a dynamic pharmacokinetic based model to predict human AChE or BChE activity after exposure to nerve agent surrogates (NEMP and NIMP) and the oximes (44.08 and 44.25).

DEDICATION

I dedicate this work to my family, Jessica and Sean. Their love and support and patience through the years has allowed me to accomplish many academic endeavors and also serve my country. They have made the greatest sacrifice for me as we travel around the country away from family and friends. I want them to know everything I do is for them and they are always in my heart. Thank you for everything and I love you guys!

I also want to dedicate this work to my Dad for teaching me discipline and humility, and for instilling in me the drive to work harder. To my Mom thanks for teaching me compassion, dedication, and courage. To my Stepdad thanks for teaching me the importance of actively listening and understanding those around me. To my Sister thank you for all your love and support; your selfless devotion to the family is inspiring. To my Storm family thank you for all your love and support throughout the years, I couldn't ask for a better family to learn about life and share in our adventures throughout the country.

Finally, I dedicate this work to Howard Chambers it has been an honor having you as a mentor and a blessing having you as a friend. Rest in peace and God bless you.

ACKNOWLEDGEMENTS

I would like to thank all of my committee members for their mentorship and guidance as I developed my research project, conducted my experiments, and authored my dissertation. Dr. Janice Chambers thank you for recruiting and accepting me into the program and brining me into your laboratory family. It has been an honor working for you and learning from you. It has been a true blessing being here under your tutelage. Dr. Russell Carr thank you for all your help troubleshooting my kinetic experiments and setting up my data analysis. Dr. Allen Crow thank you for your input for improving aspects of my kinetic protocols and calculations. Dr. Ken Willeford thank you for providing me with some great kinetic references and advice that helped me build a strong base for setting up my experiments. Finally, thanks to Dr. Xueyan Shan, whom I spent a whole year learning about biochemistry and enzymes. Her knowledge was very helpful in providing a backbone for my kinetics focused research. Thanks to everyone in my committee for their overall mentorship and friendship.

Thanks to the National Institute of Health for their partial support of this research U01 NS083430. I would also like to thank my Air Force sponsors at the Air Force Institute of Technology for their monetary support and Keesler Air Force Base for their specimen support. In particular thanks to Maria Miah for her support throughout the years coordinating my Air Force education from continuing medical education, to my master's degree, and now my doctoral degree.

Finally, a huge thanks to my research laboratory family at the Center for Environmental Health Sciences for all their help and support. Big thanks to Edward Meek for his technical expertise and wealth of knowledge. He was my go to guy for everything. Everyone in the laboratory helped me out at one point in time so huge thanks to Shane Bennett, Dr. Ron Pringle, Erle Cheney, Marybeth Dail, Dr. Drew Leach, Jason Garcia, Royce Nichols, Dr. Russell Carr and his group, Dr. Matthew Ross and his group, Dr. Barbara Kaplan and her group. Also thanks to the support staff that have helped with the administrative aspects, Jeanne Whitehead, Tia Perkins, and Stephanie Huffman.

The views expressed in this dissertation are those of the author and do not reflect the official policy or position of the United States Air Force, Department of Defense, or the U.S. Government.

TABLE OF CONTENTS

LIST OF TABLES

LIST OF FIGURES

LIST OF ABBREVIATIONS

2-PAM – 2-pyridine aldoxime methyl chloride

AAALAC – Association for Assessment and Accreditation of Laboratory Animal Care

abs – rate of absorption

ACh – acetylcholine

AChE – acetylcholine

ATCh – acetylthiocholine

BBB – blood brain barrier

BCh – butyrylthiocholine

BChE – butyrylcholinesterase

BTCh – butyrylthiocholine

ChE – cholinesterase inhibitor

CNS – central nervous system

DFP – diisopropyl-fluorophosphate

DTNB – 5,5'-dithiobis(2-nitrobenzoate)

EDTA – ethylenediaminetetraacetic acid

E – enzyme

e – exponential function

el – rate of excretion

FC – final concentration

FDA – Food and Drug Administration

GA – tabun

GABA – gamma-aminobutyric acid

GB – sarin

GD – soman

GF – cyclosarin

HI-6 – asoxime

HPB – hypotonic phosphate buffer

I – inhibitor

IACUC – Institutional Animal care and Use Committee

IC_{50} – fifty percent inhibitory concentrations

IRB – Institutional Review Board

K_A – association constant for enzyme and inhibitor

k_a – rate of aging of enzyme, permanent inhibition of enzyme via dealkylation

k_{abs} – rate constant for absorption

K_D – dissociation constant for enzyme and inhibitor

k_{el} – rate constant for excretion

k_i – rate of inhibition of enzyme by inhibitor

K_{mapp} – apparent Michaelis-Menten constant for enzyme and substrate

K_{obs} – observed Michaelis-Menten constant for enzyme and substrate

k_p – rate of phosphorylation of enzyme by inhibitor

k_r – rate of reactivation of inhibited enzyme by oxime

k_s – spontaneous reactivation of enzyme via hydrolysis

LC-ESI-MS – liquid chromatography/electrospray ionization/mass spectrophotometry

LD_{50} – lethal dose at which fifty percent of animals expire

NCMP – 4-nitrophenyl cyclohexyl methylphosphonate

NEMP – 4-nitrophenyl ethyl methylphosphonate

NIMP – 4-nitrophenyl isopropyl methylphosphonate

NMR – nuclear magnetic resonance

OP – organophosphate

PB – pyridostigmine bromide

PBPK – physiologically based pharmacokinetic model

PI – phosphatidylinositol

SEM – standard error of the mean

SPB – sodium phosphate buffer

t – time

UN – United Nations

V_{DSS} – volume of distribution

CHAPTER I

INTRODUCTION

Historical Background of Organophosphates

Organophosphates (OPs) were first discovered in the 19th century by Jean Louis Lassaigne and Philippe de Clermont. Lassaigne synthesized the compound by reacting alcohol with phosphoric acid and Clermont presented tetraethyl pyrophosphate at a French Academy of Science meeting (Fest and Schmidt 1982). The effect on the cholinergic system was described in 1932 by German chemist Willy Lange and Gerduh von Krueger. The scientists observed that OP exposure caused eye sight problems via pupil dilation with the resulting increased light sensitivity. Most importantly they observed that OP exposure induced respiratory distress and shortness of breath. Around the late 1930s, Gerhard Schrader began to develop the OPs for insecticidal use. Under German law all research with the potential for warfare applications were required to be reported to the Nazi government. Dr. Schrader was eventually ordered to develop OPs into weapons of war (Tucker 2007). The compounds were classified as organophosphates since they contain a phosphorus element in their structure.

The G-series nerve agents were the first developed and the most widely used historically. They include GA (tabun) created in 1936, GB (sarin) created in 1938, GD (soman) created in 1944, and GF (cyclosarin) created in 1949. The V agents were developed around 1954 by the British. They include VE, VG, VM, and VX. The

Russians developed VR in the 1960s. The biggest strategic difference between the G and V-series agents is persistence. G agents are considered non-persistent, while V agents are very persistent and do not degrade or wash away easily. GB and VX are the only agents fielded by the US military as munitions in rockets, aerial bombs, and artillery shells (United States. Department of the Army, Institute of Land Warfare et al. 1967). Currently nerve agents have been classified as chemical weapons and are considered by the United Nations (UN) as weapons of mass destruction. The terms of this ruling are described in UN Resolution 687 which was passed in 1991. The Chemical Weapons Convention of 1993 outlaws the production of and stockpiling of any chemical weapons. In addition, the use of chemical weapons during warfare is not permitted by treaties signed during the Hague Conventions of 1899 and 1907 and the 1925 Geneva Protocol (Tuorinsky, United States. Dept. of the Army. Office of the Surgeon General. et al. 2008).

After WWII, American companies used Dr. Schrader's research to create several OP pesticides, some of which are still in use today like malathion, parathion, and many others. OPs became increasingly popular with the banning of organochlorines in the 1970s. As an insecticide, OPs are used extensively throughout the world. Most poisonings occur as a result of work related exposures and lapses in the use of personal protective equipment and contamination of food sources (van Heel and Hachimi-Idrissi 2011, Vučinić, Antonijević et al. 2014, Coskun, Gundogan et al. 2015, Muñoz-Quezada, Lucero et al. 2016). In some cases, particularly in rural areas of undeveloped and developed countries, OPs are used in suicides (Eddleston 2000, Buckley, Karalliedde et al. 2004, Pandit, Seshadri et al. 2011).

Besides OPs being used as pesticides, there is a concern that OP nerve agents may be used as weapons during warfare and also as a means of terrorist attacks throughout the world. Prime examples of nerve agent being used in war include the Iran-Iraq War, and recently the Syrian civil war (Tuorinsky, United States. Dept. of the Army. Office of the Surgeon General. et al. 2008). During the end of the Iran-Iraq War in 1988, the Iraqi forces unleashed a chemical attack on Iranian forces in the city of Halabjah, leaving over 4000 dead and 6000 injured combatants and civilians (Rose and Baravi 1988). More recently in 2013, a nerve agent attack was conducted in Damascus with the Syrian Civil War. Death estimates ranged from 1400 to 1500 with 426 of those children and around 3600 more severely affected (Dolgin 2013, Pita and Domingo 2014, Rosman, Eisenkraft et al. 2014).

Even more dangerous are terrorists who are using unconventional methods, such as nerve agents to strengthen their position and/or force their beliefs on the whole of society. One example is the Tokyo subway attacks in 1995 (Tuorinsky, United States. Dept. of the Army. Office of the Surgeon General. et al. 2008). The Aum Shinrikyo religious sect launched a sarin gas attack in the Tokyo subways during rush hour. The result was 12 killed, over 1000 temporarily injured, and 50 permanently injured neurologically. The rising concerns of homegrown terrorist attacks brought on by the surge in ISIS propaganda has also increased the necessity for improved prevention of nerve agent attacks and treatment of those exposed. It is imperative that better nerve agent antidotes be developed to counteract and/or deter possible terrorist attacks and also decrease detrimental effects of pesticide poisonings throughout the world.

Organophosphate Mechanism of Action

The nervous system helps coordinate a majority of the voluntary and involuntary functions and assists in the coordination between various parts of the body (Tortura 2011, Kandel 2013). It consists of the brain, spinal cord, and peripheral nerves (Tortura 2011, Kandel 2013). It accomplishes communication primarily through the formation of nerve impulses or action potentials (Tortura 2011, Kandel 2013). As a whole, it plays a vital role in our perceptions, behaviors, memories, movements, and control of homeostasis throughout the body (Kandel 2013). Within the system there are various elements that play a role in conducting the complex network of communication. Some of those elements include concentration gradients of potassium, sodium, and calcium. Along with their corresponding membrane ion channels, they work together to help with the conduction of electrical signals. Other components of the nervous system provide vital cellular support like oligodendrocytes, astrocytes, and Schwann cells that assist with overall maintenance and up keep of the system streamlining the communication (Tortura 2011, Kandel 2013). One of the most important components of the nervous system are the neurotransmitters which provide communication between separate nerve cells via the synaptic cleft that separates them (Tortura 2011, Kandel 2013).

In the normal nerve, a presynaptic cell and a postsynaptic cell provide an important junction in the nerve cell communication and provide the main means utilized by nerve agents for their mechanism of toxicity. At the transition point between the two neurons, the electrical signal turns into a chemical signal via the acetylcholine (ACh) ligand. The ligand communicates to the next cell by binding a receptor (nicotinic or muscarinic) on the postsynaptic cell. When an action is no longer needed the ligand is

cleared by acetylcholinesterase (AChE; EC 3.1.1.7) which is bound to the postsynaptic cell membranes and the nerve cell stimulation is stopped. In the nicotinic system, the ACh binds to nicotinic cholinergic receptors that open to allow flux of ions and initiates the next nerve impulse (Kabbani, Nordman et al. 2013). In mammals, the nicotinic receptors mainly control voluntary muscle movements. In the muscarinic system, the ACh binds to receptors that affect G-protein signaling, which signals either the cAMP or phosphatidylinositol (PI) pathways (Strader, Fong et al. 1994). The muscarinic receptors mainly affect the autonomic nervous system and control actions like salivation, lacrimation, digestion, and sexual arousal. At a molecular level, cAMP and PI can play a role in intracellular signal transduction, lipid signaling, cell signaling, membrane trafficking, and activation of protein kinases (Rosenbaum, Rasmussen et al. 2009). OPs block AChE from interacting with the ACh ligand and prevent its subsequent metabolism into acetate and choline. The latter of which is recycled by the presynaptic cell to create more ACh. The loss of AChE activity results in ACh buildup in the synapse and causes continued stimulation of the affected receptors. Generally, the concentration and type of OP exposure determines the signs and symptoms of those exposed and can range from irritation to death (Tuorinsky, United States. Dept. of the Army. Office of the Surgeon General. et al. 2008).

Biological Importance of Acetylcholine and Butyrylcholinesterase

The most important and best-studied neurotransmitter when discussing nerve agents is acetylcholine (ACh). ACh is utilized in neuromuscular junctions of the autonomic and the somatic nervous systems and also at various sites within the central nervous system (Purves D 2001). Within the nerve cell, ACh is derived from the

conversion of glucose into pyruvate (Taylor 1999). Glycolysis is the process that converts glucose into pyruvate. Once pyruvate is formed, then it is converted to acetyl coenzyme A (acetyl CoA). In nerve cells, choline acetyl transferase interacts with acetyl CoA and choline to form ACh. The ACh is then placed in vesicles for release into the synapse when electrically stimulated by a nerve impulse. Once released into the synaptic cleft, the ACh in the cleft binds to ACh receptors on the adjacent nerve or effector cell as mentioned previously. The bound ACh stimulates another electrical signal, and then is released from the ACh receptor. The stimulation continues as long as the ACh remains in the synapse or neuromuscular junction. To clear the synapse of ACh, acetylcholinesterase (AChE) within the synapse or neuromuscular junction cleaves the ACh into acetate and choline. Choline is actively taken back into the presynaptic nerve terminal via a Na^+/choline transporter for reuse (Purves D 2001, Amenta and Tayebati 2008).

Butyrylcholinesterase (BChE; EC 3.1.1.8) is an enzyme primarily suspended in the plasma (Kolarich, Weber et al. 2008). A natural ligand for the enzyme would be butyrylcholine (BCh) but it does not occur in the body naturally. It can be used to help distinguish between AChE and BChE activity. BChE is also known as pseudocholinesterase or plasma cholinesterase and interacts with many different choline esters making it a non-specific cholinesterase. This non-specific nature allows BChE to play a significant role in the metabolism of procaine, heroin, cocaine, mivacurium, succinylcholine, and a variety of similar compounds (Cook, Stiller et al. 1989, Carmona, Jufer et al. 2000, Hou, Zhan et al. 2014). Though BChE is primarily located in the plasma, recent studies have found BChE in the brain and cerebrospinal fluid and have

demonstrated possible reactivity with ACh (Nordberg, Ballard et al. 2013). In the realm of chemical warfare, BChE has been sought out as a possible countermeasure against nerve agents by acting as a scavenger of OPs (Masson and Lockridge 2010, Nachon, Brazzolotto et al. 2013). It can interact with the nerve agent while it is in the bloodstream decreasing nervous system interaction (Raveh, Grunwald et al. 1993, Lenz, Yeung et al. 2007).

OP Poisoning Signs and Symptoms and Diagnostic Testing

According to the Centers for Disease Control and Prevention website page on emergency preparedness there are a variety of signs and symptoms for OP poisoning and a variety of diagnostic testing options are available (Peter, Sudarsan et al. 2014). Central nervous system toxicity causes miosis, headache, restlessness, convulsions, loss of consciousness, and coma. Respiratory system toxicity can lead to rhinorrhea, bronchorrhea, wheezing, dyspnea, chest tightness, hyperpnea, and bradypnea. Cardiovascular system toxicity can result in tachycardia, bradycardia, other arrhythmias, hypertension and hypotension arrhythmias. Gastrointestinal system toxicity results in abdominal pain, nausea, vomiting, and diarrhea. Toxicity can also lead to urinary incontinence. Musculoskeletal system toxicity causes weakness and fasciculation. Skin and mucous membrane toxicity leads to profuse sweating, lacrimation, and conjunctival hyperemia (Tuorinsky, United States. Dept. of the Army. Office of the Surgeon General. et al. 2008). Once OP exposure is suspected, blood testing for cholinesterase activity can be performed by assessing plasma BChE or erythrocyte AChE activity (Bajgar 2004, Worek, Koller et al. 2005). Erythrocyte AChE better reflects CNS AChE activity than plasma does and is also more specific than plasma assays. On the other hand, plasma

BChE is easier to assay than erythrocyte AChE and is more commonly available and widely used in clinical chemistry analyzers (van Heel and Hachimi-Idrissi 2011, Worek, Schilha et al. 2016). Decreases in BChE or AChE activity only suggest poisoning, but cannot rule out specifically the cause, but patient history can further validate the source of poisoning (Bajgar 2004). Once OP poisoning is identified, immediate treatment involves enzyme reactivation via oximes and blocking nerve cell receptors with atropine.

Nerve Agent Antidotes

The general treatment involves the administration of atropine to block the effects of the nerve agent and 2-pyridine aldoxime methyl chloride (2-PAM Cl, also called 2-pralidoxime chloride; pyridine-2-aldoxime methyl chloride; 2-formyl-1-methylpyridinium chloride) to reactivate inhibited AChE (Kassa 2002, Smythies and Golomb 2004). The 2-PAM oxime reactivates AChE by removing the phosphyl moiety. In general, most reactivators remove inhibitors via their attached nitrogen-associated hydroxyl group. The hydroxyl loses its hydrogen and becomes bound to the phosphorous group of the inhibitor. The phosphorous group releases its bond with AChE. AChE is thereby reactivated and once again is able to break down ACh. Atropine is administered to temporarily block the muscarinic ACh receptors, preventing further stimulation by ACh that is building up in the synapse. The temporary blocking of the ACh receptors prevents continued stimulation by ACh until the ACh can be cleared from the synapse.

2-PAM is only effective against an OP that has not released any of its side groups while attached to AChE, in other words it has not “aged”. The OP side groups help to pull electrons away from the OP phosphorous core maintaining a neutral charge easily broken by 2-PAM. By losing a side group while covalently attached to an OP, the AChE

is “aged” and is resistant to reactivation by hydrolysis or an oxime antidote because of the phosphylated enzyme (Tuorinsky, United States. Dept. of the Army. Office of the Surgeon General. et al. 2008). The reaction for aging or dealkylation is centered on the interaction of amino acids located in the active site gorge with the phosphyl moiety of the OP and the splitting of the complex that forms the alcohol and nonreactivatable AChE (Bajgar 2004). Normally AChE bound by an OP can be naturally reactivated by hydrolysis within the normal operating nervous system, until aging takes place. The only way to combat inhibited AChE that has aged is to generate a new AChE molecule. Other antidotes similar to 2-PAM include asoxime (HI-6) and obidoxime chloride (Yang 2003). 2-PAM is the only antidote approved by the Food and Drug Administration (FDA) for use in the United States.

Another means to combat nerve agent poisoning is to provide prophylactic drugs like pyridostigmine bromide (PB) which is a carbamate AChE inhibitor (Tuorinsky, United States. Dept. of the Army. Office of the Surgeon General. et al. 2008). PB has been tested in primate models demonstrating 40 to 50% protection over a period of 1 to 6 hours and several other animal models (Shiloff and Clement 1986, von Bredow, Adams et al. 1991, Maxwell, Brecht et al. 1993). Prophylactic drugs like PB temporarily bind AChE and prevent OP nerve agents from binding. The carbamylated enzyme can regenerate naturally via hydrolysis much more quickly than the phosphylated AChE can regenerate spontaneously. Once AChE function is restored then ACh is metabolized and returned to normal levels.

Diazepam (valium), a benzodiazepine, has been used to prevent convulsions and enhance nerve agent antidotes during moderate to severe exposures (Marrs 2003). The

action of diazepam is mediated through gamma-aminobutyric acid (GABA) receptors which activates ligand-gated chloride ion channels to inhibit neurotransmission with the influx of chloride ions to dissipate the electrical signal. This reduces convulsions and prevents nervous system damage from overstimulation.

Improving Nerve Agent Antidote by Crossing Blood Brain Barrier

In the late 19th century scientists noticed that certain dyes administered peripherally did not stain tissue in the CNS (Davson and Segal 1996, Banks 2008). Many explored theories focused on differences in CNS tissue affinity to vasculature of the brain, but it was not until the 1960s and 1970s that scientists began to explore the ultra-structures of the body (Davson and Segal 1996). It was then that Karnovsky, Reese, and Brightman found that brain capillary beds had tight junctions, pinocytosis was decreased significantly, and fenestrations were absent (Brightman 1977). These structural modifications prevent plasma ultra filtrate from forming and hence plasma proteins like albumin could not cross the blood brain barrier (BBB). Since the dyes adhere to albumin they were unable to stain CNS tissue. Transport systems were later identified that allowed a variety of substances to enter the CNS circulation like glucose, amino acids, vitamins, minerals, fatty acids, and electrolytes. Many researchers have exploited all these avenues of transport, but the primary mechanism utilized for drug delivery is transmembrane diffusion and saturable transport (Begley 2004). The major hindrance to diffusion is the polarity of a molecule where highly polar molecules are prevented from crossing the BBB. Lipophilic molecules can easily diffuse through the BBB and passively enter the CNS (Levin 1980). This is not the case for some lipophilic molecules which can be actively transported out of the CNS in some situations. To cross the BBB,

Dr. Howard Chambers synthesized phenoxyalkyl pyridinium oximes with a variety of R-group attachments that provide a more lipophilic structure. This lipophilicity may allow for improved BBB crossing and reactivation of brain AChE for some of the developed chemicals, but the exact mechanism has yet to be determined (Chambers, Chambers et al. 2013). Dr. Janice Chambers and her laboratory have successfully tested a variety of these novel oximes in *in vivo* rat models and demonstrated a few can cross the BBB and restore OP inhibited AChE. This is an improvement from the currently used oxime antidote, pralidoxime chloride (2-PAM), which only reverses inhibited AChE in the peripheral nervous system (Kassa 2002, Smythies and Golomb 2004). The polarity of 2-PAM prevents it from crossing the BBB (Worek, Eyer et al. 2007, Joosen, van der Schans et al. 2011). Bis-quaternary oxime compounds like HI-6, MMB-4, and obidoxime improve their reactivation capabilities with a second cation, but also have problems crossing the BBB because of their positive charge (Kalisiak, Ralph et al. 2011). The nomenclature for Dr. Chambers' novel oximes is defined by the first digit which is the position of the oxime in relationship to the quaternary nitrogen in the pyridinium ring, second digit is the n describing number of methylene's in the methylene bridge, and the final double digit is the sequence of the compound within the series.

The recent development of novel nerve agent surrogates has allowed for easier testing of nerve agents without the usual scrutiny and security required for military grade nerve agent usage (Meek, Chambers et al. 2012). The developed nerve agent surrogates provide the same inhibitor-AChE complex as seen with the normal nerve agents. The difference is in the leaving group, which decreases the potency compared to the actual nerve agent. Utilizing these nerve agent surrogates, the novel oxime antidotes were

tested and demonstrated their potential for BBB crossing in rats (Chambers, Chambers et al. 2013). Nerve agents that reach the brain can have permanent detrimental effects to higher level motor and cognitive function. OP compounds are lipophilic and are able to cross the BBB to inhibit AChE. Besides the novel oximes currently being developed, there are a few other antidotes that explore other mechanisms to cross the BBB. Non-polar neutral compounds in development have demonstrated effectiveness in crossing the BBB in mice (Radic, Sit et al. 2012). These neutral hydroxyimino-acetamido alkylamine compounds have been successfully tested *in vivo* with mice models and refined *in vitro* using purified commercial human AChE (Sit, Radic et al. 2011, Radic, Sit et al. 2012, Radić, Sit et al. 2013). The compounds are devoid of charge, but the oxime group and amine group causes a coexistence of a charge and uncharged states at physiological pH. The charged state assists with AChE reactivation and the uncharged state allows BBB penetration. Another approach for BBB crossing uses amidine-oxime reactivators which are also more lipophilic than 2-PAM and have resulted in 24 hour mice survival after sarin exposure (Kalisiak, Ralph et al. 2011, Kalisiak, Ralph et al. 2012). The amidine moiety provides a pseudo charge that allows efficient binding of OP-inhibited ChEs, while the oxime group reactivates the phosphylated ChE. Researchers have also developed novel sugar-oxime conjugates to reactivate inhibited CNS AChE by attaching glucose to 2-PAM (Garcia, Campbell et al. 2010). The sugar oximes have the potential to be transported across the BBB via glucose transporters and have demonstrated effectiveness in peripheral AChE restoration. Prodrugs associated with 2-PAM have also been considered, but synthesis is difficult and autoxidation is common (Shek, Higuchi et al. 1976, Shek, Higuchi et al. 1976, Demar, Clarkson et al. 2010). Pro-2-PAM has

demonstrated effectiveness in guinea pig models exposed to a sarin surrogate diisopropyl-fluorophosphate (DFP) (Demar, Clarkson et al. 2010).

Choosing the Best Kinetic Model

Over 100 years ago Leonor Michaelis and Maud Menten published their work on enzyme kinetics and their famous Michaelis-Menten equation. In their work, they demonstrated that the rate of an enzyme-catalyzed reaction is proportional to the enzyme-substrate complex. The equation follows a mechanism in which substrate binds reversibly to an enzyme to form an enzyme-substrate complex, which then reacts irreversibly and generates a product and the free enzyme. In 2011, their work was officially translated to English, reevaluated using computer programs, and published by Kenneth Johnson and Roger Goody (Michaelis, Menten et al. 2011). Utilizing modifications of the original equation, many nerve agent researchers use the equation to demonstrate how effective their oximes, nerve agents, or nerve agent surrogates work kinetically. This provides a basis from which researchers can compare and help determine the effectiveness of their compounds.

The current research continues to utilize the kinetic concepts developed by Michaelis -Menten to demonstrate the effectiveness of AChE and BChE inhibition by new nerve agent surrogates and subsequent reactivation by novel oximes. The kinetic data generated will provide additional support towards demonstrating the viability of the compounds for nerve agent research and further antidote testing. Demonstrating kinetic differences between rat and human AChE and BChE will provide a better knowledge base for determining human modeling based on rat experimental data. Three of the most utilized kinetic models derived from the Michaelis-Menten equation include a standard

Briggs-Haldane plot, an Eadie-Hofstee plot, and a Lineweaver-Burk plot (Briggs and Haldane 1925, Michaelis, Menten et al. 2011). These various plots were utilized to obtain the best fit line equation with a coefficient of determination statistic, R^2-value, greater than 0.9. Choosing the best kinetic model plot requires continued monitoring of the data as it is being generated and determining which of the three plots provides consistent best fit lines. From this line equation the necessary rate constants were calculated for all the data.

The Briggs-Haldane model plots the velocity versus the inhibitor concentration (v_o versus inhibitor concentration). The inhibitor concentration could also be replaced with substrate concentration depending on what kinetic values are required. It provides direct analysis of the data without any adjustment to the original data. In most cases linear lines were demonstrated with R^2-values greater then 0.9, occasionally the R^2-value was less than 0.9. The Eadie-Hofstee model plots the velocity versus the velocity divided by the inhibitor concentration (v_o versus v_o/inhibitor concentration). In a few data sets, dividing the velocity by the inhibition concentration on the x-axis provided improved linearity. Yet in some cases the adjustment resulted in outliers and nonlinear equations with a correlation coefficient far less than 0.9. The nonlinear data may be due to the strong dependence of both the x and y-axis on the velocity data. Another concern is the smaller concentrations and their increased weight when forming the linear equation and best fit line. The weight of these smaller concentrations can sway the line dramatically (Dowd and Riggs 1965). The various kinetic models have strengths and weaknesses when investigating particular biological functions.

The Lineweaver-Burk model plots the reciprocal of both velocity versus the inhibitor concentration ($1/v_o$ versus 1/inhibitor concentration). All data sets demonstrated the best linearity when using this model and the best correlation coefficient always greater than 0.9. The major concern with this model was the smaller concentrations and their increased weight when forming the linear equation and best fit line (Ritchie and Prvan 1996, Ritchie and Prvan 1996). Utilizing this model, all the necessary kinetic values were calculated utilizing kinetic calculations adopted from Worek et al. and Carr et al. (Carr and Chambers 1996, Worek, Eyer et al. 1998, Worek, Reiter et al. 2002, Worek, Thiermann et al. 2004). Ideally, studying enzymes in their natural environment is considered to be the best approach, but experimentally it is hard to account for the variety of conditions in such an environment. Consequently, extracted and purified enzymes analyzed *in vitro* are the controlled experimental option. The current research maintains some biological relevancy using plasma and purified membranes, but the downside is the introduction of some unknown factors. Choosing the correct consistent model helps negate some of these biological factors that can influence the kinetic values.

Kinetic Analysis and Bridging Rat and Human Models

Kinetic analysis of biological systems is important for understanding and comparing systems (Resat, Petzold et al. 2009). To further understand the interactions between the nerve agent surrogates and novel oxime antidotes it is imperative that a kinetic analysis be performed. The knowledge of reaction rates is critical in providing a means for comparative analysis between 2-PAM and any proposed replacements. 2-PAM is currently the FDA approved antidote in the United States. Many researchers have utilized kinetic analysis to quantify reactions occurring with various oximes and

OPs. Researchers have also performed similar kinetic analyses to look at acetylcholinesterase activity in various animal and human models (Worek, Reiter et al. 2002, Worek, Aurbek et al. 2007, Aurbek, Herkert et al. 2010, Herkert, Freude et al. 2012, Coban, Carr et al. 2016) Utilizing their research precedent, procedures for kinetic analysis of our nerve agent surrogates and oximes were adapted to further validate their capabilities compared to 2-PAM. The current research provides analytical results of rat and human blood AChE and BChE and rat brain and skeletal muscle AChE activity levels when exposed to our nerve agent surrogates (NIMP – 4-nitrophenyl isopropyl methylphosphonate, NEMP – 4-nitrophenyl ethyl methylphosphonate, and NCMP – 4-nitrophenyl cyclohexyl methylphosphonate), and novel oximes (oxime 44.08 and oxime 44.25), and 2-PAM (Worek, Thiermann et al. 2004, Worek, Aurbek et al. 2007). Kinetic reaction rates were determined for initial inhibition, spontaneous reactivation, aging, and oxime reactivation. Using reaction rates and standard variables determined by other researchers, a pharmacokinetic model and calculations were hypothesized, focusing on key body compartments involved acutely with nerve agent exposure (Munro 1994, Baker and Sedgwick 1996, Marino, Schuster et al. 1998, van der Schans, Lander et al. 2003, Bide, Armour et al. 2005, Whalley, McGuire et al. 2007).

Classical Versus Physiological Based Pharmacokinetic Model

Physiologically based pharmacokinetic (PBPK) models utilize a mathematical description of the physiologic, biochemical, and physicochemical reactions that contribute to the pharmacokinetics of the nerve agent in question (Emond, Michalek et al. 2005). In these models, the mathematical descriptors take into account the various compartments and the variations within these compartments. Each compartment could

have a variety of metabolizing enzyme rates, a variety of enzyme types, diffusion rates, and accessibility requirements. There are a variety of different PBPK models utilized based on the chemical or toxicant investigated. Considerations of which type to use must be made based on mode of entry, elimination, dosage, enzyme induction capability, and many other factors that may be specific to the chemical or toxicant. Chemical or toxicant factors could include volatility, chemical structure, molecular weight, and other factors that affect entry and interaction in the biological system. Well calculated and thorough PBPK models can provide very accurate predictions for short term and long term studies of pharmacokinetics (Emond, Michalek et al. 2005). The downside to precision is the numerous parameters that must be determined experimentally to obtain the necessary information. The more information obtained for use in the model can increase precision and produce more accurate projections. This approach can be very informative and useful in situations of long term exposure, but the costs could be restraining if an acute exposure is more clinically relevant. Such is the case with nerve agent or other OP exposures, where brain damage or death can occur in minutes or hours. In such cases, elimination from the body, metabolism in the liver, and or interactions in non-essential peripheral tissues is not an immediate concern. In these cases, a more simplified classical model would be more relevant.

Classical pharmacokinetic models can provide a more cost effective look into the interactions occurring within the simplified biological system. In the case of nerve agent or OP poisoning, the primary concerns with nerve agent OP exposure would be the effect on the respiratory and central nervous system. Both of these systems can easily be reached via the circulating blood. In a classical model the metabolism of the nerve agent

in the blood, brain, and skeletal muscle would be primary compartments of concern and therefore the most efficient to research.

Overall Research Summary

The main objective of the research was to characterize the reactions occurring with the sarin and VX surrogates and the novel oxime antidotes, and provide a quantifiable comparison with 2-PAM utilizing kinetic data. In addition, the research provided preliminary data for combined oxime therapies and the necessary protocols to conduct such analytical testing. Finally, the kinetic data obtained from rat and human models provided critical information for future extrapolation of human parameters in regards to our novel oxime antidotes and possible therapeutic utilization in the future.

Chapter Two describes the experiments conducted to evaluate the best 46-series oximes for reactivating the cyclosarin surrogate, NCMP. To date the laboratory has done preliminary testing utilizing the novel oximes and nerve agent surrogates. Rat tissue types tested *in vitro* include brain, diaphragm, and skeletal muscle. Rat and human blood have also been tested. Measuring AChE levels in various tissues after exposure to the novel nerve agent surrogates and novel oximes has partly been accomplished utilizing a modified Ellman's AChE activity assay (Ellman, Courtney et al. 1960, Worek, Diepold et al. 1999, Worek, Mast et al. 1999, Coban, Carr et al. 2016). Similar experiments were utilized for the NCMP testing. Some of the initial testing conducted by the laboratory involved the sarin surrogates (NIMP and PIMP) and VX surrogate (NEMP). The oximes showing the most reactivation for further testing with these agents were oximes 44.08 and 44.25 (Meek, Chambers et al. 2012, Chambers, Chambers et al. 2013). Oximes 44.08 and 44.25 were chosen for further kinetic testing experiments as described in the results

of this dissertation. Any successful 46-series oximes for NCMP will also be utilized for kinetic testing as the results are described in this dissertation.

Using a slight modification to Ellman's AChE activity assay protocol, a novel cyclosarin surrogate (NCMP) developed by our laboratory was tested with a different series of novel oximes. The oximes from this series that showed the most promise for further testing were 46.21, 46.43 and 46.49. Another, modification to the protocol was necessary since cyclosarin and its corresponding novel surrogates are very potent inhibitors and reactivation is hard to accomplish as demonstrated by the preliminary data described in this dissertation and past experiments carried out by the Worek and the Chambers labs (Worek, Eyer et al. 2007, Chambers, Chambers et al. 2013). The oximes and NCMP were simultaneously incubated at various incubation times (15, 30, and 45 minutes). It was determined that 15 minutes was the most advantageous incubation time to analyze AChE activity for these oximes after exposure to NCMP. In addition to these initial experiments, information was also gathered on possible synergistic effects of combining the most effective novel oximes and 2-PAM for reactivation after NCMP exposure in the pooled rat brain tissue.

Chapter Three describes the AChE and BChE activity of various human, rat blood components, and rat tissues over time for the novel surrogates and novel oximes developed in the laboratory. The kinetic values were used to calculate the inhibition, aging and reactivation rate constants and to compare against 2-PAM. The laboratory had previously performed AChE and BChE experiments on intact human and rat erythrocytes, but extensive kinetic analysis of the different enzyme sources like erythrocyte membranes, blood plasma, brain and skeletal muscle has not been done

(Coban, Carr et al. 2016). The current research focused on analysis of human and rat purified erythrocyte membrane AChE and plasma AChE and BChE and rat brain and skeletal muscle tissue AChE. The additional kinetics data provided more information on the novel oxime reactivation capabilities and also provided a critical comparison between human and rat models for the novel oximes. The data will provide a better perspective when it comes to drawing conclusions to what needs to be done when transitioning from initial rat experiments to testing clinically safe antidote doses in humans.

Chapter Four describes a hypothesized pharmacokinetic model to be used with the current rat and human data, in conjunction with known constants from other researchers, and tested via published case study data. The kinetic data generated from the rat and human erythrocyte and plasma will provide the essential kinetic parameters. To complete the data, clearance rates have yet to be determined for the novel oximes and surrogates. This dissertation describes the findings, and provides additional experimental support for the further development of the novel oximes as a possible improved nerve agent antidote, that can penetrate the BBB.

References

Amenta, F. and S. K. Tayebati (2008). "Pathways of acetylcholine synthesis, transport and release as targets for treatment of adult-onset cognitive dysfunction." Curr Med Chem **15**(5): 489-496.

Aurbek, N., N. M. Herkert, M. Koller, H. Thiermann and F. Worek (2010). "Kinetic analysis of interactions of different sarin and tabun analogues with human acetylcholinesterase and oximes: is there a structure-activity relationship?" Chem Biol Interact **187**(1-3): 215-219.

Bajgar, J. (2004). Organophosphates / Nerve Agent Poisoning: Mechanism of Action, Diagnosis, Prophylaxis, And Treatment. Advances in Clinical Chemistry, Elsevier. **Volume 38:** 151-216.

Baker, D. J. and E. M. Sedgwick (1996). "Single fibre electromyographic changes in man after organophosphate exposure." Hum Exp Toxicol **15**(5): 369-375.

Banks, W. A. (2008). "Developing drugs that can cross the blood-brain barrier: applications to Alzheimer's disease." BMC Neuroscience **9**(Suppl 3): S2-S2.

Begley, D. J. (2004). "Delivery of therapeutic agents to the central nervous system: the problems and the possibilities." Pharmacol Ther **104**(1): 29-34.

Bide, R. W., S. J. Armour and E. Yee (2005). "GB toxicity reassessed using newer techniques for estimation of human toxicity from animal inhalation toxicity data: new method for estimating acute human toxicity (GB)." J Appl Toxicol **25**(5): 393-407.

Briggs, G. E. and J. B. S. Haldane (1925). "A Note on the Kinetics of Enzyme Action." Biochemical Journal **19**(2): 338-339.

Brightman, M. W. (1977). "Morphology of blood-brain interfaces." Exp Eye Res **25 Suppl**: 1-25.

Buckley, N., L. Karalliedde, A. Dawson, N. Senanayake and M. Eddleston (2004). "Where is the Evidence for Treatments used in Pesticide Poisoning? - Is Clinical Toxicology Fiddling while the Developing World Burns?" Journal of toxicology. Clinical toxicology **42**(1): 113-116.

Carmona, G. N., R. A. Jufer, S. R. Goldberg, D. A. Gorelick, N. H. Greig, Q. S. Yu, E. J. Cone and C. W. Schindler (2000). "Butyrylcholinesterase accelerates cocaine metabolism: *in vitro* and *in vivo* effects in nonhuman primates and humans." Drug Metab Dispos **28**(3): 367-371.

Carr, R. L. and J. E. Chambers (1996). "Kinetic analysis of the *in vitro* inhibition, aging, and reactivation of brain acetylcholinesterase from rat and channel catfish by paraoxon and chlorpyrifos-oxon." Toxicol Appl Pharmacol **139**(2): 365-373.

Chambers, J. E., H. W. Chambers, E. C. Meek and R. B. Pringle (2013). "Testing of novel brain-penetrating oxime reactivators of acetylcholinesterase inhibited by nerve agent surrogates." Chem Biol Interact **203**(1): 135-138.

Coban, A., R. L. Carr, H. W. Chambers, K. O. Willeford and J. E. Chambers (2016). "Comparison of inhibition kinetics of several organophosphates, including some nerve agent surrogates, using human erythrocyte and rat and mouse brain acetylcholinesterase." Toxicology Letters **248**: 39-45.

Cook, D. R., R. L. Stiller, J. N. Weakly, S. Chakravorti, B. W. Brandom and R. M. Welch (1989). "*In Vitro* Metabolism of Mivacurium Chloride (BW B1090U) and Succinylcholine." Anesthesia & Analgesia **68**(4): 452-453.

Coskun, R., K. Gundogan, G. C. Sezgin, U. S. Topaloglu, G. Hebbar, M. Guven and M. Sungur (2015). "A retrospective review of intensive care management of organophosphate insecticide poisoning: Single center experience." Nigerian Journal of Clinical Practice **18**(5): 647-648.

Davson, H. and M. B. Segal (1996). Physiology of the CSF and blood-brain barriers. Boca Raton, CRC Press. p. 49-91

Demar, J. C., E. D. Clarkson, R. H. Ratcliffe, A. J. Campbell, S. G. Thangavelu, C. A. Herdman, H. Leader, S. M. Schulz, E. Marek, M. A. Medynets, T. C. Ku, S. A. Evans, F. A. Khan, R. R. Owens, M. P. Nambiar and R. K. Gordon (2010). "Pro-2-PAM therapy for central and peripheral cholinesterases." Chem Biol Interact **187**(1-3): 191-198.

Dolgin, E. (2013). "Syrian gas attack reinforces need for better anti-sarin drugs." Nat Med **19**(10): 1194-1195.

Dowd, J. E. and D. S. Riggs (1965). "A COMPARISON OF ESTIMATES OF MICHAELIS-MENTEN KINETIC CONSTANTS FROM VARIOUS LINEAR TRANSFORMATIONS." J Biol Chem **240**: 863-869.

Eddleston, M. (2000). "Patterns and problems of deliberate self-poisoning in the developing world." Qjm **93**(11): 715-731.

Ellman, G., K. Courtney, V. Andres and R. Featherstone (1960). "A new and rapid colorimetric determination of acetylcholinesterase activity." Biochemical Pharmacology **7:** 88-95.

Emond, C., J. E. Michalek, L. S. Birnbaum and M. J. DeVito (2005). "Comparison of the Use of a Physiologically Based Pharmacokinetic Model and a Classical Pharmacokinetic Model for Dioxin Exposure Assessments." Environmental Health Perspectives **113**(12): 1666-1668.

Fest, C. and K.-J. Schmidt (1982). The Chemistry of Organophosphorus Pesticides. Berlin, Heidelberg, Springer Berlin Heidelberg,**:** 1 online resource 13-14.

Garcia, G. E., A. J. Campbell, J. Olson, D. Moorad-Doctor and V. I. Morthole (2010). "Novel oximes as blood-brain barrier penetrating cholinesterase reactivators." Chem Biol Interact **187**(1-3): 199-206.

Herkert, N. M., G. Freude, U. Kunz, H. Thiermann and F. Worek (2012). "Comparative kinetics of organophosphates and oximes with erythrocyte, muscle and brain acetylcholinesterase." Toxicol Lett **209**(2): 173-178.

Hou, S., M. Zhan, X. Zheng, C.-G. Zhan and F. Zheng (2014). "Kinetic characterization of human butyrylcholinesterase mutants for hydrolysis of cocaethylene." The Biochemical journal **460**(3): 447-457.

Joosen, M. J. A., M. J. van der Schans, C. G. M. van Dijk, W. C. Kuijpers, H. M. Wortelboer and H. P. M. van Helden (2011). "Increasing oxime efficacy by blood–brain barrier modulation." Toxicology Letters **206**(1): 67-71.

Kabbani, N., J. C. Nordman, B. A. Corgiat, D. P. Veltri, A. Shehu, V. A. Seymour and D. J. Adams (2013). "Are nicotinic acetylcholine receptors coupled to G proteins?" Bioessays **35**(12): 1025-1034.

Kalisiak, J., E. C. Ralph and J. R. Cashman (2012). "Nonquaternary reactivators for organophosphate-inhibited cholinesterases." J Med Chem **55**(1): 465-474.

Kalisiak, J., E. C. Ralph, J. Zhang and J. R. Cashman (2011). "Amidine-oximes: reactivators for organophosphate exposure." J Med Chem **54**(9): 3319-3330.

Kandel, E., Jessell T, Schwartz J, Hudspeth, AJ, Siegelbaum (2013). "Principles of Neural Science." New York, McGraw-Hill. p. 9-10, 19-34.

Kassa, J. (2002). "Review of oximes in the antidotal treatment of poisoning by organophosphorus nerve agents." J Toxicol Clin Toxicol **40**(6): 803-816.

Kolarich, D., A. Weber, M. Pabst, J. Stadlmann, W. Teschner, H. Ehrlich, H. P. Schwarz and F. Altmann (2008). "Glycoproteomic characterization of butyrylcholinesterase from human plasma." Proteomics **8**(2): 254-255.

Lenz, D. E., D. Yeung, J. R. Smith, R. E. Sweeney, L. A. Lumley and D. M. Cerasoli (2007). "Stoichiometric and catalytic scavengers as protection against nerve agent toxicity: A mini review." Toxicology **233**(1–3): 31-39.

Levin, V. A. (1980). "Relationship of octanol/water partition coefficient and molecular weight to rat brain capillary permeability." J Med Chem **23**(6): 682-684.

Marino, M. T., B. G. Schuster, R. P. Brueckner, E. Lin, A. Kaminskis and K. C. Lasseter (1998). "Population pharmacokinetics and pharmacodynamics of pyridostigmine bromide for prophylaxis against nerve agents in humans." J Clin Pharmacol **38**(3): 227-235.

Marrs, T. C. (2003). "Diazepam in the treatment of organophosphorus ester pesticide poisoning." Toxicol Rev **22**(2): 75-81.

Masson, P. and O. Lockridge (2010). "Butyrylcholinesterase for protection from organophosphorus poisons; catalytic complexities and hysteretic behavior." Archives of biochemistry and biophysics **494**(2): 107.

Maxwell, D. M., K. M. Brecht, B. P. Doctor and A. D. Wolfe (1993). "Comparison of antidote protection against soman by pyridostigmine, HI-6 and acetylcholinesterase." Journal of Pharmacology and Experimental Therapeutics **264**(3): 1085-1089.

Meek, E. C., H. W. Chambers, A. Coban, K. E. Funck, R. B. Pringle, M. K. Ross and J. E. Chambers (2012). "Synthesis and *in vitro* and *in vivo* inhibition potencies of highly relevant nerve agent surrogates." Toxicol Sci **126**(2): 525-533.

Michaelis, L., M. L. Menten, K. A. Johnson and R. S. Goody (2011). "The original Michaelis constant: translation of the 1913 Michaelis-Menten paper." Biochemistry **50**(39): 8264-8269.

Muñoz-Quezada, M. T., B. A. Lucero, V. P. Iglesias, M. P. Muñoz, C. A. Cornejo, E. Achu, B. Baumert, A. Hanchey, C. Concha, A. M. Brito and M. Villalobos (2016). "Chronic exposure to organophosphate (OP) pesticides and neuropsychological functioning in farm workers: a review." International Journal of Occupational and Environmental Health **22**(1): 68-79.

Munro, N. (1994). "Toxicity of the Organophosphate Chemical Warfare Agents GA, GB, and VX: Implications for Public Protection." Environmental Health Perspectives **102**(1): 18-37.

Nachon, F., X. Brazzolotto, M. Trovaslet and P. Masson (2013). "Progress in the development of enzyme-based nerve agent bioscavengers." Chemico-Biological Interactions **206**(3): 536-544.

Nordberg, A., C. Ballard, R. Bullock, T. Darreh-Shori and M. Somogyi (2013). "A Review of Butyrylcholinesterase as a Therapeutic Target in the Treatment of Alzheimer's Disease." The Primary Care Companion for CNS Disorders **15**(2): PCC.12r01412. pp. 1-2.

Pandit, V., S. Seshadri, S. N. Rao, C. Samarasinghe, A. Kumar and R. Valsalan (2011). "A case of organophosphate poisoning presenting with seizure and unavailable history of parenteral suicide attempt." Journal of Emergencies, Trauma and Shock **4**(1): 132-134.

Peter, J. V., T. I. Sudarsan and J. L. Moran (2014). "Clinical features of organophosphate poisoning: A review of different classification systems and approaches." Indian Journal of Critical Care Medicine : Peer-reviewed, Official Publication of Indian Society of Critical Care Medicine **18**(11): 735-745.

Pita, R. and J. Domingo (2014). "The Use of Chemical Weapons in the Syrian Conflict." Toxics **2**(3): 391-393.

Purves D, A. G., Fitzpatrick D, et al. (2001). "Acetylcholine." Neuroscience (2nd Edition). Online source https://www.ncbi.nlm.nih.gov/books/NBK11143/.

Radić, Z., R. K. Sit, E. Garcia, L. Zhang, S. Berend, Z. Kovarik, G. Amitai, V. V. Fokin, K. B. Sharpless and P. Taylor (2013). "Mechanism of Interaction of Novel Uncharged, Centrally Active Reactivators with OP-hAChE Conjugates." Chemico-biological interactions **203**(1): 67-71.

Radic, Z., R. K. Sit, Z. Kovarik, S. Berend, E. Garcia, L. Zhang, G. Amitai, C. Green, B. Radic, V. V. Fokin, K. B. Sharpless and P. Taylor (2012). "Refinement of structural leads for centrally acting oxime reactivators of phosphylated cholinesterases." J Biol Chem **287**(15): 11798-11809.

Raveh, L., J. Grunwald, D. Marcus, Y. Papier, E. Cohen and Y. Ashani (1993). "Human butyrylcholinesterase as a general prophylactic antidote for nerve agent toxicity. *In vitro* and *in vivo* quantitative characterization." Biochem Pharmacol **45**(12): 2465-2474.

Resat, H., L. Petzold and M. F. Pettigrew (2009). "Kinetic Modeling of Biological Systems." Methods in molecular biology (Clifton, N.J.) **541**: 311-314.

Ritchie, R. J. and T. Prvan (1996). "Current statistical methods for estimating the Km and Vmax of Michaelis-Menten kinetics." Biochemical Education **24**(4): 196-206.

Ritchie, R. J. and T. Prvan (1996). "A Simulation Study on Designing Experiments to Measure theKmof Michaelis-Menten Kinetics Curves." Journal of Theoretical Biology **178**(3): 239-254.

Rose, S. and A. Baravi (1988). "The meaning of Halabja: chemical warfare in Kurdistan." Race & Class **30**(1): 74-77.

Rosenbaum, D. M., S. G. F. Rasmussen and B. K. Kobilka (2009). "The structure and function of G-protein-coupled receptors." Nature **459**(7245): 356-363.

Rosman, Y., A. Eisenkraft, N. Milk, A. Shiyovich, N. Ophir, S. Shrot, Y. Kreiss and M. Kassirer (2014). "Lessons learned from the Syrian sarin attack: evaluation of a clinical syndrome through social media." Annals of internal medicine **160**(9): 644-648.

Shek, E., T. Higuchi and N. Bodor (1976). "Improved delivery through biological membranes. 2. Distribution, excretion, and metabolism of N-methyl-1,6-dihydropyridine-2-carbaldoxime hydrochloride, a pro-drug of N-methylpyridinium-2-carbaldoxime chloride." J Med Chem **19**(1): 108-112.

Shek, E., T. Higuchi and N. Bodor (1976). "Improved delivery through biological membranes. 3. Delivery of N-methylpyridinium-2-carbaldoxime chloride through the blood-brain barrier in its dihydropyridine pro-drug form." J Med Chem **19**(1): 113-117.

Shiloff, J. D. and J. G. Clement (1986). "Effects of subchronic pyridostigmine pretreatment on the toxicity of soman." Can J Physiol Pharmacol **64**(7): 1047-1049.

Sit, R. K., Z. Radic, V. Gerardi, L. Zhang, E. Garcia, M. Katalinic, G. Amitai, Z. Kovarik, V. V. Fokin, K. B. Sharpless and P. Taylor (2011). "New structural scaffolds for centrally acting oxime reactivators of phosphylated cholinesterases." J Biol Chem **286**(22): 19422-19430.

Smythies, J. and B. Golomb (2004). "Nerve gas antidotes." Journal of the Royal Society of Medicine **97**(1): 32-32.

Strader, C. D., T. M. Fong, M. R. Tota, D. Underwood and R. A. Dixon (1994). "Structure and function of G protein-coupled receptors." Annu Rev Biochem **63**: 101-132.

Taylor, P., Brown, JH (1999). "Synthesis, Storage and Release of Acetylcholinesterase." Basic Neurochemistry: Molecular, Cellular and Medical Aspects. 6th Edition. online resource https://www.ncbi.nlm.nih.gov/books/NBK28051/

Tortura, G. J. D., Bryan H. (2011). "Principle of Anatomy & Physiology." 415-459.

Tucker, J. (2007). War of Nerves: Chemical Warfare from World War I to Al-Qaeda, Anchor Books. pp 331-347, 349-371.

Tuorinsky, S. D., United States. Dept. of the Army. Office of the Surgeon General. and Borden Institute (U.S.) (2008). Medical aspects of chemical warfare. Falls Church, Va. Washington, DC, Office of the Surgeon General Borden Institute For sale by the Supt. of Docs., U.S. G.P.O. pp. 45-77, 113-146, 155-205, 243-253.

United States. Department of the Army., Institute of Land Warfare (Association of the United States Army) and United States. Department of the Army. (1967). "U.S. Army Field Manual 3-8 Chemical Reference Handbook." pp. 65-87.

van der Schans, M. J., B. J. Lander, H. v. d. Wiel, J. P. Langenberg and H. P. Benschop (2003). "Toxicokinetics of the nerve agent (±)-VX in anesthetized and atropinized hairless guinea pigs and marmosets after intravenous and percutaneous administration." Toxicology and Applied Pharmacology **191**(1): 48-62.

van Heel, W. and S. Hachimi-Idrissi (2011). "Accidental organophosphate insecticide intoxication in children: a reminder." International Journal of Emergency Medicine **4**(1): 32.

von Bredow, J. D., N. L. Adams, W. A. Groff and J. A. Vick (1991). "Effectiveness of oral pyridostigmine pretreatment and cholinolytic-oxime therapy against soman intoxication in nonhuman primates." Fundam Appl Toxicol **17**(4): 761-770.

Vučinić, S., B. Antonijević and D. Brkić (2014). Occupational and environmental aspects of organophosphorus compounds. Basic and Clinical Toxicology of Organophosphorus Compounds**:** 213-244.

Whalley, C. E., J. M. McGuire, D. B. Miller, E. M. Jakubowski, R. J. Mioduszewski, S. A. Thomson, L. A. Lumley, J. H. McDonough and T. M. Shih (2007). "Kinetics of sarin (GB) following a single sublethal inhalation exposure in the guinea pig." Inhal Toxicol **19**(8): 667-681.

Worek, F., N. Aurbek, M. Koller, C. Becker, P. Eyer and H. Thiermann (2007). "Kinetic analysis of reactivation and aging of human acetylcholinesterase inhibited by different phosphoramidates." Biochem Pharmacol **73**(11): 1807-1817.

Worek, F., C. Diepold and P. Eyer (1999). "Dimethylphosphoryl-inhibited human cholinesterases: inhibition, reactivation, and aging kinetics." Arch Toxicol **73**(1): 7-14.

Worek, F., P. Eyer, N. Aurbek, L. Szinicz and H. Thiermann (2007). "Recent advances in evaluation of oxime efficacy in nerve agent poisoning by *in vitro* analysis." Toxicology and Applied Pharmacology **219**(2–3): 226-234.

Worek, F., P. Eyer and L. Szinicz (1998). "Inhibition, reactivation and aging kinetics of cyclohexylmethylphosphonofluoridate-inhibited human cholinesterases." Arch Toxicol **72**(9): 580-587.

Worek, F., M. Koller, H. Thiermann and L. Szinicz (2005). "Diagnostic aspects of organophosphate poisoning." Toxicology **214**(3): 182-189.

Worek, F., U. Mast, D. Kiderlen, C. Diepold and P. Eyer (1999). "Improved determination of acetylcholinesterase activity in human whole blood." Clin Chim Acta **288**(1-2): 73-90.

Worek, F., G. Reiter, P. Eyer and L. Szinicz (2002). "Reactivation kinetics of acetylcholinesterase from different species inhibited by highly toxic organophosphates." Arch Toxicol **76**(9): 523-529.

Worek, F., M. Schilha, K. Neumaier, N. Aurbek, T. Wille, H. Thiermann and K. Kehe (2016). "On-site analysis of acetylcholinesterase and butyrylcholinesterase activity with the ChE check mobile test kit—Determination of reference values and their relevance for diagnosis of exposure to organophosphorus compounds." Toxicology Letters **249**: 22-28.

Worek, F., H. Thiermann, L. Szinicz and P. Eyer (2004). "Kinetic analysis of interactions between human acetylcholinesterase, structurally different organophosphorus compounds and oximes." Biochem Pharmacol **68**(11): 2237-2248.

Yang, G. Y. Y., Joong-Ho; Seong, Churl-Min; Park, No-Sang; and Jung, Young-Sik (2003). "Synthesis of Bis-pyridinium Oxime Antidotes Using Bis(methylsulfonoxymethyl) Ether for Organphosphate Nerve Agent." Bull. Korean Chem. Soc. **24**(9): 1368-1370.

CHAPTER II

ANALYSIS OF CYCLOSARIN SURROGATE AND NOVEL OXIMES

Introduction

Chapter II describes the research with the cyclosarin surrogate, 4-nitrophenyl cyclohexyl methylphosphonate (NCMP) and determining the best oximes for reactivating rat brain inhibited by NCMP. The current research demonstrates a few novel oximes that are capable of reactivating rat brain AChE after NCMP inhibition. In addition, co-administration studies with 2-PAM and the novel oximes demonstrate increased AChE reactivation after inhibition with NCMP. This information provides initial data for a possible combined oxime therapy with the novel oximes and 2-PAM.

Materials and Methods

Nerve agent surrogate

The cyclosarin surrogate (NCMP) was synthesized from commercially available compounds and all reagent grade chemicals were purchased from Thermo Fisher Scientific (Waltham, MA) or Sigma Chemical Co. (St Louis, MO). NCMP was developed, synthesized, and characterized in the laboratory as previously described (Meek, Chambers et al. 2012). The structure and purity were respectively confirmed using liquid chromatography/electrospray ionization/mass spectrophotometry (LC-ESI-MS) and ^{1}H nuclear magnetic resonance (NMR). Figure 1 displays the chemical

structure differences between cyclosarin and the corresponding nerve agent surrogate NCMP.

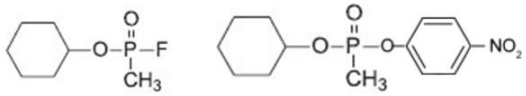

Figure 1 Chemical structure of cyclosarin and NCMP

Novel oxime reactivators

The novel oximes are substituted phenoxyalkyl pyridinium oximes that have incorporated lipophilic moieties with the expectation that the charged quaternary ammonium will counterbalance the lipophilic moiety and impart the oxime with an ability to cross the BBB. In addition, it is expected that the reactivating ability of the oxime will be retained. The overall structure of this oxime series is shown in Figure 2 below and the specific substitutions are listed in Table 1 in the results section. The oxime numbering is defined by: First number is the location of the oxime in relationship to the quaternary nitrogen in the pyridinium ring, second number is the n describing number of methylene's in the methylene bridge, and the final double digit number is the sequence of the compound in the series. The structure for 2-PAM from Sigma-Aldrich is shown in Figure 3.

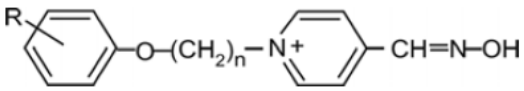

Figure 2 General structure of substituted phenoxyalkyl pyridinium oxime

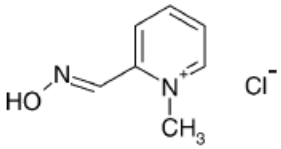

Figure 3 2-PAM chemical structure

Animals

Adult male Sprague Dawley-derived rats were used as the animal model for *in vitro* screening of the oximes. All animal protocols received prior approval from the Mississippi State University Animal Care and Use Committee.

Standard *in vitro* reactivation screening

The initial screening of the novel oximes for reactivation potential was conducted with NCMP as previously described (Chambers, Chambers et al. 2013). The criterion for moving forward was set at 5% reactivation. Three different pools of Sprague-Dawley-derived rat brains were utilized for each experiment. Each pool consisted of five rat brains. The brains were homogenized with a Heidolph Homogenizer and diluted with 0.05 M Tris-HCl buffer (pH 7.4 at 37 ºC). Specimens were stored at -80 ºC until testing. Each pooled specimen was diluted to 40 mg/ml with Tris-HCl buffer. The final concentration (FC) for each experiment was 1 mg equivalent/ml of tissue.

Rat brain AChE was inhibited at approximately 80 percent using a NCMP FC of 3 nM and incubated for 15 minutes at 37 ºC in a shaking water bath. The inhibited rat brain AChE was immediately reactivated using the various oximes in ethanol at a FC of 100 µM for 30 minutes at 37 ºC in a shaking water bath. The samples were diluted with TRIS-HCl buffer 1/25 to stop inhibition and reactivation. The AChE activity was measured by adding the substrate acetylthiocholine (ATCh) at a FC of 1 mM and incubating for 15 minutes at 37 ºC in a shaking water bath. 5,5'-dithiobis(2-nitrobenzoate) (DTNB) was used as the chromogen to detect activity at 412 nm on a Thermo Scientific Biomate 3 Spectrophotometer.

Percent reactivation was determined by subtracting the total inhibition percentage, I_T, minus the total inhibition percentage after reactivation, I_R, and then dividing that value by the total inhibition percentage. Solvent controls were utilized to eliminate extraneous activity. The criteria for continued testing was set at 5% reactivation. Equation 1 below describes the calculation utilized.

$$\%Reactivation = \frac{\%I_T - \%I_R}{\%I_T} \qquad (1)$$

Simultaneous inhibition and reactivation *in vitro* studies

The standard *in vitro* reactivation protocol above was modified by adding the NCMP and oxime simultaneously one after the other at the initial start time. The AChE activity was measured at 15, 30, and 45 minute intervals using the modified Ellman's assay previously described above (Chambers, Chambers et al. 2013). The criteria for continued testing was set at 30%.

Combined 2-PAM and novel oxime studies

A similar protocol was used as described above, but the 100 µM FC of oxime normally added was divided into 50 µM of 2-PAM and 50 µM of the best novel oxime. The criterion for advancing each oxime forward for further testing was set at 40% reactivation in the *in vitro* screening.

Results

The 17 novel oxime antidotes for NCMP were tested alongside 2-PAM. The best AChE reactivation activity ranged from 4 to 5 percent and included 2-PAM, Oximes 46.21, 46.43, and 46.49 as seen in Table 1 below. Using these four oximes, simultaneous testing was conducted. NCMP was simultaneously incubated with 2-PAM, Oximes 46.21, 46.43, or 46.49 and AChE activity was measured at 15, 30, and 45-minute time points after incubation. Simultaneous incubation increased AChE activity for specimens with NCMP and Oximes 46.43 or 46.49. Peak reactivation of 26 and 34 percent, respectively, was observed for the 15-minute time point and progressively decreasing values for the 30 and 45-minute time points. 2-PAM and Oxime 46.21 did not show any improvement and continued to have reactivation ranging from 4 to 5 percent as previously observed for all time points. Finally, concentrating on the successful data from the simultaneous experiments and using a 15-minute incubation we tested the successful oximes in combination with 2-PAM. A nearly 40 percent reactivation of AChE was observed with Oxime 46.43 with 2-PAM and nearly 35 percent reactivation with Oxime 46.49 and 2-PAM.

Table 1 *In vitro* NCMP inhibited rat brain AChE reactivation by novel oximes.

Oxime	n[a]	R[b]	In vitro percent reactivation NCMP[c]	Simultaneous incubation of NCMP and Oxime[d]			Simultaneous incubation of NCMP, 2-PAM, and Oxime[e]
				15 min	30 min	45 min	
2-PAM	**NA**	**NA**	**5.7 ± 2.8**	**7.8 ± 1.6**	**5.3 ± 1.2**	**3.5 ± 1.8**	
46.01	6	H-	3.1 ± 1.3				
46.06	6	4-CH_3-O-	2.7 ± 0.4				
46.10	6	4-O_2N	2.0 ± 1.2				
46.12	6	4-$CH_3C(:O)$-	2.1 ± 0.6				
46.16	6	4-Ph-	2.6 ± 0.4				
46.21	**6**	**4-Ph-C(:O)-**	**5.5 ± 0.7**	**4.1 ± 2.8**	**5.8 ± 0.7**	**3.7 ± 1.7**	**5.0 ± 0.7**
46.23	6	4-Ph-O-	2.1 ± 0.7				
46.24	6	4-Ph-CH_2-	1.3 ± 0.3				
46.25	6	4-Ph-CH_2-O-	2.2 ± 0.6				
46.26	6	2,4,5-Cl_3-	0.9 ± 0.4				
46.28	6	2,4.6-Cl_3-	2.2 ± 0.5				
46.35	6	4-Cl-3,5-$(CH_3)_2$-	2.0 ± 0.4				
46.43	**6**	**4-$(CH_3)_3CCH_2C(CH_3)_2$-**	**4.4 ± 0.6**	**30.5 ± 12.8**	**23.7 ± 5.5**	**6.3 ± 3.7**	**39.5 ± 2.0**
46.49	**6**	**4-Ph-$C(CH_3)_2$-**	**5.1 ± 1.0**	**50.1 ± 8.1**	**28.2 ± 7.0**	**16.6 ± 3.6**	**34.2 ± 2.5**
46.55	6	3-O-C(:O)CH=CH-4-	2.2 ± 1.0				
46.56	6	3-CHCH=C(Br)CH-4-	1.0 ± 0.8				
46.57	6	(Phthalimidyl-)	0.0 ± 0.6				

Bold print indicates the oximes that showed best reactivation for further testing. [a] Number of C's in alkyl chain (n in Figure 2). [b] Substitutions on the phenoxy moiety (R in Figure 2). [c] 30-min incubation with 10 mM oxime following 15-min incubation with $10^{-5.5}$ M NCMP, n = 3, mean ± SEM. [d] Simultaneous incubation of 10 mM oxime and $10^{-5.5}$ M NCMP, n = 3, mean ± SEM. [e] This simultaneous incubation of 10 mM novel oxime, 10 µM 2-PAM, and $10^{-5.5}$ M NCMP, n = 3, mean ± SEM.

Discussion

All 17 novel phenoxyalkyl pyridinium oximes and 2-PAM were highly ineffective against NCMP. This was expected considering the historical data demonstrating the difficulty in reactivating cyclosarin inhibited AChE with the current approved US antidote of 2-PAM (Worek, Thiermann et al. 2004, Moshiri, Darchini-Maragheh et al. 2012). Further investigation of the novel oximes and 2-PAM demonstrated increased reactivation percentages with simultaneous exposure of rat brain AChE to NCMP and two of the novel oximes and 2-PAM. Possible explanations for these observations were made by reviewing the discoveries of other researchers looking into the interactions between other nerve agents and oximes (Worek, Thiermann et al. 2004). Researchers have suggested that differences in oxime structure, acidity, R-group attachment position on the pyridinium ring, and also structural fit into the active site may play a role.

A number of mechanisms were considered in the interpretation of the research results. The size of the oximes and the particular structure demonstrates a possible link to improved reactivation. Oxime 46.43 is structurally one of the largest novel oximes that were tested with the R-group containing only methyl groups. Oxime 46.49 was also one of the structurally largest novel oximes tested with the R-groups containing a phenol and methyl groups. When compared to 2-PAM and the other 14 novel oximes, these oximes were structurally smaller then these two compounds. The exception is the oxime containing the phthalimidyl group which is the largest structure tested of all the oximes. This suggests that these two particular oximes may have been the perfect size for reactivating with NCMP inhibited AChE in these conditions. In addition, structures with R-groups containing oxygen, nitrogen, chloride, and bromine did not reactivate as well as

the two successful oximes. These atoms may have played a role in binding activity, but had less of a factor towards reactivation. When considering that commercial oximes like HI6 and HLö 7 contain additional oxygen, nitrogen, and chloride elements and are very successful at reactivating cyclosarin inhibited AChE, then the atoms mentioned may not play a critical role at all (Worek, Thiermann et al. 2004). What may matter most is the tertiary conformation of the protein that is dictated by the atoms present, instead of the individual atoms themselves. The size of the two oximes most likely played an important role in their success under these conditions. Three-dimensional modeling may be helpful in further characterizing size relationships and interactions taking place.

The position of the oxime group on the pyridinium ring has been demonstrated by other researchers to play a role in reactivation, with position 2 and 4 being critical (de Jong, Verhagen et al. 1989). Worek et al. also demonstrated that position 4 is usually associated with better organophosphate reactivation versus position 2 (Worek, Thiermann et al. 2004). This is supported in the experimental findings with both of the oximes located at position 4.

The addition of a second pyridinium ring to oximes has been demonstrated by researchers to play a role in orienting some oximes into the active site of the AChE. In particular, Ashani et al. performed active site substitutions to elucidate the interaction of HI-6 with AChE during reactivation and discovered the importance of the second pyridinium ring (Ashani, Radic et al. 1995). In this case, the three rings of the oxime 46.49 may play a role in orienting the oxime for improved reactivation. Amino acid substitution testing of key elements at the active site of AChE may be beneficial in determining the specific interaction of the oxime 46.49 with AChE, and help determine

possible structural improvements with this NCMP antidote. Also, substitution experiments with the previous nerve agent surrogates tested (NIMP and NEMP) and their corresponding successful 44-series oximes may be beneficial in improving the antidotes further (Chambers, Chambers et al. 2013).

The last significant observation is the difference in reactivation seen between adding the oxime after the NCMP inhibition has occurred versus adding it concurrently. One explanation to this observation is the possibility of noncompetitive or competitive non-covalent binding of the oxime with AChE at the active site or at another location on the enzyme. Researchers have demonstrated that allosteric changes to human AChE can be caused by the binding of peripheral ligands noncompetitively to AChE and this subsequently leads to modulation of paraoxon inhibition (Barak, Ordentlich et al. 1995). Using amino acid substitutions, the researchers demonstrated that the modulation of allosteric sites can cause conformational changes to the active site of human AChE. This research finding could explain the possibility that the novel oximes may be interacting with peripheral sites on the AChE and causing active site changes that temporarily prevent inhibition by NCMP. Following the amino acid substitutions on AChE conducted by Barak et al., this possibility could be tested for the 46-series oxime and NCMP. A kinetic analysis may be able to demonstrate competitive inhibition as well (Gawron and Keil 1960, Čolović, Krstić et al. 2013). Researchers have demonstrated the use of kinetic inhibition constants to demonstrate that certain compounds can be competitive inhibitors of AChE. This approach could be used with the 46-series oximes and NCMP.

A second possibility may be that the oximes are noncovalently binding to the NCMP, and temporarily preventing it from interacting with the AChE. Researchers have demonstrated that radiolabeled sarin can be attached to molecules in the blood with molecular weights of 10000 and a majority of these molecules were actually AChE (Polak and Cohen 1970). The molecular weight of the various oximes is less than 10000, so direct binding of the oximes with NCMP is not probable.

The last observation in the data is the decreased reactivation activity observed in the timed studies. This may be a result of normal degradation of the oximes over time (Meek, Chambers et al. 2012, Chambers, Chambers et al. 2013). In addition, the formation of phosphyloximes after AChE reactivation has been demonstrated to inhibit AChE after reactivation (Worek, Szinicz et al. 2005). This inhibition could account for the decreased reactivation over time and also the ineffectiveness of some of the many oximes tested in initial experiments.

Conclusion

It was surprisingly unexpected to see stronger reactivation after simultaneous incubation with NCMP and two of the better performing novel oximes, 46.43 and 46.49. The literature provides some very important possible explanations for these observations. Our results further emphasize the importance of oxime size, location of the R-group attachment on the phenoxy ring, and the possible importance of additional phenoxy rings when orienting the active site.

Also the success of our combined oxime experiments with 2-PAM and oxime 46.43 or oxime 46.49, helps support the possibility of future such experiments. In particular combined oxime experiments with 2-PAM and the other successful oximes

44.08 and 44.25 could be useful in developing actual *in vivo* therapies in the future for reactivating the sarin and VX surrogates (Chambers, Chambers et al. 2013).

References

Ashani, Y., Z. Radic, I. Tsigelny, D. C. Vellom, N. A. Pickering, D. M. Quinn, B. P. Doctor and P. Taylor (1995). "Amino acid residues controlling reactivation of organophosphonyl conjugates of acetylcholinesterase by mono- and bisquaternary oximes." J Biol Chem **270**(11): 6370-6380.

Barak, D., A. Ordentlich, A. Bromberg, C. Kronman, D. Marcus, A. Lazar, N. Ariel, B. Velan and A. Shafferman (1995). "Allosteric modulation of acetylcholinesterase activity by peripheral ligands involves a conformational transition of the anionic subsite." Biochemistry **34**(47): 15444-15452.

Chambers, J. E., H. W. Chambers, E. C. Meek and R. B. Pringle (2013). "Testing of novel brain-penetrating oxime reactivators of acetylcholinesterase inhibited by nerve agent surrogates." Chem Biol Interact **203**(1): 135-138.

Čolović, M. B., D. Z. Krstić, T. D. Lazarević-Pašti, A. M. Bondžić and V. M. Vasić (2013). "Acetylcholinesterase Inhibitors: Pharmacology and Toxicology." Current Neuropharmacology **11**(3): 315-335.

de Jong, L. P., M. A. Verhagen, J. P. Langenberg, I. Hagedorn and M. Loffler (1989). "The bispyridinium-dioxime HLo-7. A potent reactivator for acetylcholinesterase inhibited by the stereoisomers of tabun and soman." Biochem Pharmacol **38**(4): 633-640.

Gawron, O. and J. Keil (1960). "Competitive inhibition of acetylcholinesterase by several thiazolines and oxazolines." Archives of Biochemistry and Biophysics **89**(2): 293-295.

Meek, E. C., H. W. Chambers, A. Coban, K. E. Funck, R. B. Pringle, M. K. Ross and J. E. Chambers (2012). "Synthesis and *in vitro* and *in vivo* inhibition potencies of highly relevant nerve agent surrogates." Toxicol Sci **126**(2): 525-533.

Moshiri, M., E. Darchini-Maragheh and M. Balali-Mood (2012). "Advances in toxicology and medical treatment of chemical warfare nerve agents." DARU Journal of Pharmaceutical Sciences **20**(1): 81-81.

Polak, R. L. and E. M. Cohen (1970). "The binding of sarin in the blood plasma of the rat." Biochemical Pharmacology **19**(3): 877-881.

Worek, F., L. Szinicz, P. Eyer and H. Thiermann (2005). "Evaluation of oxime efficacy in nerve agent poisoning: Development of a kinetic-based dynamic model." Toxicology and Applied Pharmacology **209**(3): 193-202.

Worek, F., H. Thiermann, L. Szinicz and P. Eyer (2004). "Kinetic analysis of interactions between human acetylcholinesterase, structurally different organophosphorus compounds and oximes." Biochem Pharmacol **68**(11): 2237-2248.

CHAPTER III

KINETIC COMPARISON

Introduction

Testing of nerve agent exposure and corresponding antidote efficacy is primarily accomplished via *in vitro* and *in vivo* animal models (Thiermann, Kehe et al. 2007). The primary cost effective animal model is centered on the Sprague Dawley-derived rat or other similar research rats. Actual nerve agent testing on humans is limited to blood components (Worek, Eyer et al. 1998). Kinetic testing of enzymes provides a quantitative means to evaluate the effects of various substrates, inhibitors, and reactivators on the active site of an enzyme (Valiveti, Bhalerao et al. 2015). To improve data extrapolation from rat to humans, a comparative kinetic analysis was performed to provide the initial information for translating antidote dosing for humans via a future pharmacokinetic model (Worek, Reiter et al. 2002, Eyer, Szinicz et al. 2007).

To accomplish the kinetic analysis rat and human blood were processed to analyze acetylcholinesterase (EC 3.1.1.7, AChE) on the erythrocyte membrane, and AChE and butyrylcholinesterase (EC 3.1.1.8; BChE) suspended in the plasma. In addition, rat brain and skeletal muscle (SKM) were also processed to analyze AChE in these tissues. A modified Ellman's AChE and BChE activity assay using a 96-well plate was developed and utilized to determine the necessary kinetic values. Inhibitors used were a VX nerve agent surrogate (4-nitrophenyl ethyl methylphosphonate; NEMP) and a

sarin nerve agent surrogate (4-nitrophenyl isopropyl methylphosphonate; NIMP). AChE and BChE reactivators tested were pralidoxime chloride (2-PAM), and novel oximes 44.08 and 44.25. The AChE and BChE kinetic values obtained from the experiments include the maximum velocity (V_{max}), the apparent Michaelis-Menten (K_{mapp}) constant, the association constant (K_A), the rate of phosphorylation (k_p), the rate of inhibition (k_i), the rate of reactivation (k_r), the rate constant for aging (k_a), and the rate constant for spontaneous reactivation (k_s).

The kinetic values provided important measurements of enzyme activity in the tested specimens and allowed for points of comparison (Voet and Voet 2011). The Michaelis constant (K_m) is a measure of the affinity of the enzyme for its substrate as long as the k_2 is less than k_{-1}. A small K_m value means an enzyme reaches maximal catalytic efficiency at low substrate concentrations. It is the substrate concentration at which the reaction rate is half of V_{max}. The V_{max} value is the maximum rate achieved when enzyme concentration is saturated. In the presence of an inhibitor the K_m is called K_{mapp}, because the inhibitor alters the true K_m and V_{max} values. Though the K_m and V_{max} values are altered in the presence of an inhibitor, their true underlying values are still the same without the inhibitor. The K_{mapp} varies based on the inhibitor and inhibitor concentration. The rate of inhibition k_i describes the inhibition rate of an enzyme in the presence of specific inhibitors and can be described as k_i for a forward reaction and k_{-i} for a reverse reaction. The K_i is the inhibition constant that describes the forward and reverse inhibition rates, where $K_i = k_i/k_{-i}$. For the inhibition rates, the higher the number the faster the rate of inhibition. The K_A is the association constant that describes the strength of the enzyme inhibitor association (Carr and Chambers 1996). The higher the

number the greater the association. The k_p is the phosphorylation rate of the enzyme forming the inhibited enzyme. The higher the number, the faster the rate of phosphorylation of the enzyme by the inhibitor. The binding affinity to the active site and the rate of phosphorylation, respectively K_A and k_p, together determine the bimolecular rate constant, k_i, which is the measurement of the inhibitory power of an inhibitor (Coban, Carr et al. 2016). The phosphylated enzyme is susceptible to spontaneous hydrolysis of the phosphylated enzyme resulting in spontaneous reactivation and the associated k_s rate (Worek, Thiermann et al. 2004). The phosphylated enzyme is also susceptible to spontaneous hydrolysis of one alkyl-ester bond and the resulting negatively charged residue that is resistant to nucleophile attack by oximes or spontaneous reactivation, and is termed aged with its corresponding aging rate constant k_a. Aged enzyme is permanently inhibited. The higher the k_s and k_a value the faster the rate.

This chapter describes the experimental procedures used to conduct the kinetic experiments, describes the findings of the analyses and discusses the results.

Materials and Methods

Nerve agent surrogates

The sarin surrogate (4-nitrophenyl isopropyl methylphosphonate; NIMP) and VX surrogate (4-nitrophenyl ethyl methylphosphonate; NEMP) were synthesized from commercially available compounds by Dr. Howard Chambers and all reagent grade chemicals were purchased from Thermo Fisher Scientific (Waltham, MA) or Sigma Chemical Co. (St Louis, MO) (Meek, Chambers et al. 2012). Figure 4 depicts the chemical structure of the real nerve agents and the nerve agent surrogates.

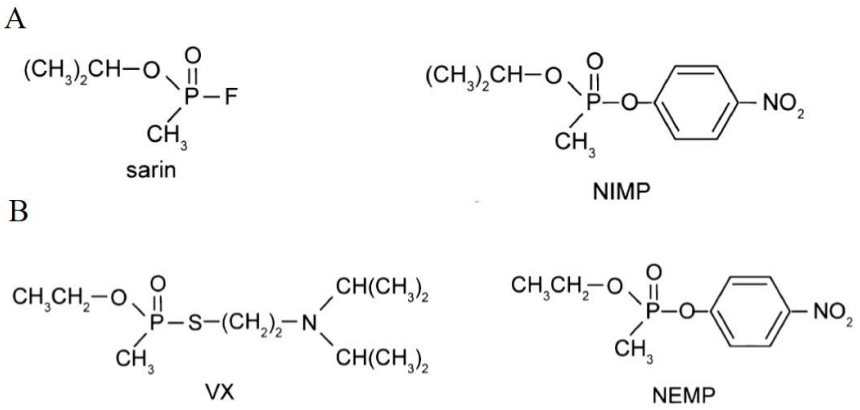

Figure 4 Chemical structures of nerve agents and surrogates

Side by side chemical structure comparison between (A) sarin and the corresponding surrogate NIMP and (B) VX and the corresponding surrogate NEMP.

Novel oxime reactivators

The novel oximes are substituted phenoxyalkyl pyridinium oximes and have incorporated lipophilic moieties with the expectation that the charged quaternary ammonium will counterbalance the lipophilic moieties and impart the oxime with an ability to cross the BBB (US Patent 9,277,937). In addition, it is expected that the reactivating ability of the oxime will be retained. These were synthesized by Dr. Howard Chambers. The overall structure of this oxime series is shown in Figure 5.A. and the specific substitutions are shown in Figure 5.B.

A

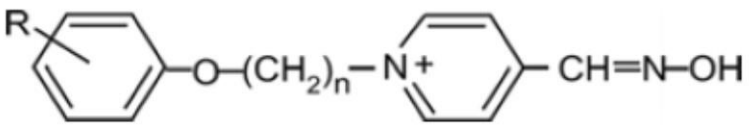

B

Oxime	R Group
44.08	4-Cl-
44.25	4-Ph-CH_2-O-

Figure 5 General chemical structure of novel oximes and R-group

(A) General structure of substituted phenoxyalkyl pyridinium oximes. R can represent a variety of chemical substitutions on the phenoxy moiety and n indicates the number carbons in the alkyl chain. For the compounds tested n = 4. Oxime 44.08 and oxime 44.25 are also referred to respectively as MSU 01 and MSU 20. (B) Chemical structure of the substitutions for the chemicals tested. The first digit of the code number is the location of the oxime in relationship to the quaternary nitrogen in the pyridinium ring, the second digit represent the n in the structure and denotes the number of methylene groups in the chain, and the last double digit is the sequence number of the compound in the series.

Animals

Adult male Sprague Dawley-derived rats (250-300 g) were housed in AAALAC accredited facilities with temperature controlled environments and 12 h dark-light cycle. LabDiet and tap water were provided ad libitum. All animal protocols received prior approval from the Mississippi State University Animal Care and Use Committee. All blood samples were collected via cardiac puncture and collected in ethylenediaminetetraacetic acid (EDTA) tubes (Parasuraman, Raveendran et al. 2010). All rat brain and skeletal muscle specimens were homogenized in a 15 ml ground glass Pyrex homogenizer and washed with Tris buffer, described below. Final experimental

concentration of 1 mg/ml of tissue was made with Tris buffer. Sample pools consisted of 5 different rats.

Human Blood

All human samples were collected at Columbus Air Force Base Medical Group (Columbus, MS) by medical laboratory technicians. Human blood samples were collected in EDTA tubes, and were ready to be discarded by the laboratory. Samples were de-identified and no patient demographics or information was provided. All human protocols were reviewed and approved by the IRBs at Mississippi State University and at Keesler Air Force Base research center. Sample pools consisted of 5 different human specimens. 20 human samples were collected in all and 4 pools created.

Buffers and Reagents

Sodium phosphate wash buffer (SPB) was made at 100 mM at pH 7.4. Hypotonic hemolysis buffer (HPB) was made at 6.7 mM at pH 7.4. The SPB and HPB were used for all blood experiments. Tris HCl buffer was made at 0.05 M at pH 7.7 at 25 ºC which results in a pH of 7.4 at 37 ºC. The Tris HCl buffer was used for rat brain and skeletal muscle experiments. The substrates acetylthiocholine (ATCh) and butyrylthiocholine (BTCh) were made at 0.1 M at pH 4.5. ATCh and BTCh were aliquoted into 1 ml conical tubes and frozen at 4 ºC until testing. The chromagen DTNB was made at 0.03 M. The DTNB was aliquoted into 5 ml glass vials and frozen at 4 ºC until testing. The cholinesterase (ChE) inhibitor eserine sulfate was made at 10^{-3} M. The eserine sulfate was aliquoted into 1 ml conical tubes and frozen at 4 ºC until testing.

AChE and BChE Preparation

Blood specimens were centrifuged for 10 minutes at 1500xg at 4 ºC (Eppendorf Centrifuge 5702R, A-4-38 rotor). The plasma was removed, aliquoted, pooled, and stored at -80 ºC until testing. Erythrocytes were washed with SPB (0.1M, pH 7.4) and then lysed with HPB (6.7 mM, pH 7.4). The erythrocyte solution was ultracentrifuged to remove hemoglobin for 30 minutes at 4 ºC (Beckman Coulter Avanti Centrifuge, JA-20 rotor). The supernatant was discarded and the pelleted samples were pooled. The lysed erythrocytes, now ghosts, were washed and returned to original volume with SPB (0.1 M, pH 7.4). A 15 ml ground glass Pyrex homogenizer was used to thoroughly resuspend and mix samples and then aliquot 250 µl into conical tubes which were stored at -80 ºC until testing (Dodge, Mitchell et al. 1963, Worek, Reiter et al. 2002).

Rat cerebral cortex and medulla oblongata and skeletal muscle were ground with a Polytron PT 10-35 Grinder and then homogenized with a Heidolph Homogenizer with a Teflon pestle in cold 0.05 M Tris-HCl buffer (pH 7.4 @ 37°C) at a concentration of 40 mg/ml for brain or 100 mg/ml for skeletal muscle. The homogenate was filtered through glass wool or gauze. Five rat samples were utilized per pooled sample. Samples were aliquoted into 4 ml glass vials and maintained at -80 ºC until testing. Prior to testing, rat brain and skeletal muscle were washed with Tris buffer to reduce turbidity. To accomplish this the specimens were centrifuged for 5 minutes at 5000xg and the supernatant was discarded (Eppendorf Centrifuge 5415C, F-45-18-11 rotor). The sample was returned to the original volume with Tris buffer. All testing was performed on the tissue pellet. After washing the samples were diluted appropriately with Tris buffer for a final testing concentration of 1 mg equivalent/ml per well.

AChE and BChE Substrate Kinetics Procedure

The sample analysis was conducted using a 96-well plate with a final testing volume of 300 µl per well. Samples were diluted to obtain a consistent absorbance of approximately 0.3 units. ATCh and BTCh concentrations were used to produce a range of enzyme activity in the experimental wells. The chromagen DTNB was added to the testing wells for a final concentration (FC) of 0.002 M. In addition to experimental wells, control wells were also included. Eserine sulfate, a ChE inhibitor, was added to the appropriate blank wells to obtain a FC 10^{-5} M and displayed absence of ChE activity to allow correction of non-ChE-mediated absorbance. Ethanol vehicle was added to the appropriate control wells to demonstrate maximum ChE activity. The appropriate substrate was added to the control wells for a FC of 2.5 mM. The experimental wells had a range of substrate concentrations from 0.02 mM to 2.5 mM. Enzyme activity was measured using a modified Ellman's assay as previously described (Ellman, Courtney et al. 1960, Carr and Chambers 1996, Chambers, Chambers et al. 2013). The same protocol was utilized for rat brain and skeletal muscle substrate kinetics, but the final testing concentration was 1 mg equivalent/ml and the 96-well plate volume was 200 µl per well.

For each concentration and control, the velocity was calculated. The velocities were then used to formulate a Lineweaver Burk plot with the reciprocal of each velocity on the y-axis and the reciprocal of each ATCh (BTCh) concentration on the x-axis as depicted in Figure 6. The resulting data were used to formulate a linear line with the coefficient of determination statistic (R^2-value) greater than 0.9 for acceptable results. The K_{mapp} = -slope and V_{max} = x-intercept (Hofstee 1959, Carr and Chambers 1996).

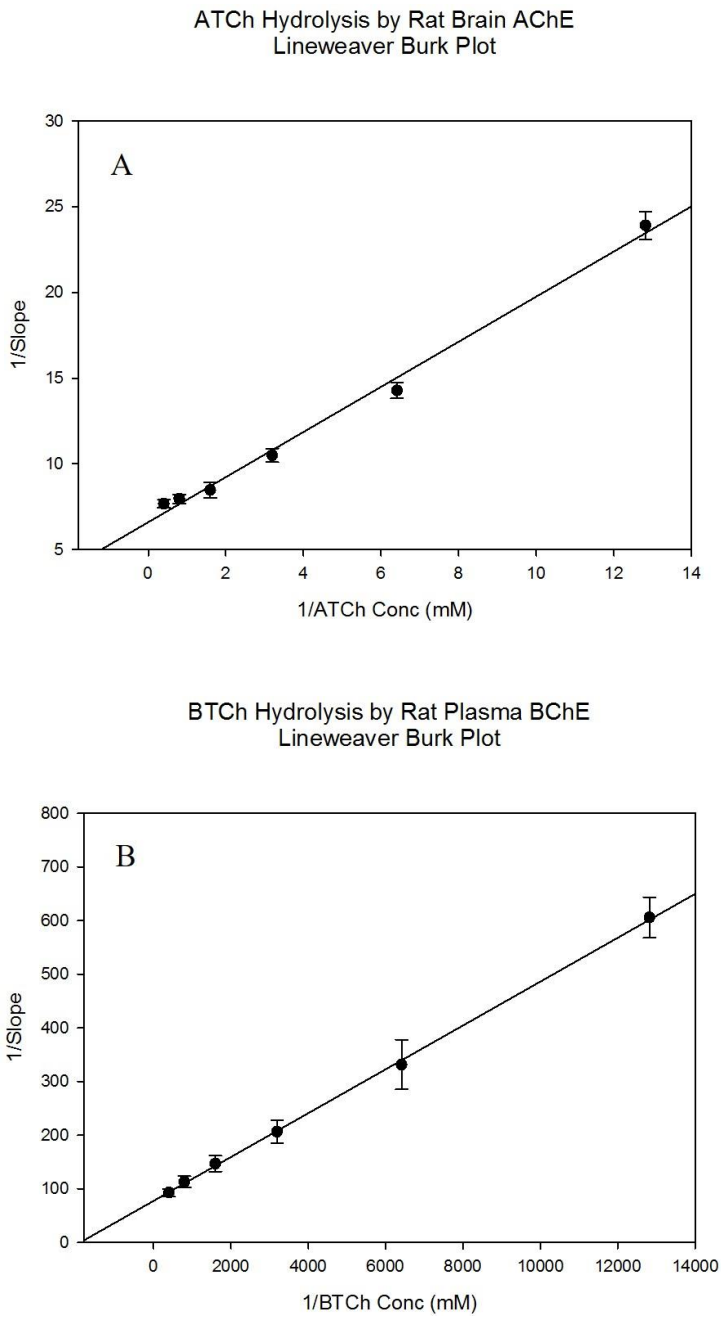

Figure 6 Lineweaver Burk plots for ATCh and BTCh substrate hydrolysis.

Lineweaver Burk plots used for determination of (A) ATCh and (B) BTCh substrate hydrolysis kinetics by AChE and BChE respectively.

AChE and BChE Inhibition Kinetics Procedure

The sample analysis for blood fractions was conducted using a 96-well plate with a final testing volume of 300 µl per well. Samples were diluted to obtain an absorbance of approximately 0.3 units. NEMP and NIMP concentrations were selected to effectively produce a range of 10 to 90 percent enzyme inhibition as depicted in Table 2 below. The chromagen DTNB was added to the testing wells for a FC of 0.002 M. Eserine sulfate, the ChE inhibitor, was added to the appropriate blank wells to obtain a FC 10^{-5} M. The substrate was added to the testing wells for a FC of 0.0025 M. Enzyme activity was measured using a modified Ellman's assay as previously described (Chambers, Chambers et al. 2013). Kinetic readings were performed at 0, 1, 2, 3, 4, and 5-minute time points. At each time point 12 continuous kinetic readings of the 96-well plate were obtained and enzyme activity was measured as mentioned above. The same protocol was utilized for rat brain and skeletal muscle substrate kinetics, but the final testing concentration was 1 mg equivalent/ml of tissue and the 96-well plate volume was 200 µl per well.

Table 2 NEMP and NIMP inhibition concentrations

Enzyme Source	NEMP Concentrations (µM)	NIMP Concentrations (µM)
Rat RBC AChE	0.003 to 0.054	0.004 to 0.078
Human RBC AChE	0.005 to 0.067	0.012 to 0.183
Rat Plasma AChE	0.067 to 0.207	0.004 to 0.300
Human Plasma AChE	0.067 to 1.130	0.400 to 16.67
Rat Plasma BChE	0.067 to 0.207	0.025 to 0.850
Human Plasma BChE	0.067 to 1.130	0.400 to 16.67
Rat Brain AChE	0.031 to 0.510	0.019 to 0.250
Rat SKM AChE	0.004 to 0.080	0.001 to 0.180

Eight concentrations of NEMP and NIMP were utilized to obtain 10% to 90% inhibition for rat and human AChE and BChE blood sources as displayed in the table below.

For each concentration and control, the velocity of each incubation period was calculated. For each preincubation time, the fraction of AChE or BChE velocity left was calculated by dividing the AChE or BChE velocity following inhibition ($[E]_t$) by the original uninhibited velocity ($[E]_0$) as described in the Equation 2 below.

$$\frac{[E]_t}{[E]_0} = \textit{Ratio of inhibited sample by control sample} \quad (2)$$

Using the linear regression of the natural log (ln) of the $[E]_t/[E]_0$ value as a function of time provided a line at each inhibitor concentration with slope equal to $-k_{app}$ as described with Equation 3 below.

$$\ln \frac{[E]_t}{[E]_0} = -k_{app}t \quad (3)$$

The $-k_{app}$ value was the apparent rate of AChE or BChE phosphorylation. A double reciprocal plot of the k_{app} as a function of the inhibitor concentration, depicted in Figure 7 below, provided a line equation to determine the necessary kinetic values.

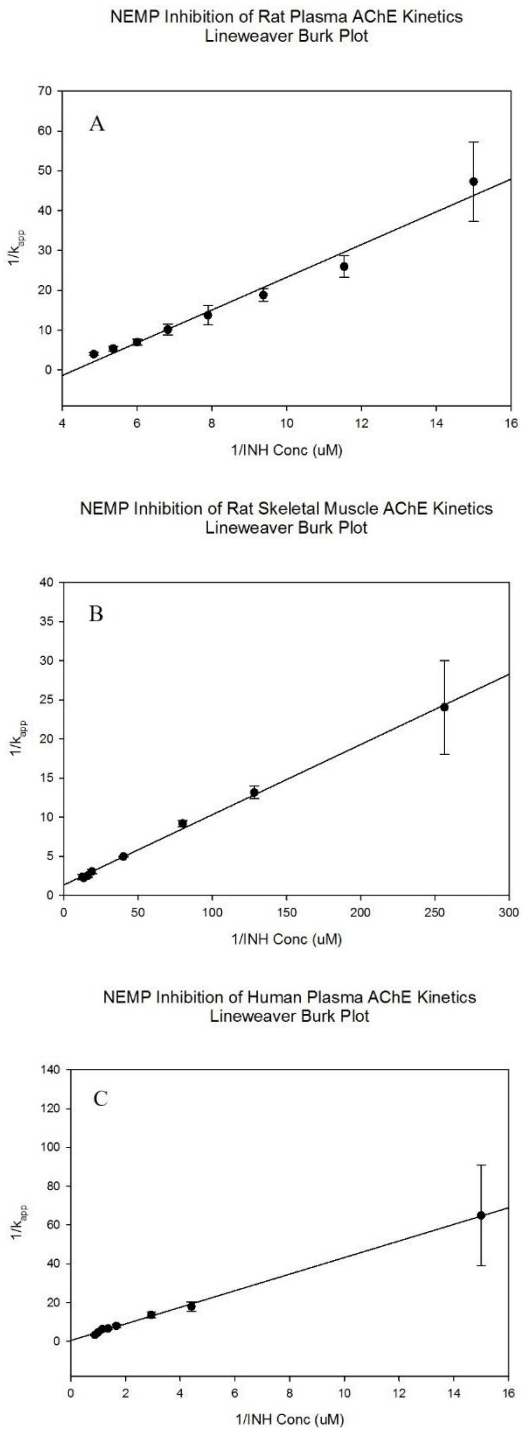

Figure 7 Lineweaver Burk plots for inhibition kinetics

Lineweaver Burk plots used for determination of inhibition kinetics. Represented are NEMP inhibition of (A) rat plasma AChE, (B) rat SKM AChE, and (C) human plasma AChE.

From the line equation the kinetic values are determined with, the slope equal to $1/k_i$, the y-intercept equal to $1/k_p$, and the x-intercept equal to $-K_A$, as seen in Equation 4 below (Segel 1975, Carr and Chambers 1996, Worek, Thiermann et al. 2004).

$$y = mx + b \tag{4}$$

$$Slope\ m = \frac{1}{k_i}$$

$$y - intercept\ = \frac{1}{k_p}$$

$$\text{x}-intercept\ = -K_A$$

Equation 5 below describes the overall reaction and summarizes the basis of the calculations to obtain the necessary kinetic values. Symbols are defined as: [E] is concentration of free enzyme, [I] is concentration of free inhibitor, $[EI]_R$ is the reversible enzyme-inhibitor complex, $[EI]_I$ is the irreversible phosphorylated enzyme-inhibitor complex, and [EI]a is the aged enzyme-inhibitor complex. The reaction rates were previously described. Equation 6 assumes the reaction primarily flows forward with the k_p and not reverse with the k_{-1}. Equation 7 describes the rates associated with inhibition, while Equation 8 demonstrates the relationship between all rates for the reaction scheme. The K_D rate constant was not previously described and represents the dissociation constant between the inhibitor and enzyme.

$$[E] + [I] \underset{k_{-1}}{\overset{k_1}{\leftrightarrow}} [EI]_R \overset{k_p}{\rightarrow} [EI]_I \begin{matrix} \overset{k_r}{\rightarrow} \\ \underset{k_a}{\rightarrow} \end{matrix} \begin{matrix} [E] + [Oxime\ I] \\ [EI]_a \end{matrix} \quad (5)$$

$$\text{Assuming } k_p \ll k_{-1} \quad (6)$$

$$(K_A)(k_p) = k_i \quad (7)$$

$$k_i = (K_A)(k_p) = \frac{k_p}{K_D} = \frac{(k_1)(k_p)}{k_{-1}} \quad (8)$$

AChE and BChE Reactivation Kinetics Procedure

The sample analysis for blood fractions was conducted using a 96-well plate with a final testing volume of 300 µl per well (200 µl per well for rat brain and skeletal muscle). Enzyme activities were inhibited by about 90 percent utilizing an appropriate concentration of NEMP or NIMP. Inhibited erythrocyte AChE and rat brain and skeletal muscle AChE samples were washed two times with the appropriate buffer by centrifugation and removal of supernatant to remove excess inhibitor and then resuspension with buffer. Centrifugation was done at 5 minutes at 5000xg and samples were returned to their original volumes (Eppendorf Centrifuge 5415C, F-45-18-11 rotor). Since AChE and BChE are suspended in the plasma, removing the inhibitor via centrifugation was not possible. To decrease or stop additional inhibition, the plasma was diluted. Pre-testing was done to determine the minimal volume of sample and inhibitor necessary for optimal inhibition, and the minimal dilution necessary to eliminate or reduce further inhibition without compromising overall enzyme activity and subsequent absorbance. The amount of dilution varied by pool of plasma, enzyme being tested (AChE or BChE), or species (rat or human). The inhibited sample was split into five equal portions. To two portions, 30 µl (10 µl for rat brain and skeletal muscle) of

ethanol was added per ml to measure spontaneous reactivation and aging. To three separate portions, oximes were added to measure reactivation, FC 0.3 mM (2-PAM, oxime 44.08, and oxime 44.25). For rat brain and skeletal muscle, oximes were added at FC 0.1 mM. Utilizing the same concentration of chromagen, eserine sulfate, and substrate listed above, kinetic readings were performed at 0, 15, 30, 45, and 60-minute time points by withdrawing a sample from each portion and assaying. At each time point 12 continuous kinetic readings of the 96-well plate were performed and enzyme activity was measured as mentioned above.

Determination of the ratio of AChE (BChE) activity at each time interval was calculated by dividing the AChE (BChE) activity in the inhibited samples by the matching control activity as seen in Equation 9 below (Kitz and Wilson 1962).

$$\frac{[E]_t}{[E]_0} = \textit{Ratio of inhibited sample by control sample} \quad (9)$$

Using the natural log of the ratio of inhibited versus control activity (y-axis) at each time point (x-axis), the various rate constants described below were obtained (k_r, k_s, k_a) with the slope of the best fit line with R^2-value no less than 0.9. All rate constant variables were on the y-axis and the time points were on the x-axis. First order rate constants were calculated from linear regression of the natural log (ln) of the ratio of AChE (BChE) activity as a function of time. Using the vehicle (control) plots, the spontaneous reactivation (s) rate constant, k_s, was estimated from the slope of the line described by Equation 10 below (Kitz and Wilson 1962).

$$\ln \frac{[E]_t}{[E]_0} = k_s t \quad (10)$$

Using the oxime reactivation plots, the oxime reactivation rate (r) constant, k_r, was estimated from the slope of the line described by Equation 11 below (Kitz and Wilson 1962).

$$\ln \frac{[E]_t}{[E]_0} = k_r t \quad (11)$$

Using the oxime reactivation plots from the 2-PAM aging data, the aging rate (a) constant, k_a, was estimated from the slope of the line described by the Equation 12 below (Kitz and Wilson 1962).

$$\ln \left(1 - \frac{[E]_t}{[E]_0}\right) = k_a t \quad (12)$$

Aging was determined by incubating a portion of the inhibited sample with the oxime reactivator 2-PAM at a concentration determined in preliminary experiments to reactivate 100% of AChE(BChE) at each of the set time points (15, 30, 45, and 60 minutes) and calculating if any AChE(BChE) was not reactivated by subtracting from 1. The percent not reactivated was considered the aged AChE(BChE). The difference between the reactivation and aging rate constant provided the true reactivation rate constant.

Statistical Analysis

Data were analyzed using Sigma Plot software on a PC. Blood sample data were analyzed by two-way or three-way ANOVA when appropriate, $p \leq 0.001$. Pairwise comparisons were made with Holm-Sidak method, $p < 0.05$. Rat brain and skeletal muscle data were analyzed by one-way ANOVA when appropriate, $p \leq 0.001$. Pairwise comparisons were made with Holm-Sidak method, $p < 0.05$. All data with comparisons of two values were analyzed with t-test when appropriate, $p < 0.05$. When distribution was not normal and variances were unequal, the data were analyzed nonparametrically with Mann-Whitney Rank Sum Test ($T = 6\text{-}18$, $n_1 = 3$, $n_2 = 3\text{-}4$, $P < 0.05$).

Results

Nerve agent surrogate concentrations needed for AChE and BChE inhibition are presented in Table 3 below. The data demonstrated differences between IC_{50} concentrations of rat and human and NEMP and NIMP. Rat plasma AChE and BChE had significantly lower NEMP and NIMP IC_{50} concentrations compared to their corresponding human AChE and BChE samples. All other rat and human comparison differences were not statistically significant. When comparing NEMP versus NIMP for different specimen types, only half of the specimens demonstrated significant differences. Human plasma AChE and BChE, rat plasma BChE, and rat skeletal muscle AChE demonstrated NIMP IC_{50} concentrations that were significantly higher than corresponding NEMP IC_{50} concentrations.

Table 3 Median inhibition concentrations

Enzyme Source	NEMP IC_{50} (µM)	NIMP IC_{50} (µM)
Rat RBC AChE	0.017 ± 0.001	0.025 ± 0.001
Human RBC AChE	0.020 ± 0.003	0.048 ± 0.002
Rat Plasma AChE	0.149 ± 0.006*	0.082 ± 0.002*
Human Plasma ACHE	0.578 ± 0.047*$^{\Delta}$	2.882 ± 0.014*$^{\Delta}$
Rat Plasma BChE	0.151 ± 0.012*$^{\Delta}$	0.358 ± 0.011*$^{\Delta}$
Human Plasma BChE	0.738 ± 0.060*$^{\Delta}$	2.679 ± 0.039*$^{\Delta}$
Rat Brain AChE	0.116 ± 0.006	0.116 ± 0.011
Rat SKM AChE	0.030 ± 0.001	0.082 ± 0.005$^{\Delta}$

The original concentration ranges from table 2 above were used to calculate the designated median inhibition concentration (IC_{50}) values (mean ± SEM) in Table 3. Data transformation were not necessary due to the linearity of the original data. IC_{50} values were analyzed statistically for differences between human and rat specimens and between nerve agent surrogates NEMP and NIMP. For blood specimens a two-way ANOVA was conducted that examined the effect of species differences and inhibitor type on IC_{50} concentrations. There were statistically significant differences between effects of different species and inhibitor type on IC_{50} concentrations, $F = (1415, 1294) = 546$, $p \leq 0.001$. Pairwise comparisons were made with Holm-Sidak method for all ANOVA analyses. For rat brain and skeletal muscle specimens a two-sided t-test was performed, $p \leq 0.05$, (*) indicates statistically significant differences between rat and human blood specimen types, ($^{\Delta}$) indicates inhibitor, NEMP or NIMP, with a significantly different IC_{50} concentration

Substrate hydrolysis by AChE or BChE was analyzed using V_{max} and K_{mapp} kinetic values as depicted in Table 4 below. The V_{max} for human plasma AChE was significantly higher than the corresponding rat samples, but the p-value was greater than the $p < 0.05$ cutoff ($p = 0.07$). The closeness of the actual p-value to the cutoff, provided support for accepting the difference as significant. The V_{max} for rat plasma BChE was significantly higher than the corresponding human samples.

The K_{mapp} for human erythrocyte AChE and plasma BChE were significantly higher than the corresponding rat samples, but the p-values were greater than the $p < 0.05$ cutoff (both $p = 0.06$). The closeness of the actual p-value to the cutoff, provided support for accepting the difference as significant. The K_{mapp} for rat plasma AChE was significantly higher than the corresponding human sample. All other V_{max} and K_{mapp} comparisons between human and rat blood samples did not indicate significant differences between the species.

Table 4 Substrate Hydrolysis

Enzyme Source	V_{max} (mmol min^{-1} mg $protein^{-1}$)	K_{mapp} (mM)
Rat RBC AChE	0.531 ± 0.077	0.018 ± 0.005*
Human RBC AChE	0.360 ± 0.030	0.104 ± 0.042*
Rat Plasma AChE	0.382 ± 0.036*	0.096 ± 0.009*
Human Plasma AChE	0.634 ± 0.099*	0.031 ± 0.014*
Rat Plasma BChE	0.856 ± 0.083*	0.018 ± 0.002*
Human Plasma BChE	0.164 ± 0.022*	0.077 ± 0.026*
Rat Brain AChE	0.190 ± 0.004	0.148 ± 0.008
Rat SKM AChE	0.190 ± 0.009	0.041 ± 0.002

In vitro ATCh and BTCh hydrolysis respectively by AChE and BChE from human and rat blood, brain and skeletal muscle. For comparing only human and rat blood specimen types a two-sided t-test was performed, n = 3-4, mean ± SEM, $p \leq 0.05$, (*) indicates statistically significant differences between rat and human blood specimen types

Inhibition kinetics of nerve agent surrogates with human and rat AChE and BChE sources are depicted in Table 5 below. The data demonstrated differences in the inhibition kinetic values for rat and human specimens. The K_A values for rat NEMP inhibited erythrocyte AChE and plasma AChE and BChE were significantly higher than the corresponding human K_A values. The K_A value for NIMP inhibited rat erythrocyte AChE was significantly higher than the corresponding human samples. When comparing inhibitors using K_A values, rat plasma AChE and BChE and human erythrocyte AChE had significantly higher values for NEMP versus NIMP (respectively $p = 0.02$, 0.04, 0.006). Rat erythrocyte AChE had K_A values significantly higher for NIMP versus NEMP ($p < 0.001$). All other rat and human blood specimen type comparisons did not have statistically significant differences.

The k_p value differences for all NEMP and NIMP inhibited human and rat specimen types were not statistically significant. When comparing inhibitors using k_p values, rat plasma AChE had significantly higher values for NIMP versus NEMP ($p = 0.002$).

The k_i values for NEMP and NIMP inhibited rat erythrocyte AChE were significantly higher than human erythrocyte AChE. The k_i value for NIMP inhibited rat plasma AChE was significantly higher than human plasma AChE. When comparing k_i values between NEMP and NIMP, rat and human erythrocyte AChE had significantly higher k_i values with NEMP versus NIMP (both $p < 0.001$). The opposite occurred with rat plasma AChE which had significantly higher k_i values with NIMP versus NEMP ($p < 0.001$). Rat brain and skeletal muscle AChE also had significantly higher k_i values with

NEMP versus NIMP (respectively $p = 0.07$ and 0.02). Though the p-value for rat brain AChE was above the $p < 0.05$ cutoff, the close proximity was acceptable.

Table 5 Inhibition

Enzyme Source	NEMP Inhibition			NIMP Inhibition		
	K_A (μM^{-1})	k_p (min^{-1})	k_i (μM^{-1} min^{-1})	K_A (μM^{-1})	k_p (min^{-1})	k_i (μM^{-1} min^{-1})
Rat RBC AChE	13.6 ± 1.46*	0.88 ± 0.09	11.70 ± 0.27*$^{\Delta}$	21.55 ± 1.58*	0.48 ± 0.04	10.10 ± 0.26*$^{\Delta}$
Human RBC AChE	5.77 ± 1.60*	1.69 ± 0.78	7.50 ± 0.86*$^{\Delta}$	2.51 ± 0.23*	0.84 ± 0.07	2.08 ± 0.04*$^{\Delta}$
Rat Plasma AChE	3.81 ± 0.50*	0.08 ± 0.02	0.29 ± 0.03$^{\Delta}$	1.197 ± 0.220	1.73 ± 0.33	1.937 ± 0.068*$^{\Delta}$
Human Plasma AChE	0.20 ± 0.05*	1.33 ± 0.37	0.27 ± 0.06	0.023 ± 0.006	2.18 ± 0.69	0.042 ± 0.005*
Rat Plasma BChE	3.59 ± 0.19*	0.10 ± 0.01	0.36 ± 0.03	1.252 ± 0.224	0.57 ± 0.09	0.672 ± 0.020
Human Plasma BChE	0.15 ± 0.03*	1.14 ± 0.13	0.17 ± 0.02	0.057 ± 0.005	0.67 ± 0.08	0.038 ± 0.002
Rat Brain AChE	2.45 ± 0.08	1.05 ± 0.09	2.56 ± 0.23$^{\Delta}$	2.44 ± 0.14	0.78 ± 0.12	1.86 ± 0.18$^{\Delta}$
Rat SKM AChE	9.51 ± 2.05	1.14 ± 0.26	9.82 ± 0.01$^{\Delta}$	14.47 ± 0.49	0.45 ± 0.05	6.48 ± 0.76$^{\Delta}$

In vitro AChE and BChE inhibition by NEMP or NIMP. For blood specimens a two-way ANOVA was conducted that examined the effect of species differences and inhibitor type on the K_A, k_p, or k_i. There were statistically significant differences between effects of different species and inhibitor type on K_A, k_p, or k_i. For K_A statistic, $F = (0.04, 153) = 15$, $p \leq 0.001$, for k_p statistic $F = (1, 4) = 4$, $p = 0.009$, for k_i statistic, $F = (7, 112) = 9$, $p \leq 0.001$. Pairwise comparisons were made with Holm-Sidak method for all ANOVA analyses, $p \leq 0.05$. For rat brain and skeletal muscle specimens a two-sided t-test was performed, n = 3-4, mean ± SEM, $p \leq 0.05$, (*) indicates statistically significant differences between rat and human blood specimen types, ($^{\Delta}$) indicates inhibitor, NEMP versus NIMP, with a significantly different k_i value

Oxime reactivation kinetics of AChE or BChE inhibited by surrogates are represented in Table 6 and 7 below, respectively NEMP and NIMP. The data demonstrated *in vitro* AChE and BChE inhibition respectively by NEMP or NIMP and subsequent reactivation by various oximes. When comparing rat and human samples, only NEMP inhibited rat plasma AChE reactivated by 2-PAM and oxime 44.08 displayed significantly lower reactivation rates compared to corresponding human specimens. All other differences in rat and human comparisons did not indicate significance.

When comparing oximes, nearly all comparisons between oximes were not significantly different among the various rat and human enzyme sources. One exception was NIMP inhibited human erythrocyte AChE where 2-PAM had significantly higher reactivation rates compared to oxime 44.08. The other exception was NEMP and NIMP inhibited rat brain AChE where 2-PAM had significantly higher reactivation rates compared to oxime 44.08 and 44.25. When looking at overall oxime comparisons utilizing all the NEMP and NIMP inhibited rat and human blood sample data, 2-PAM had significantly higher reactivation rates versus oxime 44.08 and oxime 44.25 ($p = 0.004$). When using the same data, no significant differences were seen between oxime 44.08 and oxime 44.25 ($p = 0.199$). When looking at NEMP and NIMP inhibited rat brain AChE alone, 2-PAM had significantly higher reactivation rates versus oxime 44.08 and 44.25 ($p < 0.001$). When looking at NEMP and NIMP inhibited rat skeletal muscle AChE alone, there were no statistically significant differences between the oximes. In addition, NIMP inhibited rat erythrocyte AChE demonstrated 2-PAM had significantly higher reactivation rates versus oxime 44.08.

When comparing NEMP versus NIMP in terms of reactivation rates of the oximes for only the blood samples, significant differences were seen with 2-PAM which had significantly higher reactivation rates for NEMP versus NIMP ($p = 0.02$). Oximes 44.08 and 44.25 had significantly higher reactivation rates for NIMP versus NEMP (respectively $p = 0.01$ and $p = 0.03$). When looking at rat brain AChE alone, NEMP had significantly higher reactivation rates for all the oximes versus NIMP ($p < 0.001$). When looking at rat skeletal muscle AChE alone, NIMP had significantly higher reactivation rates for all the oximes versus NEMP ($p < 0.001$).

When comparing differences between oximes for all blood samples, rat plasma BChE demonstrated oxime 44.25 had significantly lower reactivation rates versus 2-PAM ($p = 0.02$). For rat and human erythrocyte AChE oxime 44.25 had significantly higher reactivation rates versus oxime 44.08 and lower reactivation rates versus 2-PAM (respectively $p = 0.004$, 0.016 for rat and $p = 0.001$, 0.003 for human).

Aging and spontaneous reactivation of AChE or BChE inhibited by surrogates are depicted in Table 6 and 7 below, respectively NEMP and NIMP. The data demonstrated *in vitro* AChE and BChE inhibition by NEMP or NIMP and subsequent aging and spontaneous reactivation over an hour time frame. All NEMP and NIMP inhibited rat and blood samples had aging and spontaneous reactivation rates that were not significantly different than corresponding human blood samples, except for NEMP inhibited rat plasma AChE which had a significantly lower spontaneous reactivation rate compared to the corresponding human plasma AChE ($p < 0.001$).

Table 6 NEMP Inhibition and Oxime Reactivation

NEMP					
Enzyme Source	k_r (min^{-1})			k_a (min^{-1})	k_s (min^{-1})
	2-PAM	Oxime 44.08	Oxime 44.25	Aging	Spontaneous Reactivation
Rat RBC AChE	0.042 ± 0.001	0.037 ± 0.002	0.041 ± 0.002	0.0085 ± 0.0004	0.0030 ± 0.0019
Human RBC AChE	0.045 ± 0.004	0.042 ± 0.005	0.043 ± 0.005	0.0093 ± 0.0003	0.0040 ± 0.0017
Rat Plasma AChE	0.029 ± 0.005*	0.025 ± 0.004*	0.025 ± 0.005	0.0074 ± 0.0006	0.0005 ± 0.0002*
Human Plasma AChE	0.048 ± 0.007*	0.044 ± 0.006*	0.040 ± 0.005	0.0082 ± 0.0005	0.0077 ± 0.0006*
Rat Plasma BChE	0.028 ± 0.002	0.019 ± 0.001	0.018 ± 0.002	0.0077 ± 0.0008	0.0016 ± 0.0009
Human Plasma BChE	0.042 ± 0.004	0.035 ± 0.005	0.030 ± 0.004	0.0056 ± 0.0014	0.0033 ± 0.0014
Rat Brain AChE	0.060 ± 0.003^{P}	0.046 ± 0.003 ^{P}	0.041 ± 0.003 ^{P}	0.0071 ± 0.0003	0.0009 ± 0.0001
Rat SKM AChE	0.025 ± 0.002	0.021 ± 0.002	0.022 ± 0.002	0.0066 ± 0.0002	0.0004 ± 0.0002

In vitro AChE and BChE inhibition by NEMP and reactivation by various oximes. For blood specimens a three-way ANOVA was conducted that examined the effect of species differences, different oximes, and different inhibitor types on the k_r. There were statistically significant differences between effects of different species, oximes, and inhibitor on k_r. $F = (14, 10, 0.07) = 0.2$, $p \leq 0.001$. Pairwise comparisons were made with Holm-Sidak method for all ANOVA analyses when indicated, $p \leq 0.05$. For rat brain and skeletal muscle specimens a one-way ANOVA was conducted comparing oximes, $F = 19$, $p \leq 0.003$. For k_a and k_s values for rat and human blood specimens a two-sided t-test was performed, n = 3-4, mean ± SEM, $p \leq 0.05$, (*) indicates statistically significant differences between rat and human blood specimen types, (^{P}) indicates significant difference between 2-PAM and one or both of the novel oximes as indicated

Table 7 NIMP Inhibition and Oxime Reactivation

NIMP					
Enzyme Source	k_r (min^{-1})			k_a (min^{-1})	k_s (min^{-1})
	2-PAM	Oxime 44.08	Oxime 44.25	Aging	Spontaneous Reactivation
Rat RBC AChE	0.040 ± 0.002	0.032 ± 0.003	0.039 ± 0.002	0.0084 ± 0.0001	0.0020 ± 0.0007
Human RBC AChE	0.036 ± 0.001^{P}	0.025 ± 0.002 ^{P}	0.033 ± 0.002^{P}	0.0089 ± 0.0008	0.0017 ± 0.0005
Rat Plasma AChE	0.034 ± 0.003	0.026 ± 0.005	0.030 ± 0.004	0.0084 ± 0.0002	0.0006 ± 0.0001
Human Plasma AChE	0.042 ± 0.004	0.033 ± 0.001	0.040 ± 0.004	0.0089 ± 0.0003	0.0003 ± 0.0001
Rat Plasma BChE	0.037 ± 0.002	0.027 ± 0.002	0.032 ± 0.001	0.0083 ± 0.0001	0.0012 ± 0.0003
Human Plasma BChE	0.043 ± 0.004	0.040 ± 0.004	0.038 ± 0.004	0.0091 ± 0.0004	0.0065 ± 0.0027
Rat Brain AChE	0.041 ± 0.001^{P}	0.026 ± 0.001^{P}	0.026 ± 0.001 ^{P}	0.0006 ± 0.0005	0.0005 ± 0.0001
Rat SKM AChE	0.034 ± 0.002	0.030 ± 0.002	0.033 ± 0.002	0.0006 ± 0.0002	0.0081 ± 0.0001

In vitro AChE and BChE inhibition by NIMP and reactivation by various oximes. For blood specimens a three-way ANOVA was conducted that examined the effect of species differences, different oximes, and different inhibitor types on the k_r. There were statistically significant differences between effects of different species, oximes, and inhibitor on k_r. $F = (14, 10, 0.07) = 0.2$, $p \leq 0.001$. Pairwise comparisons were made with Holm-Sidak method for all ANOVA analyses, $p \leq 0.05$. For rat brain and skeletal muscle specimens a one-way ANOVA was conducted comparing oximes, $F = 132$, $p \leq 0.001$. For k_a and k_s values for rat and human blood specimens a two-sided t-test was performed, $n = 3$-4, mean ± SEM, $p \leq 0.05$, (*) indicates statistically significant differences between rat and human blood specimen types, (^{P}) indicates significant difference between 2-PAM and one or both of the novel oximes as indicated

Discussion

The data demonstrated important differences between rat blood AChE and BChE versus human blood AChE and BChE when inhibited with NEMP and NIMP, and subsequent reactivation with 2-PAM and novel oximes.

NEMP and NIMP inhibitory concentrations: For half of the enzyme sources the NIMP IC_{50} concentrations were higher compared to the NEMP concentrations. This indicates that the VX surrogate is more potent than the sarin surrogate for these conditions and sample types. This is consistent with the potency of real sarin and VX, where VX is also more potent than sarin when tested against human erythrocyte AChE (Worek, Thiermann et al. 2004). The data also supported previous observations published for NEMP and NIMP, where NEMP is also more potent than NIMP (Meek, Chambers et al. 2012).

Human plasma AChE and BChE sources had greater NEMP and NIMP IC_{50} concentrations compared to corresponding rat plasma AChE and BChE sources. This is an important observation when considering nerve agent surrogate dosing in rat models and expectations in human modeling. This indicates rat samples may be more sensitive to NEMP and NIMP versus humans which suggests that the rat information may be conservative for human predictions. This could partly be explained by published research data that demonstrated rat blood AChE activity is double the activity observed in the rat brain (Habila, Inuwa et al. 2012). This may suggest that there are larger AChE concentrations in the rat blood and therefore proportionally larger AChE concentrations in the human blood. In addition, the variations in concentration may be associated with the balance of AChE and BChE in the blood and the variability in binding affinity of

AChE and BChE (Juul 1968). Another difference to consider between species is the ChE activity differences between rat males and females. Researchers have demonstrated higher concentrations of BChE in humans versus rat males (2x) and females (6x) (Ecobichon and Comeau 1973).

Substrate kinetics: The data on substrate kinetics provided further insight into what NEMP and NIMP concentration differences there are between rat and human AChE and BChE sources. The differences seen in the necessary inhibitory concentrations of NEMP and NIMP, and the variability among species kinetic rates may be a result of the composition of the AChE and BChE present in rat and human blood and rat brain and skeletal muscle. Researchers have identified 12 ChE isoenzymes which catalyze the same reaction but differ in their chemical properties or amino acid sequence (Juul 1968, Wilkinson 1970). The identified ChE isoenzymes were characterized into three components of AChE or BChE, defined by their binding affinity (low, medium, and high), in a variety of blood and solid tissues which can play a role in K_{mapp} and V_{max} values (Juul 1968, Dave, Syal et al. 2000). In human serum, there are three components of BChE present with different binding affinities versus the two components in rat serum. In this case the rat serum is missing the high-affinity component. It is reasonable to think that having more components equates to greater binding affinity or a lower K_{mapp}, but composition alone may not define binding affinity fully. The concentration of the components could also play a role and provide further variability between species. This latter explanation could account for the higher K_{mapp} value in human plasma BChE when a lower K_{mapp} would be expected compared to the corresponding rat values. In this case,

the more components of human plasma BChE with a broader affinity spectrum did not translate to a stronger BChE binding affinity.

Human erythrocytes have two components of AChE present versus the three components in rat erythrocytes (Juul 1968, Dave, Syal et al. 2000). In this case the human plasma is missing the mid-affinity component. In the current experiment, the human erythrocyte AChE maintains a higher K_{mapp} value compared to the corresponding rat values, despite missing a component. So again the concentration of each component may play a role in overall binding affinity and therefore K_{mapp}. There is no research data identifying the composition of plasma AChE, but since rat plasma AChE has a higher K_{mapp} value, then the human plasma may be missing the high affinity component. The composition makeup and concentration of the components for the analyzed specimens could provide further insight into the observations seen.

Binding affinity may also be affected by the size of the active site gorge, where AChE is more narrow and BChE is larger (Pohanka 2014). The later could allow for greater interactions with a variety of compounds and therefore increased affinity through increased interactions (Masson and Lockridge 2010). Kinetic research conducted on human plasma BChE and erythrocyte AChE, demonstrated lower K_{mapp} values for plasma BChE versus erythrocyte AChE (Kato, Hashimoto et al. 2000). The current study demonstrates the same finding for rat plasma AChE and BChE where the latter has a lower K_{mapp} value ($p < 0.05$).

The K_{mapp} value for human erythrocyte AChE was determined to be 0.10 mM, which was similar to published data of 0.18 mM and 0.08 mM (Ciliv and özand 1972, Kamal, Greig et al. 2000). The K_{mapp} value for human serum BChE was determined to be

0.1 mM, which was similar to published data of 0.1 and 0.2 mM (Simeon-Rudolf, Reiner et al. 1999). The K_{mapp} value for rat brain AChE was determined to be 0.148 mM, which was similar to the published data of 0.110 mM and 0.055 mM, and also similar to rat heart AChE 0.100 mM (Moss and Fahrney 1978, Watts and Hoogmoed 1984, Carr and Chambers 1996). The other sources of AChE and BChE did not have any published values. Overall the affinity compositions of human and rat AChE and BChE can be useful tools in defining the differences seen in inhibition and reactivation since V_{max} and K_{mapp} are important factors in the calculation of these kinetic values (Carr and Chambers 1996, Worek, Thiermann et al. 2004).

Inhibition Kinetics of AChE and BChE: The comparison between rat and human blood continues by looking at the bimolecular rate constant, which is defined here by the k_i. The k_i describes the inhibitory power of the nerve agent surrogates NEMP and NIMP. The k_i is determined by the binding affinity of the compound, defined as K_A, and the rate of phosphorylation, defined by k_p. The best inhibitory rate is therefore defined by a strong K_A value and a fast k_p rate (Coban, Carr et al. 2016).

In the inhibition experiments, the significant data for rat blood AChE sources had faster rates of inhibition (k_i) and therefore were more sensitive to inhibition by NEMP and NIMP compared to their corresponding human samples. OP experiments with paraoxon-inhibited rat and human plasma BChE also demonstrated the greater sensitivity of rats versus humans (Ecobichon and Comeau 1973). The current data demonstrated differences in BChE specimens of rats versus humans, but they were not statistically significant.

Considering the significant data, the more sensitive rat AChE and BChE were also supported with stronger enzyme affinity, K_A, as data demonstrated higher values compared to the corresponding human K_A values. Faster k_p values were seen for the human blood data versus the corresponding rat blood data, but the differences were insignificant. The discrepancy in k_p has been shown by researchers to be a result of the lesser role of phosphorylation versus binding affinity, where correlation with k_i is much stronger with the binding affinity K_A (Coban, Carr et al. 2016). In this experiment, the lack of significance may indicate such a case where k_p values have a lesser effect on the k_i value versus the K_A.

A direct comparison between NEMP and NIMP inhibition potency can also be made with the inhibition kinetics data. Researchers have demonstrated with human erythrocyte AChE that inhibition rates for VX are greater than for sarin, making the former a more potent inhibitor (Worek, Thiermann et al. 2004, Coban, Carr et al. 2016). This was also observed in the data with significant comparisons, NEMP demonstrated greater inhibitory rates compared to NIMP for rat and human erythrocyte AChE and rat brain and skeletal muscle AChE. Literature on rat plasma AChE and BChE inhibition kinetics was not available. As previously mentioned, the absence of significance for some of the specimen sources may be a result of the variability in AChE and BChE enzyme isomer types and concentrations present in the specimen sources (Lenz and Maxwell 1981, Chatonnet and Lockridge 1989).

The active site of AChE and BChE is highly conserved genetically between species, but the size of the active site gorge can vary considerably and may also play a role in AChE and BChE differences as mentioned previously (Chatonnet and Lockridge

1989, Masson and Lockridge 2010). Four polymorphisms of AChE have been identified with only two being of clinical significance and may also account for differences (Hasin, Avidan et al. 2005). One polymorphism is a glucocorticoid response element that is related to increased OP sensitivity and the other is Asn substitution of His322 that is responsible in blood typing and donor matching (Bartels, Zelinski et al. 1993, Ehrlich, Ginzberg et al. 1994). BChE polymorphisms have also been identified and could explain species differences as well (Primo-Parmo, Bartels et al. 1996, Souza, Mikami et al. 2005).

The chemical structure of the inhibitors can also influence the inhibition kinetic values as demonstrated by many researchers (Worek, Thiermann et al. 2004). Research has confirmed that small changes to alkyl residues on OPs and stereoisomers of OPs can have substantial effects on k_i (Worek, Thiermann et al. 2004). The alterations of the nerve agent surrogates to make them less potent than the original agent could account for some of the differences seen in the data.

Oxime Reactivation Kinetics of Surrogate Inhibited AChE and BChE: The reactivation data provided important information about differences between oxime reactivation of inhibited rat and human blood AChE and BChE. The data also defined differences between NEMP and NIMP. In addition, the data provided informative insight into which of the novel oximes were most effective against nerve agent surrogate inhibited AChE and BChE.

In terms of comparing rat and human reactivation of NEMP and NIMP inhibited AChE and BChE, there were only a couple differences. NEMP inhibited human plasma AChE had significant differences in reactivation rates for 2-PAM and oxime 44.08 when

compared to the corresponding rat plasma AChE. All other direct comparisons did not indicate significant differences.

Interesting observations were also seen between the current research data and the literature. Researchers have demonstrated sarin-inhibited human erythrocyte AChE had greater 2-PAM reactivation rates versus VX, while sarin and VX-inhibited rat erythrocyte AChE had similar 2-PAM reactivation rates (Worek, Reiter et al. 2002). The current research data demonstrated that 2-PAM had greater reactivation rates for NEMP (the VX surrogate) versus NIMP (the sarin surrogate). The novel oximes 44.08 and 44.25 had opposite results with NIMP having greater reactivation rates than NEMP. Published rat brain and skeletal muscle data were not available, but the current experiments demonstrated NEMP inhibited rat brain AChE had reactivation rates that were greater than NIMP for all the oximes. Rat skeletal muscle AChE had opposite results with NIMP demonstrating greater reactivation rates compared to NEMP for all the oximes. Noting differences in reactivation rates between rat skeletal muscle and brain towards NEMP and NIMP would be important when considering effects seen in the rat model.

The same researchers have also observed VX-inhibited human erythrocyte AChE had greater 2-PAM reactivation rates versus their corresponding rat specimens, while sarin-inhibited rat erythrocyte AChE had greater 2-PAM reactivation rates versus their corresponding human specimens (Worek, Reiter et al. 2002). The current research demonstrates for NEMP inhibited human plasma AChE that 2-PAM and oxime 44.08 have significantly greater reactivation rates versus corresponding rat plasma AChE. All other blood samples did not indicate significant differences between rat and human

samples. This observation means that the rat reactivation data could be more conservative versus a human model, so less oxime may be required for humans.

Researchers have also demonstrated that OP reactivation rates for rat brain AChE is lower versus human erythrocyte AChE at lower concentrations (Lugokenski, Gubert et al. 2012). This was not the case in the current experiment, but various concentrations of inhibitor were not tested. In addition, direct comparison of blood and brain AChE can be questionable due to the variations in tissue components and therefore was not analyzed statistically for the current analysis.

Differences between the current results and the published literature may be due to the, previously mentioned, variations of binding affinity seen with the different compositions of AChE and BChE observed with the plasma and membrane bound enzymes (Juul 1968, Dave, Syal et al. 2000). The affinity of AChE or BChE could translate to variations in susceptibility to inhibition as suggested by some researchers performing rat brain soman-inhibited AChE experiments on isoenzymes (Lenz and Maxwell 1981). This could explain the differences seen between membrane bound versus plasma solubilized enzyme in the current experiments as well. In addition, the chemical structure of the oxime and the interaction with the phosphylated enzyme plays a major role in the observed differences seen. The individual isoenzymes would need to be explored to pinpoint actual effects on oxime reactivation and the other kinetic values.

The data also demonstrated where Oxime 44.08 and Oxime 44.25 fit in terms of reactivation rates versus the most commonly used oxime antidote, 2-PAM, as the reference. The current data in conjunction with data from other researchers also helped predict overall rankings among the most common oximes used throughout the world. In

terms of the specific oxime reactivation only 3 out of the 16 available blood and brain and skeletal muscle sources indicated significant differences between the various oximes. These 3 enzyme sources (NIMP inhibited human erythrocyte AChE and NIMP and NEMP inhibited rat brain AChE) demonstrated that 2-PAM had significantly greater reactivation rates compared to oxime 44.08 and oxime 44.25. In addition, the overall blood data demonstrated 2-PAM had significantly greater reactivation rates versus oxime 44.08 and 44.25. Current literature demonstrates the best oxime for sarin and VX-inhibited erythrocyte AChE reactivation is obidoxime, followed by HLö 7, then HI 6, and lastly 2-PAM (Worek, Reiter et al. 2002). The obidoxime reactivation rate is around 4 times greater than 2-PAM, while HI 6 is slightly better than 2-PAM. This places oxime 44.08 and oxime 44.25 behind 2-PAM when considering the overall ranking of the oximes. When comparing oxime 44.08 and 44.25 there are no significant data to distinguish the two oximes, so the oximes are probably similar. The variability of reactivation by different oximes has been explored previously by many researchers (Worek, Thiermann et al. 2004). Further exploration into the acidity of the oximes, the position of the oxime group on the pyridinium ring, and the orientation of the oxime could help further define the effectiveness of the novel oximes for reactivation of organophosphate-inhibited enzymes (de Jong, Verhagen et al. 1989, Worek, Thiermann et al. 2004).

Aging and spontaneous reactivation of AChE and BChE: In this experimental design, the spontaneous reactivation and aging rates provided a point of reference for possible effects on inhibition and reactivation rates. In this case the effect was negligible,

but a few observations confirmed findings of other researchers in regards to OP and AChE or BChE interactions.

The longer aging of sarin was also observed in the clinical treatment records of the Tokyo subway casualties where many of the exposed had fully recoverable AChE (Yanagisawa, Morita et al. 2006, Masson and Lockridge 2010). Researchers have also shown that aging of VX-inhibited human AChE and BChE can be restored to 70% activity after 48 hours with 2-PAM treatment (Li, Schopfer et al. 2007). The same research has also demonstrated negligible aging of VX-inhibited human BChE after 28 hours. Researchers performing kinetic analysis on rat and human blood with methamidophos-inhibited AChE ghost and plasma BChE observed insignificant spontaneous reactivation, supporting the findings of this study (Lugokenski, Gubert et al. 2012). Research on cyclosarin-inhibited human erythrocyte AChE and plasma BChE, demonstrated that BChE aged at a faster rate than AChE (Worek, Eyer et al. 1998). This was also observed in the data for NIMP and NEMP inhibited human erythrocyte AChE and plasma AChE and BChE, where the BChE aging was at a higher rate but the difference was not significant. The opposite was observed with the corresponding rat specimens, but the differences were also not significant. The overall observations would be important when considering rat and human models and looking at extended exposures where spontaneous reactivation and aging are measurable for most OP exposures except for soman which ages quickly with AChE and BChE inhibition (Carletti, Li et al. 2008, Carletti, Aurbek et al. 2009, Carletti, Colletier et al. 2010).

In the experiment from the literature, the aging and spontaneous reaction was observed over many hours, so the significance of the current data could be associated to

the hour time frame of the testing. This hour time frame is suitable for all kinetic rate determinations except for spontaneous reactivation and aging which is best seen when tested periodically over 20 to 48 hours on average (Carr and Chambers 1996, Worek, Eyer et al. 1998, Li, Schopfer et al. 2007). Extending the time frame for aging and spontaneous reactivation could make the observed differences more statistically significant.

Conclusion

In general, nearly all IC_{50} concentrations of NIMP were higher than NEMP. In addition, human IC_{50} values were greater than corresponding rat IC 50 values. This indicates rat samples may be more sensitive to NEMP and NIMP versus humans which suggests that the rat information may be conservative for human predictions. Together these are important observations when considering nerve agent surrogate dosing in the laboratory rat model and expectations in human exposures. The k_i values in rats were overall greater than humans for this experiment which supports published materials (Coban, Carr et al. 2016). The overall reactivation data suggests that 2-PAM is a significantly greater reactivator for NEMP and NIMP compared to the novel oximes, but the combined rat and human reactivation data only demonstrated 3 out of 16 specimen types where the oximes were significantly different from each other. This suggests the novel oximes may be comparable to 2-PAM in potential efficacy. In addition, reactivation rate differences between the species for the various oximes were significantly different for NEMP inhibited plasma AChE. In the cases where the species did have significant differences, the humans had greater reactivation rates compared to rats. This indicates that rats may be more conservative to reactivation by the oximes

versus humans, so human dosages would need to be less. Spontaneous reactivation and aging rates were negligible, but correlated with findings of published research (Li, Schopfer et al. 2007, Lugokenski, Gubert et al. 2012). What could account for the observed differences? Researchers suggest isoenzyme variations between rat and human AChE and BChE could play a role, and AChE and BChE active site gorge size differences could also account for variations, and oxime chemical structure can make a difference (Juul 1968, Dave, Syal et al. 2000, Worek, Thiermann et al. 2004, Masson and Lockridge 2010). In summary, the humans may require more nerve agent surrogate to experience the same inhibition as rats. Also when administering novel oximes, the faster human reactivation rates may indicate less oxime is required versus rats. The overall data provide important information for extrapolating what to expect in human models when obtaining rat model experimental results for the novel oximes and nerve agent surrogates tested. The next step would be to create a pharmacokinetic model using the kinetic values.

References

Bartels, C. F., T. Zelinski and O. Lockridge (1993). "Mutation at codon 322 in the human acetylcholinesterase (ACHE) gene accounts for YT blood group polymorphism." American Journal of Human Genetics **52**(5): 928-936.

Carletti, E., N. Aurbek, E. Gillon, M. Loiodice, Y. Nicolet, J.-C. Fontecilla-Camps, P. Masson, H. Thiermann, F. Nachon and F. Worek (2009). "Structure–activity analysis of aging and reactivation of human butyrylcholinesterase inhibited by analogues of tabun." Biochemical Journal **421**(1): 97-106.

Carletti, E., H. Li, B. Li, F. Ekström, Y. Nicolet, M. Loiodice, E. Gillon, M. T. Froment, O. Lockridge and L. M. Schopfer (2008). "Aging of cholinesterases phosphylated by tabun proceeds through O-dealkylation." Journal of the American Chemical Society **130**(47): 16011-16020.

Carletti, E. n., J.-P. Colletier, F. Dupeux, M. Trovaslet, P. Masson and F. Nachon (2010). "Structural evidence that human acetylcholinesterase inhibited by tabun ages through O-dealkylation." Journal of medicinal chemistry **53**(10): 4002-4008.

Carr, R. L. and J. E. Chambers (1996). "Kinetic analysis of the *in vitro* inhibition, aging, and reactivation of brain acetylcholinesterase from rat and channel catfish by paraoxon and chlorpyrifos-oxon." Toxicol Appl Pharmacol **139**(2): 365-373.

Chambers, J. E., H. W. Chambers, E. C. Meek and R. B. Pringle (2013). "Testing of novel brain-penetrating oxime reactivators of acetylcholinesterase inhibited by nerve agent surrogates." Chem Biol Interact **203**(1): 135-138.

Chatonnet, A. and O. Lockridge (1989). "Comparison of butyrylcholinesterase and acetylcholinesterase." Biochemical Journal **260**(3): 625-634.

Ciliv, G. and P. T. özand (1972). "Human erythrocyte acetylcholinesterase purification, properties and kinetic behavior." Biochimica et Biophysica Acta (BBA) - Enzymology **284**(1): 136-156.

Coban, A., R. L. Carr, H. W. Chambers, K. O. Willeford and J. E. Chambers (2016). "Comparison of inhibition kinetics of several organophosphates, including some nerve agent surrogates, using human erythrocyte and rat and mouse brain acetylcholinesterase." Toxicology Letters **248**: 39-45.

Dave, K. R., A. R. Syal and S. S. Katyare (2000). "Tissue cholinesterases. A comparative study of their kinetic properties." Z Naturforsch C **55**(1-2): 100-108.

de Jong, L. P., M. A. Verhagen, J. P. Langenberg, I. Hagedorn and M. Loffler (1989). "The bispyridinium-dioxime HLo-7. A potent reactivator for acetylcholinesterase inhibited by the stereoisomers of tabun and soman." Biochem Pharmacol **38**(4): 633-640.

Dodge, J. T., C. Mitchell and D. J. Hanahan (1963). "The preparation and chemical characteristics of hemoglobin-free ghosts of human erythrocytes." Arch Biochem Biophys **100**: 119-130.

Ecobichon, D. J. and A. M. Comeau (1973). "Pseudocholinesterases of mammalian plasma: Physicochemical properties and organophosphate inhibition in eleven species." Toxicology and Applied Pharmacology **24**(1): 92-100.

Ehrlich, G., D. Ginzberg, Y. Loewenstein, D. Glick, B. Kerem, S. Ben-Ari, H. Zakut and H. Soreq (1994). "Population Diversity and Distinct Haplotype Frequencies Associated with ACHE and BCHE Genes of Israeli Jews from Trans-caucasian Georgia and from Europe." Genomics **22**(2): 288-295.

Ellman, G., K. Courtney, V. Andres and R. Featherstone (1960). "A new and rapid colorimetric determination of acetylcholinesterase activity." Biochemical Pharmacology **7**.

Eyer, P., L. Szinicz, H. Thiermann, F. Worek and T. Zilker (2007). "Testing of antidotes for organophosphorus compounds: experimental procedures and clinical reality." Toxicology **233**(1-3): 108-119.

Habila, N., H. M. Inuwa, I. A. Aimola, O. I. Lasisi, D. G. Chechet and I. A. Okafor (2012). "Correlation of acetylcholinesterase activity in the brain and blood of wistar rats acutely infected with Trypanosoma congolense." Journal of Acute Disease **1**(1): 26-30.

Hasin, Y., N. Avidan, D. Bercovich, A. D. Korczyn, I. Silman, J. S. Beckmann and J. L. Sussman (2005). "Analysis of genetic polymorphisms in acetylcholinesterase as reflected in different populations." Curr Alzheimer Res **2**(2): 207-218.

Hofstee, B. H. (1959). "Non-inverted versus inverted plots in enzyme kinetics." Nature **184**: 1296-1298.

Juul, P. (1968). "Human plasma cholinesterase isoenzymes." Clinica Chimica Acta **19**(2): 205-213.

Kamal, M. A., N. H. Greig, A. S. Alhomida and A. A. Al-Jafari (2000). "Kinetics of human acetylcholinesterase inhibition by the novel experimental alzheimer therapeutic agent, tolserine." Biochemical Pharmacology **60**(4): 561-570.

Kato, M., Y. Hashimoto, T. Horinouchi, T. Ando, J. Ito and H. Yamanaka (2000). "Inhibition of human plasma cholinesterase and erythrocyte acetylcholinesterase by nondepolarizing neuromuscular blocking agents." J Anesth **14**(1): 30-34.

Kitz, R. and I. B. Wilson (1962). "Esters of methanesulfonic acid as irreversible inhibitors of acetylcholinesterase." J Biol Chem **237**: 3245-3249.

Lenz, D. E. and D. M. Maxwell (1981). "Inhibition of rat cerebrum acetylcholinesterase isoenzymes after acute administration of soman." Biochemical Pharmacology **30**(11): 1369-1371.

Li, H., L. M. Schopfer, F. Nachon, M.-T. Froment, P. Masson and O. Lockridge (2007). "Aging Pathways for Organophosphate-Inhibited Human Butyrylcholinesterase, Including Novel Pathways for Isomalathion, Resolved by Mass Spectrometry." Toxicological Sciences **100**(1): 136-145.

Lugokenski, T. H., P. Gubert, D. C. Bueno, P. A. Nogara, R. de Aquino Saraiva, R. P. Barcelos, V. S. Carratu, L. Bresolin, N. B. de Vargas Barbosa, M. E. Pereira, J. B. da Rocha and F. A. Soares (2012). "Effect of different oximes on rat and human cholinesterases inhibited by methamidophos: a comparative *in vitro* and *in silico* study." Basic Clin Pharmacol Toxicol **111**(6): 362-370.

Masson, P. and O. Lockridge (2010). "Butyrylcholinesterase for protection from organophosphorus poisons; catalytic complexities and hysteretic behavior." Archives of biochemistry and biophysics **494**(2): 107.

Meek, E. C., H. W. Chambers, A. Coban, K. E. Funck, R. B. Pringle, M. K. Ross and J. E. Chambers (2012). "Synthesis and *in vitro* and *in vivo* inhibition potencies of highly relevant nerve agent surrogates." Toxicol Sci **126**(2): 525-533.

Moss, D. E. and D. Fahrney (1978). "Kinetic analysis of differences in brain acetylcholinesterase from fish or mammalian sources." Biochemical Pharmacology **27**(23): 2693-2698.

Parasuraman, S., R. Raveendran and R. Kesavan (2010). "Blood sample collection in small laboratory animals." Journal of Pharmacology & Pharmacotherapeutics **1**(2): 87-93.

Pohanka, M. (2014). "Inhibitors of Acetylcholinesterase and Butyrylcholinesterase Meet Immunity." International Journal of Molecular Sciences **15**(6): 9809-9825.

Primo-Parmo, S. L., C. F. Bartels, B. Wiersema, A. F. van der Spek, J. W. Innis and B. N. La Du (1996). "Characterization of 12 silent alleles of the human butyrylcholinesterase (BCHE) gene." American Journal of Human Genetics **58**(1): 52-64.

Segel, I. H. (1975). "Enzyme Kinetics: Behavior and Analysis of Rapid Equilibrium and Steady-State Enzyme Systems." Wiley, New York. pp. 14, 25-53, 100-108, 132-133, 208-218.

Simeon-Rudolf, V., E. Reiner, R. T. Evans, P. M. George and H. C. Potter (1999). "Catalytic parameters for the hydrolysis of butyrylthiocholine by human serum butyrylcholinesterase variants." Chem Biol Interact **119-120**: 165-171.

Souza, R. L. R., L. R. Mikami, R. O. B. Maegawa and E. A. Chautard-Freire-Maia (2005). "Four new mutations in the BCHE gene of human butyrylcholinesterase in a Brazilian blood donor sample." Molecular Genetics and Metabolism **84**(4): 349-353.

Thiermann, H., K. Kehe, D. Steinritz, J. Mikler, I. Hill, T. Zilker, P. Eyer and F. Worek (2007). "Red blood cell acetylcholinesterase and plasma butyrylcholinesterase status: important indicators for the treatment of patients poisoned by organophosphorus compounds." Arh Hig Rada Toksikol **58**(3): 359-366.

Valiveti, A. K., U. M. Bhalerao, J. Acharya, H. N. Karade, B. N. Acharya, G. Raviraju, A. K. Halve and M. P. Kaushik (2015). "Synthesis and *in vitro* kinetic evaluation of N-thiazolylacetamido monoquaternary pyridinium oximes as reactivators of sarin, O-ethylsarin and VX inhibited human acetylcholinesterase (hAChE)." Bioorganic & Medicinal Chemistry **23**(15): 4899-4910.

Voet, D. and J. G. Voet (2011). Biochemistry. Hoboken, NJ, John Wiley & Sons. pp. 487-497.

Watts, J. A. and R. P. Hoogmoed (1984). "Dimethyl sulfoxide: Inhibition of acetylcholinesterase in the mammalian heart." Biochemical Pharmacology **33**(3): 365-369.

Wilkinson, J. H. (1970). Isoenzymes. Philadelphia,, Lippincott. pp. 733-739.

Worek, F., P. Eyer and L. Szinicz (1998). "Inhibition, reactivation and aging kinetics of cyclohexylmethylphosphonofluoridate-inhibited human cholinesterases." Arch Toxicol **72**(9): 580-587.

Worek, F., P. Eyer and L. Szinicz (1998). "Inhibition, reactivation and aging kinetics of cyclohexylmethylphosphonofluoridate-inhibited human cholinesterases." Archives of Toxicology **72**(9): 580-587.

Worek, F., G. Reiter, P. Eyer and L. Szinicz (2002). "Reactivation kinetics of acetylcholinesterase from different species inhibited by highly toxic organophosphates." Arch Toxicol **76**(9): 523-529.

Worek, F., H. Thiermann, L. Szinicz and P. Eyer (2004). "Kinetic analysis of interactions between human acetylcholinesterase, structurally different organophosphorus compounds and oximes." Biochem Pharmacol **68**(11): 2237-2248.

Yanagisawa, N., H. Morita and T. Nakajima (2006). "Sarin experiences in Japan: acute toxicity and long-term effects." J Neurol Sci **249**(1): 76-85.

CHAPTER IV

PHARMACOKINETIC MODEL

Introduction

The field of pharmacokinetics studies the chemical and metabolite distribution over time in the body of a living organism (Mosby Inc. 2013). Many researchers of organophosphates (OPs) utilize pharmacokinetic modelling to predict how specific OP exposures will affect the body in certain scenarios. They explore OP pesticide exposures, nerve agent exposures, and antidote effectiveness (Gearhart, Jepson et al. 1990, Worek, Szinicz et al. 2005). Due to the ethical limitations of testing OPs in humans and species differences when using animal models, pharmacokinetic models play an important role in extrapolating animal studies into reasonable human predictions (Dawson 1994, Worek, Reiter et al. 2002, Worek, Szinicz et al. 2005).

The development of pharmacokinetic models for OP exposures takes advantage of multiple data sets from research with different animal species and human blood AChE and BChE substrate kinetics, real nerve agent inhibition kinetics, commercial and novel oxime antidotes reactivation kinetics, and aging and spontaneous reactivation kinetics (Gearhart, Jepson et al. 1990, Worek, Reiter et al. 2002, Worek, Szinicz et al. 2005, Sweeney, Langenberg et al. 2006).

Testing of nerve agent exposure and corresponding antidotes is primarily accomplished economically via the Sprague Dawley-derived rat or similar rat models

(Chambers, Chambers et al. 2013). Actual nerve agent testing on humans is limited to blood components and utilizing *in vitro* assays (Worek, Mast et al. 1999, Worek, Thiermann et al. 2004, Coban, Carr et al. 2016). To improve data extrapolation from rat to humans a comparative kinetic analysis could go a long way in providing the initial information for translating antidote dosing for humans and help develop dynamic models proposed by previous researchers (Gearhart, Jepson et al. 1990, Worek, Szinicz et al. 2005). Pharmacokinetic modeling has long been used to determine estimated rates of chemical and drug metabolism (Emond, Michalek et al. 2005). Researchers utilize known human pharmacokinetic and known animal toxicokinetic data to extrapolate the necessary information that they need. Many of these kinetic rates have been determined in the literature for real nerve agents and commercial oxime antidotes, but these rates have not been determined for the nerve agent surrogates and novel oximes used in this laboratory (Worek, Szinicz et al. 2005). Following the dynamic model developed by Worek et al. from 2005, a dynamic pharmacokinetic model is presented here using the current human kinetic data and rat kinetic data from experiments with nerve agent surrogates and novel oximes described in Chapter 3. The proposed model provides the first step towards developing a human pharmacokinetic model for the novel oximes and nerve agent surrogates.

The Worek dynamic model utilized published human pharmacokinetic data for 2-PAM, which provided critical information on absorbance and excretion rates for 2-PAM. The researchers also utilized published human plasma acetylcholinesterase (AChE) kinetic data for establishing inhibition rates for real nerve agents and reactivation rates for 2-PAM. The researchers utilized published guinea pig toxicokinetic data to determine

lethal doses, and also to determine absorbance and excretion for actual nerve agents. To test the dynamic model, the researchers utilized published human case study data from real world OP exposures to test the predictive capability of the model. The Worek group only tested intravenous and percutaneous OP exposure routes. The dynamic pharmacokinetic model proposed here follows the earlier model developed by Worek et al. from 2005, but also proposes an additional respiratory exposure route developed by Spruit et al. (Spruit, Langenberg et al. 2000). The current proposed model utilized human and rat kinetic values established with our nerve agent surrogates and novel oximes from Chapter 3. The guinea pig toxicokinetic data used by Worek will be replaced with rat toxicokinetic data that has yet to be accomplished for the nerve agent surrogates in future experiments. All graphical depictions below are hypothesized human results based on the 2-PAM data used in Worek's dynamic model and the kinetic similarities seen with the oximes and 2-PAM from Chapter 3. Data charts below are from the published literature when indicated or from the kinetic work from Chapter 3.

Materials and Methods

Model development

The proposed model was based on previous work done by Worek et al. and their dynamic model from 2005 (Worek, Thiermann et al. 2004, Worek, Szinicz et al. 2005). The premise behind a dynamic model requires the creation of equations that take into account the inhibition of AChE or BChE, the reactivation of the inhibited enzymes via oximes, and natural mechanisms of aging and spontaneous reactivation. All of these parameters can be described by kinetic rate constants which have been determined previously. The rate constants can then be expressed in differential equations for input

into a proposed model. Figure 8 below displays the breakdown of the standard kinetic equation into separate components and then subsequent equations for the pharmacokinetic model. All equations in Figure 8, except for Equation 13, were slightly modified from Worek's original equations from 2005 and assume that the forward reaction is primarily occurring.

The list of equations below describe: (13) Standard overall equation describing AChE or BChE inhibition, phosphorylation, reactivation, and aging. Brackets depict concentration, [E] is enzyme, [I] is enzyme inhibitor, [OX] is oxime reactivator, [EI] is enzyme inhibitor complex, $[EI]_R$ is reversible enzyme inhibitor complex, $[EI]_I$ is inhibited enzyme inhibitor complex, $[EI]_a$ is aged enzyme inhibitor complex, [EIOX] is enzyme inhibitor oxime complex. Equations (14), (15), (16), and (17) describe the separate equations for the necessary kinetic reactions that play roles in calculating an overall dynamic model. Equation (18) describes the combined dynamic model equation with all the necessary kinetic parameters included. [OXI] is the oxime inhibitor complex. [EP] is the enzyme product complex. The rate constants are similar to previous Chapter descriptions. The k_{obs} is the same as k_{app}.

Overall Equation $$[E] + [I] \underset{k_{-1}}{\overset{k_1}{\leftrightarrow}} [EI]_R \overset{k_p}{\rightarrow} [EI]_I \begin{matrix} \overset{k_r}{\rightarrow} [E] + [OXI] \\ \underset{k_a}{\rightarrow} [EI]a \end{matrix} \quad (13)$$

Inhibition Equation $$[E] + [I] \overset{k_i}{\leftrightarrow} [EI]_R \quad (14)$$

$$-\frac{dE}{dt} = \frac{d(EI)}{dt} = k_i * [E] * [EI]$$

Reactivation Equation $$[EI] + [OX] \overset{K_D}{\leftrightarrow} [EIOX] \overset{k_r}{\rightarrow} [E] + [OXI] \quad (15)$$

$$\frac{d[E]}{dt} = k_{obs} * [EI + EIOX]$$

$$k_{obs} = \frac{k_r * [OX]}{K_{D+[OX]}}$$

Spontaneous Reactivation Equation $$\frac{d[E]}{dt} = k_s * [EI] \quad (16)$$

Aging Equation $$\frac{d[EA]}{dt} = k_a * [EI] \quad (17)$$

Combined Dynamic Equation

$$\frac{d[E]}{dt} = -k_i * [OXI] * [E] + k_s * [EI] + k_{obs} * [EI + EIOX] \quad (18)$$

$$\frac{d[EP]}{dt} = -k_i * [OXI] * [E] - k_s * [EI] - k_{obs} * [EI + EIOX] - k_a * [EP]$$

Figure 8 List of equations

Equation 16 is the raw equation used by researchers to demonstrate dynamic changes of AChE or BChE activity while accounting for enzyme kinetics, inhibitor toxicokinetics, and oxime pharmacokinetics (Worek, Szinicz et al. 2005). A dynamic pharmacokinetic model is proposed utilizing these calculations along with the previously generated data on human blood AChE and BChE kinetics, nerve agent surrogate's inhibition kinetics for nitrophenyl ethyl methylphosphonate (NEMP for VX) and nitrophenyl isopropyl methylphosphonate (NIMP for sarin), and novel oxime reactivation kinetics for oxime 44.08 and 44.25.

The time course for the oxime concentrations will be calculated using a Bateman function equation described below as Equation 19 (Bateman 1931, Worek, Szinicz et al. 2005). [OX] is the oxime concentration, Dose is oxime dose from start, V_{DSS} is volume of distribution, k_{abs} is rate constant of absorption, k_{el} is rate constant of excretion, t is time, and e is an exponential function.

$$[OX] = \frac{Dose}{V_{Dss}} * \frac{k_{abs}}{k_{abs} - k_{el}} * (e^{-k_{el}*t} - e^{-k_{abs}*t}) \quad (19)$$

The time course for the NEMP and NIMP inhibitor concentrations will need to be determined with a multi-exponential function similar to the equations described by the Worek group for intravenous (IV) and percutaneous exposure, but for the proposed model a respiratory, intravenous, and percutaneous exposure to NEMP and NIMP will be considered as well (Spruit, Langenberg et al. 2000, van der Schans, Lander et al. 2003, Worek, Szinicz et al. 2005). Equations 20, 21, and 24 below are from Worek's 2005 work with VX and sarin. Equations 22 and 23 below are from Spruit's 2000 work with

sarin. These equations will be used to determine rat toxicokinetic data and along with human pharmacokinetic data a prediction of human plasma NEMP or NIMP concentrations will be made with the overall dynamic model described earlier. For the equations below, brackets represent final concentration of inhibitor, and A, B, C, D represent doses of NIMP or NEMP and a, b, c, d represent rate constants, and e is an exponential function, and t is time. The multiple concentrations of inhibitor (A, B, C, D) and their corresponding rates (a, b, c, d) provide a means for determining the best exponential equation for specific exposure types. Based on research by Van der Shans et al. a bi- or tri-exponential equation can be used to improve data accuracy for each model described below based on the type of exposure (van der Schans, Lander et al. 2003). Researchers have confirmed through published research that the below exponential equations are suitable for toxicokinetic determination for VX and sarin (Spruit, Langenberg et al. 2000, Worek, Szinicz et al. 2005). Doses were adjusted from mg/kg to molar units using the molecular weight of the compound being used and a standard human weight of 70 kg (Spruit, Langenberg et al. 2000, Worek, Szinicz et al. 2005). Since NEMP and NIMP have been proven to be effective surrogates for VX and sarin, it is reasonable that the models below may be effective at determining rat toxicokinetics for the overall predictive model. Adjustments can be made as necessary to the proposed exponential models below to improve the toxicokinetic data.

IV NEMP Exposure $$[I] = A * e^{-at} + B * e^{-bt} \quad (20)$$

IV NIMP Exposure $$[I] = A * e^{-at} + B * e^{-bt} + C * e^{ct} \quad (21)$$

Respiratory NEMP/NIMP exposure

Absorption $$[I] = A + B * e^{-bt} \quad (22)$$

Distribution $$[I] = C * e^{-a} + D * e^{dt} \quad (23)$$

Percutaneous NEMP/NIMP exposure

$$[I] = [I_0]e^{-et} - [I]e^{-at} \quad (24)$$

Model Validation

The model validation would be done using data from published cases of OP exposed and treated human patients. The same data used by Worek et al. from 2005 will be used to test the proposed model. The data required would be the amount of OP exposure, the results for periodic blood samples to determine OP and oxime levels, and the AChE activity. Using the kinetic data for inhibition from Table 8 below, and the reactivation rates from Table 9 below, and the concentrations of the OP (I in the equation) and oxime (OX in the equation), the expected AChE activity can be calculated and compared to the actual data. Equation 25 can be applied to determine the AChE activity. K_D is the oxime dissociation constant which must be determined for each oxime and AChE and BChE source.

$$\frac{[E]}{[EI+EIOX]} = \frac{k_r}{k_i*[OXI]*(\frac{1+K_D}{[OX]})} \quad (25)$$

Table 8 Rate constants for inhibition

OP	Human Enzyme Source	k_i ($\mu M^{-1}min^{-1}$)	k_a (min^{-1})	k_s (min^{-1})
NEMP	RBC AChE	7.50	0.0093	0.0030
	Plasma AChE	0.27	0.0082	0.0077
	Plasma BChE	0.17	0.0056	0.0033
NIMP	RBC AChE	2.08	0.0089	0.0017
	Plasma AChE	0.042	0.0089	0.0003
	Plasma BChE	0.038	0.0091	0.0065

Rate constants for inhibition of AChE and BChE by OP (k_i) and for aging (k_a) and spontaneous reactivation of OP inhibited AChE and BChE (k_s). Data for human erythrocyte AChE, pH 7.4, 37 ^oC, was obtained from Chapter 3.

Table 9 Rate constants for dissociation (K_D) and reactivation (k_r)

OP	Human Enzyme Source	2-PAM		Oxime 44.08		Oxime 44.25	
		K_D (μM)	k_r (min^{-1})	K_D (μM)	k_r (min^{-1})	K_D (μM)	k_r (min^{-1})
NEMP	RBC AChE	ND	0.045	ND	0.042	ND	0.043
	Plasma AChE	ND	0.048	ND	0.044	ND	0.040
	Plasma BChE	ND	0.042	ND	0.035	ND	0.030
NIMP	RBC AChE	ND	0.036	ND	0.025	ND	0.033
	Plasma AChE	ND	0.042	ND	0.033	ND	0.040
	Plasma BChE	ND	0.043	ND	0.040	ND	0.038

Rate constants for dissociation (K_D) and reactivation (k_r) for various oximes after NEMP or NIMP inhibition of blood sources of AChE or BChE. Data for human erythrocyte AChE, pH 7.4, 37 ^oC, was obtained from Chapter 3. ND = Not Done

Calculations of enzyme activities

In experimental scenarios conducted by researchers, the real sarin nerve agent is considered to have a short biological half-life and is tested via intravenous and respiratory exposures (Spruit, Langenberg et al. 2000, Worek, Szinicz et al. 2005). Real VX nerve agent is considered a persistent OP and would be tested via intravenous and percutaneous exposure routes (van der Schans, Lander et al. 2003, Worek, Szinicz et al. 2005). The experimental model assumes a simultaneous intravascular or percutaneous exposure to nerve agent and intramuscular administration of oxime. The oxime dosage will be based on current dosing regimens for 2-PAM with 600-1800 mg (MW 172.6). The dosing for oxime 44.08 (MW 400.88) and oxime 44.25 (MW 472.55) have yet to be determined (Sidell, Takafuji et al. 1997, Worek, Szinicz et al. 2005, Chambers, Chambers et al. 2013).

Known human pharmacokinetic data can be used to calculate 2-PAM concentrations in plasma, but the same data for humans have not been determined yet for the novel oximes 44.08 and 44.25. Rat model pharmacokinetic data can be used to determine initial plasma concentration for the novel oximes. Actual toxicokinetic data for human nerve agent exposure is not available because of ethical reasons. Guinea pig data are commonly used for estimating human nerve agent exposure and calculating plasma concentrations of nerve agent (Spruit, Langenberg et al. 2000, van der Schans, Lander et al. 2003, Worek, Szinicz et al. 2005). Using rat models, NEMP and NIMP toxicokinetic data can be generated for determining nerve agent surrogate concentrations in plasma and have yet to be determined.

The AChE IC_{50} for brain tissue is considered a great predictor for nerve agent lethality (Fawcett, Aracava et al. 2009, Meek, Chambers et al. 2012). Based on research conducted with IC_{50}s for NEMP and NIMP for brain, the estimated LD_{50} can be determined and used in the pharmacokinetic analyses. Since IC_{50}s for NEMP and NIMP were determined to be slightly higher than their corresponding real nerve agent, then the LD_{50} may also be slightly higher as well (Meek, Chambers et al. 2012).

The proposed model will utilize intravenous and percutaneous nerve agent surrogate exposure scenarios and calculations established by Worek, but will also utilize the respiratory scenario and pertinent calculations set by Spruit (Spruit, Langenberg et al. 2000, Worek, Szinicz et al. 2005). In conjunction with rat toxicokinetic data and human pharmacokinetic data the calculations will help predict the AChE and BChE activity for each scenario.

Results

Following the findings of Worek's 2005 research on kinetic-based dynamic modeling and the data generated from kinetic analysis of 2-PAM, oximes 44.08 and 44.25, and NEMP and NIMP inhibition, some predictions can be made for the proposed model (Worek, Szinicz et al. 2005). In Worek's dynamic model it was demonstrated that sarin-inhibited AChE, via intravenous (IV) injection, was easily restored after simultaneous intramuscular (IM) oxime injection of 600 mg of 2-PAM. At high sarin doses it was also demonstrated that AChE activity can be quickly restored. For the VX testing the results were different. VX is described by the researchers as having a high persistence and despite the maximum 2-PAM oxime dose, the AChE activity increased

and then decreased over time. This is described as a result of quick oxime elimination and continued VX inhibition (Worek, Szinicz et al. 2005).

Considering the published kinetic values for VX and sarin with subsequent reactivation by 2-PAM, and the 2-PAM data obtained with NEMP and NIMP along with the oximes, some reasonable conclusions can be made (Worek, Szinicz et al. 2005, Meek, Chambers et al. 2012). Work described in Chapter 3 has demonstrated 2-PAM, oxime 44.08 and 44.25 have similar reactivation rates in a variety of rat and human AChE and BChE sources inhibited by NEMP and NIMP. So some of the dynamic modeling data from Worek's 2005 paper for sarin and VX exposure and 2-PAM reactivation may be similar for NEMP and NIMP exposure and subsequent oxime 44.08 and 44.25 reactivation. In Figures 3 to 6 below, hypothesized human data graphs are displayed based on Worek's 2005 data and the observations from published work of Meek and Chambers (Worek, Szinicz et al. 2005, Meek, Chambers et al. 2012, Chambers, Chambers et al. 2013). NEMP, NIMP, novel oxime pharmacokinetic and toxicokinetic data have yet to be determined to compare against real VX and sarin in rat models. Respiratory dynamic modeling was not determined by Worek et al. in 2005, but Equations 22 and 23 above have been proposed using literature from Spruit et al. (Spruit, Langenberg et al. 2000).

The information for Table 10 below is taken from Worek's 2005 data for calculated human plasma concentrations of 2-PAM after IM injection of 1 to 3 autoinjectors equivalent per 70 kg person (600mg, 1200 mg, and 1800 mg) (Worek, Szinicz et al. 2005). The V_{Dss} value was normalized for a 70 kg body weight and the oxime plasma concentrations were calculated with the Bateman Equation 19 described

above. The human experimental 2-PAM values from Table 10 for the different parameters were obtained from the following as indicated: [a](Sidell, Groff et al. 1972), [b](Jovanovic 1989). Similar human pharmacokinetic data would need to be generated for oxime 44.08 and 44.25 to determine the needed variables. The Figure 9 graphical depiction below is hypothesized results for human plasma concentrations for oxime 44.08 and 44.25 except for the doses identifying the three curves has yet to be determined and are identified generically as high, medium and low doses.

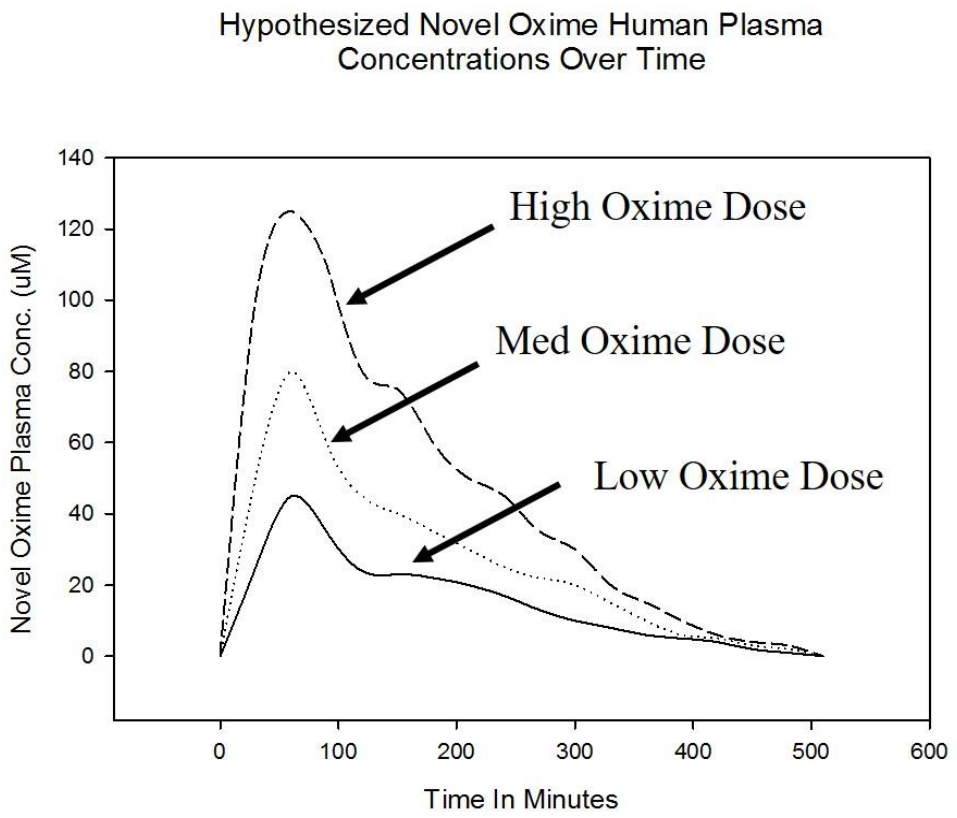

Figure 9 Hypothesized human plasma oxime concentration data

The dose is based on average human weight of 70 kg.

Table 10 Oxime parameter data

Parameter	2-PAM	Oxime 44.08	Oxime 44.25
Dose (g)	0.6/1.2/1.8	TBD	TBD
Dose (mmol)	3.48/6.95/10.43	TBD	TBD
V_{Dss} (ml/kg)	815[a]	TBD	TBD
k_{abs} (min^{-1})	0.103[d]	TBD	TBD
k_{el} (min^{-1})	0.0088[a]	TBD	TBD

Dose was transformed using the oxime molecular weight. TBD = to be determined

The information for Table 11 below is taken from Worek's 2005 data for calculated human AChE activities after IV sarin injection followed simultaneously with IM 2-PAM injection (Worek, Szinicz et al. 2005). The AChE activity changes were calculated with published toxicokinetic guinea pig sarin data and pharmacokinetic human 2-PAM data (Spruit, Langenberg et al. 2000, Worek, Szinicz et al. 2005). Based on published data on NIMP and the novel oximes from Meek et al from 2012 and Chambers et al. from 2013 and the sarin and 2-PAM data from Worek's 2005 paper, the hypothesized human plasma AChE activity depicted in Figure 10 was generated below. Equation 20 previously displayed above $[\text{sarin/NIMP}] = A \times e^{at} + B \times e^{bt}$ allows the determination of human sarin serum concentrations from the guinea pig toxicokinetic data and human 2-PAM pharmacokinetic data (Spruit, Langenberg et al. 2000). The results for NIMP and oxime 44.08 and 44.25 could be similar to the information depicted here when conducted via rat experiments for the toxicokinetics and human experiments for the pharmacokinetics.

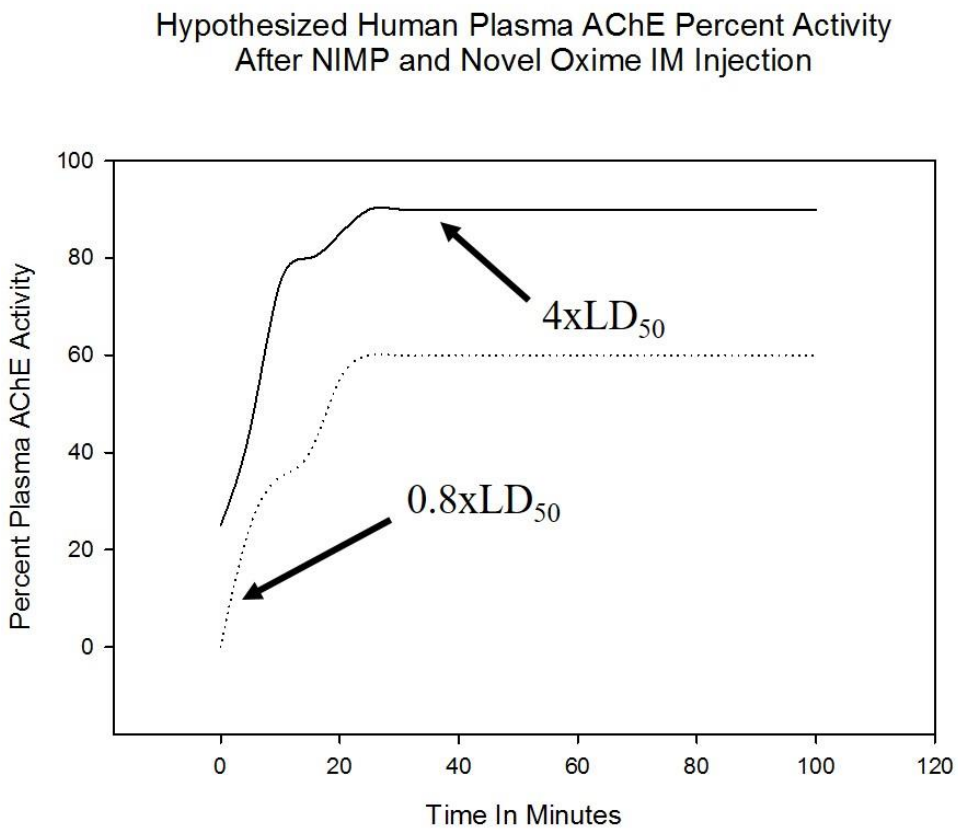

Figure 10 Hypothesized NIMP human IM exposure data

Table 11 Animal LD_{50} data

	Sarin Guinea Pig Data			NIMP Rat Data		
	0.8 x LD_{50}		**4 x LD_{50}**	**0.8 x LD_{50}**		**4 x LD_{50}**
A (nM)	256.24		1281	TBD		TBD
B (nM)	0.642		3.21	TBD		TBD
a (min^{-1})		4.6			TBD	
b (min^{-1})		0.012			TBD	

TBD = to be determined

The information for Table 12 below is taken from Worek's 2005 data for calculated human AChE activities after IV VX injection followed simultaneously with IM 2-PAM injection at 600 mg and 1800 mg (Worek, Szinicz et al. 2005). NEMP and Oxime 44.08 and 44.25 would be injected similar to VX and 2-PAM, but dosage levels still have to be determined. VX guinea pig exposure was at 1, 3, and 5 x LD_{50} and provided measurable plasma concentrations for reference. NEMP rat data would need to be determined to provide corresponding LD_{50} information. The VX animal concentrations along with human pharmacokinetic data for the oximes were used to calculate the corresponding human VX plasma concentrations listed below in the table. Equation 21 above, a three-exponential equation for VX concentration $A \times e^{at} + B \times e^{bt} + C \times e^{ct}$ was used to determine the human values below in Table 12 (van der Schans, Lander et al. 2003). A linear relationship was expected with A, B, and C for guinea pig VX dosing and for the elimination constants a, b, and c, the mean values were used (van der Schans, Lander et al. 2003). Similar protocol for VX will be used for NEMP, but rat NEMP data still needs to be generated and could be used in place of the guinea pig data for generating the corresponding human data. Figure 11 below is a graphical depiction of what human AChE activity levels may look like for various NEMP LD_{50}s.

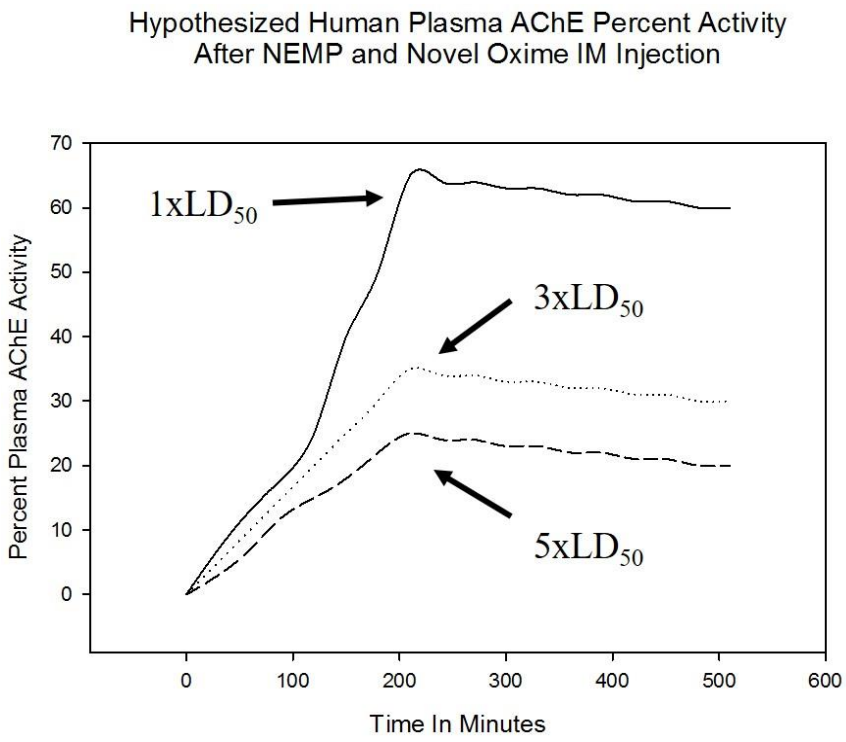

Figure 11 Hypothesized NEMP human IM exposure data

Table 12 Calculated human from animal data

	VX					NEMP				
	Guinea pig VX data		Calculated human data from guinea pig data used for simulation			Rat data for NEMP		Calculated human data from rat data used for simulation		
	1 x LD_{50}	2 x LD_{50}	1 x LD_{50}	3 x LD_{50}	5 x LD_{50}	1 x LD_{50}	2 x LD_{50}	1 x LD_{50}	3 x LD_{50}	5 x LD_{50}
A (nM)	179.5	288.0	151.1	453.3	755.5	TBD	TBD	TBD	TBD	TBD
B (nM)	32.5	63.6	32.9	98.8	164.7	TBD	TBD	TBD	TBD	TBD
C (nM)	1.46	1.80	1.01	3.03	5.06	TBD	TBD	TBD	TBD	TBD
a (min-1)	0.71	0.67		0.69		TBD	TBD		TBD	
b (min-1)	0.045	0.033		0.039		TBD	TBD		TBD	
c (min-1)	0.0071	0.0042		0.0057		TBD	TBD		TBD	

TBD = to be determined

The information for Table 13 below is taken from Worek's 2005 data for calculated human AChE activities after percutaneous VX exposure followed simultaneously with IM 2-PAM injection. The guinea pig information provided VX toxicokinetics and the human 2-PAM data provided pharmacokinetics to determine the necessary information below (Worek, Szinicz et al. 2005). Oxime 44.08 and 44.25 would be injected similar to 2-PAM, but dosage levels still have to be determined. VX guinea pig exposure at 1, 3, and 5 x LD_{50}, would have to be done for rats exposed to NEMP, so the human plasma AChE activity could be determined as hypothesized in the graphical depiction below in Figure 12. The VX animal concentrations along with human pharmacokinetic data for 2-PAM were used by Worek to calculate the VX human LD_{50} estimates in the table below (Worek, Szinicz et al. 2005). Equation 24 from above, $[VX] = [VX_0] \times e^{el*t} - [VX_0] \times e^{abs*t}$ was used to determine the human values below (van der Schans, Lander et al. 2003). Human VX concentrations were determined assuming linear dose relationship for VX (van der Schans, Lander et al. 2003). Similar protocol for VX will be used for NEMP, but rat NEMP dosing concentrations still need to be determined.

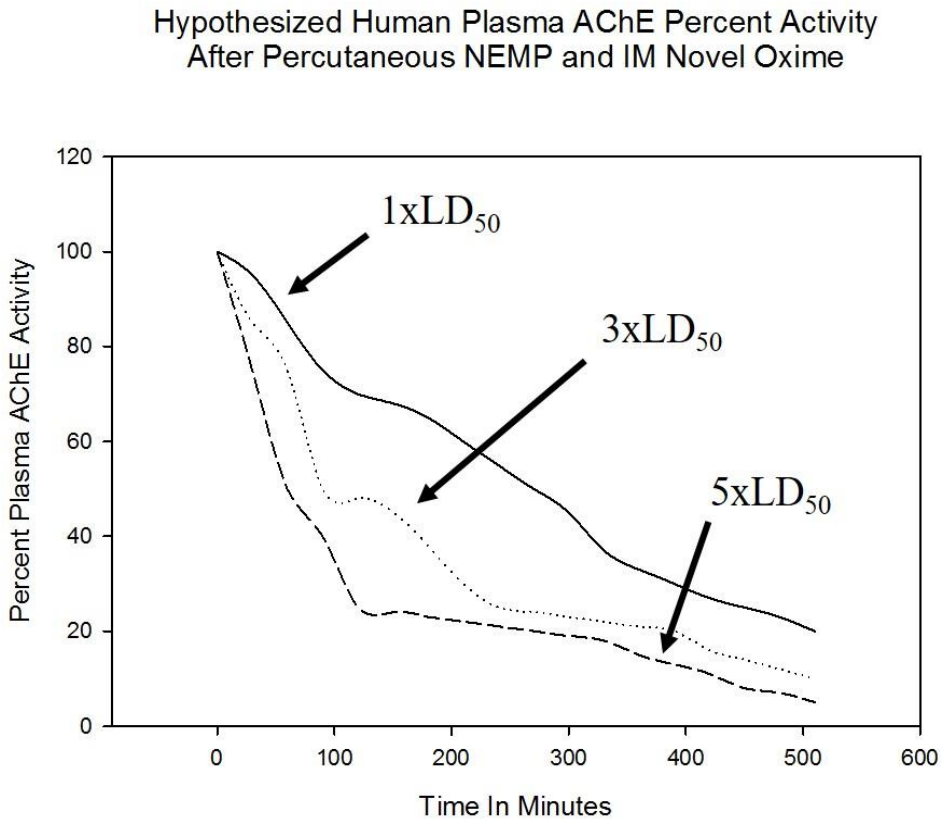

Figure 12 Hypothesized human percutaneous exposure data

Table 13 Human estimates using dynamic model

	VX human estimates			NEMP human estimates		
	1 x LD_{50}	3 x LD_{50}	5 x LD_{50}	1 x LD_{50}	3 x LD_{50}	5 x LD_{50}
VX_0 (nM)	4.784	14.35	23.92	TBD	TBD	TBD
abs (min^{-1})		0.005005			TBD	
el (min^{-1})		0.003375			TBD	

TBD = to be determined

Discussion and Conclusion

Research from Worek et al. have demonstrated the validity of the dynamic model for reactivating sarin and VX inhibited AChE using 2-PAM (Worek, Szinicz et al. 2005). Considering the recent comparison between 2-PAM and oximes 44.08 and 44.25 seen in Chapter 3, it is expected that the oximes will perform similar to 2-PAM in the dynamic modeling. As demonstrated above, critical rat and human data have yet to be determined that could provide a better prediction for the novel oximes and nerve agent surrogates performance in a calculated human model. LD_{50} values in rats would be critical to predict the nerve agent surrogates' abilities to inhibit in the human model. In addition, the novel oxime dosing in the human model is also an important parameter that needs to be determined for the dynamic model to be a better predictor. Another factor to consider is the greater lipophilicity of the novel oximes compared to 2-PAM which could play a role in overall absorption, distribution, and excretion. The increased lipophilicity could cause distribution into lipophilic cellular material and require increased doses compared to 2-PAM. Once all these parameters have been determined and explored, the model testing for the surrogates and novel oximes can be accomplished using the same case study data used by Worek et al. in 2005 (Sidell, Takafuji et al. 1997, Spruit, Langenberg et al. 2000, Worek, Szinicz et al. 2005). The proposed model will help lead the way with the optimization of treatment protocols for NIMP and NEMP exposed rats and subsequent optimization of protocols for treating humans with our novel oximes.

References

Bateman, H. (1931). "The k-Function, A Particular Case of the Confluent Hypergeometric Function." Transactions of the American Mathematical Society **33**(4): 817-831.

Chambers, J. E., H. W. Chambers, E. C. Meek and R. B. Pringle (2013). "Testing of novel brain-penetrating oxime reactivators of acetylcholinesterase inhibited by nerve agent surrogates." Chem Biol Interact **203**(1): 135-138.

Coban, A., R. L. Carr, H. W. Chambers, K. O. Willeford and J. E. Chambers (2016). "Comparison of inhibition kinetics of several organophosphates, including some nerve agent surrogates, using human erythrocyte and rat and mouse brain acetylcholinesterase." Toxicology Letters **248**: 39-45.

Dawson, R. M. (1994). "Review of oximes available for treatment of nerve agent poisoning." J Appl Toxicol **14**(5): 317-331.

Emond, C., J. E. Michalek, L. S. Birnbaum and M. J. DeVito (2005). "Comparison of the Use of a Physiologically Based Pharmacokinetic Model and a Classical Pharmacokinetic Model for Dioxin Exposure Assessments." Environmental Health Perspectives **113**(12): 1666-1668.

Fawcett, W. P., Y. Aracava, M. Adler, E. F. Pereira and E. X. Albuquerque (2009). "Acute toxicity of organophosphorus compounds in guinea pigs is sex- and age-dependent and cannot be solely accounted for by acetylcholinesterase inhibition." J Pharmacol Exp Ther **328**(2): 516-524.

Gearhart, J. M., G. W. Jepson, H. J. Clewell, 3rd, M. E. Andersen and R. B. Conolly (1990). "Physiologically based pharmacokinetic and pharmacodynamic model for the inhibition of acetylcholinesterase by diisopropylfluorophosphate." Toxicol Appl Pharmacol **106**(2): 295-310.

Jovanovic, D. (1989). "Pharmacokinetics of pralidoxime chloride. A comparative study in healthy volunteers and in organophosphorus poisoning." Arch Toxicol **63**(5): 416-418.

Meek, E. C., H. W. Chambers, A. Coban, K. E. Funck, R. B. Pringle, M. K. Ross and J. E. Chambers (2012). "Synthesis and *in vitro* and *in vivo* inhibition potencies of highly relevant nerve agent surrogates." Toxicol Sci **126**(2): 525-533.

Mosby Inc. (2013). Mosby's dictionary of medicine, nursing & health professions. St. Louis, Mo., Elsevier/Mosby.

Sidell, F. R., W. A. Groff and A. Kaminskis (1972). "Toxogonin and pralidoxime: Kinetic comparison after intravenous administration to man." Journal of Pharmaceutical Sciences **61**(11): 1765-1769.

Sidell, F. R., E. T. Takafuji and D. R. Franz (1997). Medical aspects of chemical and biological warfare. Washington, D.C., Falls Church, Va., Fort Sam Houston, Tex., Fort Detrick, Frederick, Md., Bethesda, Md., Borden Institute, Office of the Surgeon General, United States Army Medical Department Center and School ; United States Army Medical Research and Material Command ; Uniformed Services University of the Health Sciences. pp. 29-45, 111-196

Spruit, H. E., J. P. Langenberg, H. C. Trap, H. J. van der Wiel, R. B. Helmich, H. P. van Helden and H. P. Benschop (2000). "Intravenous and inhalation toxicokinetics of sarin stereoisomers in atropinized guinea pigs." Toxicol Appl Pharmacol **169**(3): 249-254.

Sweeney, R. E., J. P. Langenberg and D. M. Maxwell (2006). "A physiologically based pharmacokinetic (PB/PK) model for multiple exposure routes of soman in multiple species." Arch Toxicol **80**(11): 719-731.

van der Schans, M. J., B. J. Lander, H. v. d. Wiel, J. P. Langenberg and H. P. Benschop (2003). "Toxicokinetics of the nerve agent (±)-VX in anesthetized and atropinized hairless guinea pigs and marmosets after intravenous and percutaneous administration." Toxicology and Applied Pharmacology **191**(1): 48-62.

Worek, F., U. Mast, D. Kiderlen, C. Diepold and P. Eyer (1999). "Improved determination of acetylcholinesterase activity in human whole blood." Clin Chim Acta **288**(1-2): 73-90.

Worek, F., G. Reiter, P. Eyer and L. Szinicz (2002). "Reactivation kinetics of acetylcholinesterase from different species inhibited by highly toxic organophosphates." Arch Toxicol **76**(9): 523-529.

Worek, F., L. Szinicz, P. Eyer and H. Thiermann (2005). "Evaluation of oxime efficacy in nerve agent poisoning: Development of a kinetic-based dynamic model." Toxicology and Applied Pharmacology **209**(3): 193-202.

Worek, F., H. Thiermann, L. Szinicz and P. Eyer (2004). "Kinetic analysis of interactions between human acetylcholinesterase, structurally different organophosphorus compounds and oximes." Biochem Pharmacol **68**(11): 2237-2248.

CHAPTER V

CONCLUSION

The risk of exposure to OPs as pesticides and nerve agents continues to be a problem throughout the world. Though current antidotes do provide reactivation for the peripheral nervous system, there has yet to be discovered a viable antidote to effectively reactivate AChE in the central nervous system. The results of our research have provided additional support for the efficacy of newly developed oximes that can penetrate the blood brain barrier and reactivate the central nervous system.

The cyclosarin surrogate, NCMP, has proven to be a formidable agent for inhibiting AChE, similar to the real nerve agent cyclosarin. The inability of the novel oximes to generate appreciable reactivation is similar to 2-PAM. Despite this finding, preliminary data for combined antidote testing did demonstrate an interesting increase in rat brain reactivation *in vitro* when simultaneously incubated with NCMP, 2-PAM, and novel oxime 46.43 or 46.49. Exploring the interaction within the testing system between the NCMP, 2-PAM, and novel oximes could provide critical insight into the mechanisms occurring. Discoveries at the molecular level could provide information for further refinement of the oximes for reactivating NCMP more effectively.

Kinetic analyses provide a quantitative means to evaluate the effects of inhibitors and reactivators on different enzymes. In addition, kinetic analyses can also provide a means to quantitate differences between the same enzyme in different species. In the

current research the kinetic analysis of rat and human erythrocyte acetylcholinesterase (AChE) and plasma AChE and butyrylcholinesterase (BChE) and rat brain and skeletal muscle AChE provided important kinetic data for making critical comparisons. The current research confirmed the potency differences between the VX nerve agent surrogate, NEMP, and the sarin surrogate, NIMP, where NEMP was more potent for both humans and rats. In addition, differences between human and rat blood AChE and BChE inhibition by the surrogates demonstrated the increased sensitivity of the rat enzymes. Finally, the overall oxime reactivation data suggests 2-PAM is a greater reactivator compared to oxime 44.08 and 44.25, but the close proximity of the rates suggests they are still comparable.

The necessary deficiency in nerve agent research is the inability of *in vivo* human testing due to ethical limitations. Researchers are therefore limited to using pharmacokinetic data from humans and toxicokinetic data from animal models. The current research has not reached the stage of toxicokinetic animal testing of the nerve agent surrogates or real nerve agent with subsequent use of the novel oximes. In addition, the novel oximes have not yet reached the stage for generating human pharmacokinetic data. Despite the lack of some data, a dynamic pharmacokinetic model was proposed using the kinetic values from the rat and human blood experiments described here and available published human data. Proposed calculations, data tables, and graphs were generated to provide the initial step towards a rat-based dynamic pharmacokinetic model for predicting human results and improving rat model testing of the nerve agent surrogates and novel oximes.

The future direction of this research could include further exploration of NCMP and the interaction it had with 2-PAM and oximes 46.43 and 46.49. This could be done via amino acid substitutions on acetylcholinesterase and determining sites on the enzyme that are interacting with the NCMP or oximes. The results could help pinpoint ways the oximes could be improved. Another future direction for the research could be to continue acquiring the necessary rat OP toxicokinetic and human oxime pharmacokinetic data needed to implement the proposed rat-based dynamic pharmacokinetic model. Completing the model will help with the development of optimized treatment protocols for the nerve agent surrogate exposed rats and subsequently help project protocols for human treatment using the novel oximes. Together the research further validates the effectiveness of the nerve agent surrogates for evaluating the novel oximes and also strengthens the novel oximes use as an improved nerve agent antidote

APPENDIX A

EXPERIMENTAL PROTOCOLS

Blood AChE and BChE Preparation Procedure

Sources of AChE in human and rat blood are found on the erythrocyte outer membrane and also in the plasma. The source of BChE in human and rat blood is primarily suspended in the plasma. The preparation of human and rat erythrocyte ghost and separation of the plasma was accomplished with modified procedures from Dodge et al. and Worek et al. The pools of erythrocyte ghost or plasma were created with at least five different specimens from rats or human sources. For erythrocyte ghost preparation, blood was collected in vacutainers containing EDTA anticoagulant and kept on ice throughout the processing. The amount of blood in each container was approximately recorded. This value was used to return the erythrocyte ghost back to the original volume at the end of the procedure. Blood containers were spun at 3000xg for 10 minutes at 4 ºC (Eppendorf Centrifuge 5702R, A-4-38 rotor). After centrifugation the specimen tubes should have a layer of erythrocytes at the bottom and a layer of plasma at the top. The top plasma layer was removed from each blood container and pooled into a single glass test tube. The amount of plasma removed was recorded for each blood container and this volume removed was used to determine the amount of SPB used for the erythrocyte washing steps. The removed pooled plasma was allocated into 1 ml conical tubes with 250 µl of plasma in each tube and frozen at -80 ºC until testing. The remaining erythrocytes were washed with 2 times the plasma volume removed from each sample. All washes and dilutions were accomplished with SPB (0.1 M, pH 7.4). The samples were washed 3 times by spinning at low speed for 1000xg for 10 minutes at 4 ºC, supernatant was discarded and SPB was added and mixed, then the cycle repeated (Eppendorf Centrifuge 5702R, A-4-38 rotor). After the final wash, the packed

erythrocytes were diluted with hypotonic phosphate buffer by 20 times the volume of plasma originally removed from each tube. The diluted samples were mixed and cells allowed to lyse for 10 minutes. The lysed mixtures were centrifuged at 50,000xg for 30 minutes at 4 ºC (Beckman Coulter Avanti Centrifuge, JA-20 rotor). The supernatant was removed, samples were pooled, and the erythrocytes were diluted to the original sample volume from the original specimens. To remove excess hemoglobin, the samples were washed 1 time by spinning at low speed for 5000xg for 5 minutes at 4 ºC, supernatant was discarded and SPB (0.1 M, pH 7.4) was added to the original sample volume (Eppendorf Centrifuge 5415C, F-45-18-11 rotor). A 15 ml glass Pyrex homogenizer was used to thoroughly mix samples and then aliquot 250 µl into conical tubes and store at -80 ºC. To ensure optimal testing, pooled samples were analyzed to obtain baseline activity and testing protocol parameters were adjusted accordingly.

Rat Solid Tissue AChE Preparation Procedure

Rat cerebral cortex and medulla oblongata and skeletal muscle was ground with a Polytron PT 10-35 Grinder and then homogenized with a Heidolph Homogenizer and a Teflon pestle in cold Tris-HCl buffer (0.05 M, pH 7.4) at a concentration of 40 mg/ml for brain or 100 mg/ml for skeletal muscle. The homogenate was filtered through glass wool or gauze. Five different rat samples were utilized per pooled sample. Samples were aliquoted into 4 ml glass vials and maintained at -80 ºC until testing.

AChE and BChE Substrate Kinetics Procedure

For each pool of samples, a minimum of one 96-well microtiter plate was used. The protocol for AChE and BChE testing was adapted from a modified Ellman's AChE

activity test. For each pool of samples, a minimum of one 96-well microtiter plate was used and three different pools were run for each experiment and the average was calculated along with the standard error. Ghost AChE or plasma AChE or BChE samples were thawed and kept on ice until testing. Plasma and ghost specimens were diluted with SPB (0.1M, pH 7.4) appropriately to ensure approximately 0.3 absorbance units of activity. Ghost AChE was thoroughly homogenized using a glass Tenbroek mortar and pestle and hemoglobin removed via centrifugation and removal of supernatant at 5000xg for 5 minutes at 4 °C (Eppendorf Centrifuge 5415C, F-45-18-11 rotor). To prevent decreases in enzyme activity washing was minimized. One 96-well plate was used to carry out the substrate kinetics. Each experimental parameter and control was carried out in triplicate. 250 µl of specimen was loaded in each testing well with 300 µl as the final testing volume. Eserine sulfate at FC 10^{-5} M was added to negate any cholinesterase activity in one control column. Ethanol with FC of 2% was added to demonstrate maximum activity in one control column. A blank well without substrate and just DTNB and SPB was utilized to demonstrate background absorbance. The following 8 well columns were set up for the various concentrations of substrate to be added right before reading the plate on the spectrophotometer. DTNB was added to all wells at a FC 0.002 M. The loaded plate was placed in a Jitterbug plate warmer at 37 °C for 15 minutes at a level 3 shake. A single row on a separate plate was prepared to hold the necessary substrate mixtures (160 µl per well) to be added to the experimental plate prior to testing on the plate reader. The eserine and ethanol wells (columns 1 and 3) received ATCh or BTCh at FC 0.02 mM. The blank wells (columns 2 and 4) received ethanol with FC of 2% and no substrate was added to these wells. The subsequent wells (columns 5 to 12)

received diluted ATCh or BTCh substrate solutions that provided final concentrations ranging from 0.02 mM through 2.5 mM. Substrate mixtures were kept on ice and covered with tape prior to testing. After incubation and mixing, the loaded testing plate was placed on the plate reader for analysis and a multi-channel pipette was used to dispense the various ATCh or BTCh mixtures or ethanol as necessary and the spectrophotometer was started. Table 14 below depicts plate setup for substrate kinetics.

The procedure for rat solid tissue was similar to the above protocol for blood with the following exceptions. Pooled homogenate was thawed and mixed using a glass Tenbroek mortar and pestle and then centrifuged at 5000 RCF for 5 minutes at 4 °C to remove excess cellular debris in the supernatant (Eppendorf Centrifuge 5415C, F-45-18-11 rotor). The intact pellet was returned to the same sample volume with fresh Tris buffer (0.05 M, pH 7.4) and mixed thoroughly. Each experimental parameter and control was carried out in triplicate, but 150 µl of specimen was loaded instead of 250 µl as previously performed for blood specimens. The final concentration of each tissue was 1 mg equivalent/ml per well with a final well-volume of 200 µl. Tris buffer was used to dilute specimens or perform any other action needing buffer for rat solid tissue.

Table 14 Plate schematic for substrate kinetics

	Eserine Controls		Vehicle Controls		Substrate Concentrations							
	1	2	3	4	5	6	7	8	9	10	11	12
A	Eserine Sulfate Wells	Blank Wells	Ethanol Wells	Blank Wells	Increasing Concentrations of ATCh or BTCh							
B												
C												
D												
E												
F												
G												
H												

Calculation: For each concentration and control, the velocity was calculated. The velocities were then used to formulate a Lineweaver Burk plot with the reciprocal of each velocity on the y-axis and the reciprocal of each ATCh (BTCh) concentration on the x-axis. The resulting data were used to formulate a linear line with a squared correlation coefficient (R^2-value) greater than 0.9 for acceptable results. The K_{mapp} = -slope and V_{max} = x-intercept.

AChE and BChE Inhibition Kinetics Procedure

The protocol for AChE and BChE inhibition testing was adapted from a modified Ellman's AChE activity test using a 96-well plate. For each pool of samples, a minimum of four 96-well microtiter plates were used and three different pools were run for each experiment and the average was calculated along with the standard error. Reading times

for the inhibition kinetics were 5, 4, 3, 2, 1, and 0-minutes. All time points used 3 rows and 12 columns and one plate held two time points except for the 1-minute and 0-minute time points which were performed separately. Plate 1 held the 5-minute and 3-minute reactions, plate 2 held the 4-minute and 2-minute reactions, plate 3 held the 1-minute reaction, and plate 4 held the 0-minute reaction.

The pooled plasma or ghost AChE or BChE was diluted appropriately to ensure enough sample for all experiments and that the concentration was appropriate to generate approximately 0.3 absorbance unit. Testing wells were loaded with 250 µl of the prepared sample with each testing protocol run in triplicate (eserine, ethanol, blank, and the eight increasing inhibitor concentrations). To the blank wells, DTNB and additional SPB (0.1M, pH 7.4) was added to obtain FC 0.002 M DTNB in 300 µl total volume. Eserine sulfate was added to the appropriate control wells to obtain a FC 10^{-5} M. All plates were kept on ice until testing. A solution made up of 40% 0.03 M DTNB, 10% 0.1 M ATCh or BTCh, and 50% SPB was mixed and used to initiate the kinetic run and was kept on ice throughout the experiment to decrease substrate degradation.

A separate plate containing ethanol for the control wells and the various inhibitor concentrations was set up by adding 150 µl of ethanol to the first four wells and 150 µl of increasing inhibitor concentrations to the next eight wells. The inhibitory concentrations ranged from 10% through 90% inhibition and varied depending on the AChE or BChE source. Tape was placed over the wells and the plate was placed on ice throughout the testing cycle to decrease evaporation.

Prior to testing a plate, it was warmed and mixed on a Jitterbug plate warmer for 15 minutes at 37 °C and at a level 3 shake. While the plate was shaking the

spectrophotometer plate reader was initiated to run the first plate. Using the multichannel pipette, 5 µl of the different ethanol and inhibitor solutions was added to the top three rows of plate one, mixing each time and changing the tips to prevent contamination of the original ethanol and inhibitory solutions. Once all solutions were added to the top three rows the timer was started, and a level 3 shake was initiated on the Jitterbug. Solutions were added to each row utilizing 10 second intervals to maintain uniformity. This is the initiation of the 5-minute (4-minute) shaking incubation time period.

Thirty seconds prior to the 2-minute mark on the timer, the plate was removed from the Jitterbug and prepared for the next addition of ethanol and inhibitors. Using the multichannel pipette, 5 µl of the different solutions was added to the bottom three rows of wells as performed previously. The plate was quickly returned to the Jitterbug and a level 3 shake was initiated. Solutions were added to each row utilizing 10 second intervals to maintain uniformity. This is the 3-minute (2-minute) shaking incubation time period.

While the plate is shaking in the Jitterbug, an 8-channel repeat pipette was prepared to dispense 50 µl of the previously prepared DTNB, ATCh (BTCh), and SPB solution. The incubated and inhibited plate was removed from the shaker and loaded on the plate reader and the solution was dispensed to all the testing wells, except the blank wells, and the kinetic read initiated. The 4 and 2-minute plate and 1-minute plate was performed following the same protocol above.

For the 0-minute assay plate, the plate was warmed and mixed on the Jitterbug for 15 minutes. While the plate was incubating, the plate reader was readied for a kinetic analysis. After the incubation, the fourth row on the plate was used to contain a mixture

of 90% DTNB/ATCh(BTCh)/SPB solution and 10% ethanol or inhibitor solutions (progressing from low to high concentrations). This mixture was added to all the wells directly below the testing wells except for the blank wells.

The multi-channel pipette was prepared to dispense 50 µl of the solutions in the fourth well into the three wells above. For each replicate wells above, the solution was added and thoroughly mixed using the same tip, and the tips were changed before adding the mixture to the next replicate wells. Once the solutions were added, the plate was placed on the plate reader and the kinetic program started. Table 15 below depicts the plate setup for inhibition kinetics. The procedure for rat solid tissue was similar to the above protocol for blood, but with the same exceptions mentioned in the substrate kinetics procedure.

Calculations: For each concentration and control, the velocity of each incubation period was calculated. For each preincubation time, the fraction of AChE or BChE velocity left ($[E]_t/[E]_0$) was calculated by dividing the AChE or BChE velocity following inhibition ($[E]_t$) by the original uninhibited velocity ($[E]_0$). Using linear regression of the natural log (ln) of the $[E]_t/[E]_0$ as a function of time, should provide a line at each inhibitor concentration with slope = $-k_{app}$. This was the apparent rate of AChE or BChE phosphorylation. A double reciprocal plot of the k_{app} as a function of the inhibitor concentration provided a line with slope = $1/k_i$, y-intercept = $1/k_p$, and x-intercept = $-K_A$. [E] is the concentration of free enzyme.

Table 15 Plate schematic for inhibition kinetics

	Eserine Controls		Vehicle Controls		Inhibitor Concentrations							
	1	2	3	4	5	6	7	8	9	10	11	12
A	Eserine Sulfate Wells	Blank Wells	Ethanol Wells	Blank Wells	Increasing Concentrations of NEMP or NIMP							
B												
C												
D												
E												
F	Eserine Sulfate Wells	Blank Wells	Ethanol Wells	Blank Wells	Increasing Concentrations of NEMP or NIMP							
G												
H												

Full plate used for 5 and 3-minute time points (rows A, B, C) and 4 and 2-minute time points (rows F, G, H). Only the top of plate was used for the 1 and 0-minute time points (rows A, B, C).

AChE and BChE Reactivation Kinetics Procedure

The volume of specimen required for testing varied depending on the AChE or BChE sources and the quality of the samples. Initial activity testing was conducted to determine baseline absorbance for each pool of samples. For testing, the samples were diluted as necessary to obtain baseline absorbance of approximately 0.3 units.

Preparing the Samples. For ghost AChE specimens: Ghost AChE samples were pooled and thoroughly homogenized using a glass Tenbroek mortar and pestle and hemoglobin removed via centrifugation and removal of supernatant at 5000xg for 5 minutes at 4 °C (Eppendorf Centrifuge 5415C, F-45-18-11 rotor). The intact sample pellet was returned to the original volume with SPB (0.1M, pH 7.4) and vortexed.

For plasma: Plasma samples were pooled and not diluted prior to the inhibition step. Undiluted plasma must be used since the AChE and BChE are suspended in the plasma. Before the next step, 50 µl of the ghost or plasma sample was pipetted into three 15 ml glass tubes and maintained in the 4°C freezer until protein testing was conducted to check consistency in specimen preparation.

For solid tissue: Homogenate samples were thawed, pooled and then mixed using a glass Tenbroek mortar and pestle and then centrifuged at 5000 RCF for 5 minutes at 4 °C (Eppendorf Centrifuge 5415C, F-45-18-11 rotor). Once spun down, supernatant was removed and the pellet left intact. The same volume of fresh Tris buffer (0.05 M, pH 7.4) was returned to the pelleted specimen and vortexed.

Each experimental parameter and control was carried out in triplicate. The final volume in each well for blood specimens (ghost and plasma) was 200 µl with 150 µl from

the diluted enzyme source. The final volume in each well for solid tissue specimens (brain and skeletal muscle) was 300 µl with 250 µl from the diluted enzyme source. The final concentration of each solid tissue well was 1 mg equivalent/ml.

Sample Inhibition. For ghosts: The sample was split into two vials, one vial for the uninhibited sample that was spiked with the ethanol vehicle (minimum 1 ml total volume) and a second vial for the inhibited sample that was spiked with the appropriate inhibitor (NIMP or NEMP) which yielded approximately 90% inhibition of the sample (minimum 5 ml total volume). Incubation was done in a shaking water bath at 37° C at the necessary time interval to achieve the required 90% inhibition. Once inhibition was complete the ghosts were centrifuged at 5000xg for 5 minutes at 4°C and the supernatant was removed and the pellet left intact (Eppendorf Centrifuge 5415C, F-45-18-11 rotor). Removing the supernatant helped to eliminate excess vehicle or surrogate. The pellet was resuspended to the original volume using SPB and vortexed thoroughly. This wash procedure was done twice. The last wash was saved for analysis to ensure all the inhibitor was removed. The washed and inhibited ghost were maintained on ice until testing. Rat solid tissue followed the same protocol, but Tris buffer was used for the washes instead of SPB.

For plasma: Since the AChE or BChE is suspended in the plasma, removing the inhibitor via centrifugation was not possible. To decrease inhibition, the plasma was diluted. Pre-testing was done to determine the minimal volume of sample and inhibitor necessary, and the minimal dilution necessary to eliminate further inhibition without compromising overall enzyme activity and subsequent absorbance. This varied by pool of plasma, enzyme being tested (AChE or BChE), or species (rat or human).

Approximately 5 to 15 µl of inhibitor (ethanol for uninhibited control) was used for every 60 µl of plasma. Proportional adjustments were made per pool if more plasma was needed. Adjustments to the SPB dilution was made per pool as necessary to ensure optimal enzyme activity for testing. The diluted and inhibited sample was maintained on ice until testing.

A solution made up of 40% 0.03 M DTNB, 10% 0.1 M ATCh or BTCh, and 50% SPB (Tris buffer) was mixed and used to initiate the kinetic run and was kept on ice throughout the experiment to decrease substrate degradation.

Initial Time Point. For the initial time point (0 min), cold uninhibited ghost (plasma) was vortexed and 68 µl (175 µl for plasma and 100 µl for solid tissue) was pipetted into a 3 ml glass tube with 2 ml cold buffer. The diluted samples were vortexed and 250 µl (150 µl solid tissue) pipetted into three rows of a 96-well plate with the rows representing replicates (A, B, C). Additional columns were loaded as necessary with column 1 and 2 used for eserine sulfate controls, columns 3 and 4 were ethanol controls. Rows 2 and 4 were blanks and did not have any ATCh added to them. The same setup was done for the inhibited samples, but subsequent columns 5 through 8 were set up accordingly. To the blank wells, DTNB and additional SPB was added to obtain FC 0.002 M DTNB in 200 µl (300 µl for solid tissue) total volume. Eserine sulfate was added to the appropriate control wells to obtain a FC 10^{-5} M. The plate was incubated and mixed in the Jitterbug for 15-minutes at a level 3 mix. While the plate was shaking the spectrophotometer was set up to run the preset kinetics program. The 8-channel repeat pipette was prepared to dispense 50 µl of the DTNB/ATCh(BTCh)/SPB solution

described earlier. Once incubation was done the plate was quickly loaded with the solution, except for the blank wells, and the plate reader was started.

15, 30, 45, and 60-minute time points. For the reactivation experiment the inhibited sample was split into 5 aliquots (inhibited sample to monitor spontaneous reactivation, inhibited sample used to gauge aging, inhibited sample reactivated with 2-PAM, inhibited sample reactivated with Oxime 1, and inhibited sample reactivated with Oxime 2). For each split sample the appropriate ethanol vehicle or oxime was administered 20 µl for ghost or 50 µl for plasma per 1 ml of sample and vortexed (10 µl/ml for solid tissue). Samples were incubated in a shaking water bath at 37° C and a timer initiated. The timer was maintained throughout the 60-minute incubation and not stopped.

At each time point, incubated samples were vortexed and 68 µl for ghost samples (175 µl for plasma and 100 µl solid tissue) were pipetted into separate glass tubes with 2 ml cold buffer. The aging sample was primed with 30 µl of 2-PAM and incubated in the 37 °C shaking water bath for 10 minutes. The remaining samples were vortexed and 250 µl (150 µl solid tissue) was pipetted into three rows (A, B, C or F, G, H) of a 96-well plate as appropriate. For the uninhibited sample and inhibited sample with no reactivator the three rows A, B, and C were utilized as subsamples for each parameter. For each sample type an eserine control was setup in columns 1 and 2 with the later column used as the blank, ethanol vehicle controls were setup in columns 3 and 4 with the later column used as the blank. For inhibited samples the same setup was done using columns 5 through 8.

For the inhibited samples with reactivators added, rows F, G, and H were used as subsamples. One column was used for an eserine control and two columns were used to test the amount of reactivation at the time point (3 columns per reactivator). After setup was complete, the aging sample was removed from the water bath and setup as well. To the column with the blank wells, DTNB and additional SPB was added to obtain FC 0.002 M DTNB in 200 µl (300 µl for solid tissue) total volume. Eserine sulfate was added to the appropriate control wells to obtain a FC 10^{-5} M.

Once setup was complete the plate was placed in the Jitterbug for a 15-minute warm-up incubation with a level 3 mix. While the plate was shaking the spectrophotometer was initiated to run the preset kinetics program. The 8-channel repeat pipette was prepared to dispense 50 µl of the DTNB/ATCh(BTCh)/SPB solution used earlier. Once incubation was done the plate was quickly loaded with the solution, except the blank wells, and the plate reader was started. Table 16 below depicts the plate setup for reactivation kinetics.

Table 16 Plate schematic used for reactivation kinetics

	Uninhibited Sample					Inhibited Sample						
	1	2	3	4	5	6	7	8	9	10	11	12
A	Eserine Wells	Eserine Blank Wells	Ethanol Wells	Ethanol Blank Wells	Eserine Wells	Eserine Blank Wells	Ethanol Wells	Ethanol Blank Wells				
B												
C												
D												
E												
F	Eserine Wells	Testing Wells		Eserine Wells	Testing Wells		Eserine Wells	Testing Wells		Eserine Wells	Testing Wells	
G												
H												
	Aging Control			2-Pam			Oxime 1			Oxime 2		

Calculations: Determination of the ratio of AChE (BChE) activity at each time interval was calculated by dividing the AChE (BChE) activity in the inhibited samples by the matching control activity ($[E]_t/[E]_0$). Using the natural log of the ratio of inhibited versus control activity (y-axis) at each time point (x-axis), the various rate constants described below were obtained (k_r, k_s, k_a) with the slope of the best fit line with R^2-value no less than 0.9. All rate constant variables were on the y-axis and the time points were on the x-axis. First order rate constants were calculated from linear regression of the natural log (ln) of the ratio of AChE (BChE) activity as a function of time. Using the vehicle (control) plots, the spontaneous reactivation (s) rate constant, k_s, was estimated from the slope of the line described by the equation $\ln([E]_t/[E]_0) = k_s t$. Using the oxime reactivation plots, the oxime reactivation rate (r) constant, k_r, was estimated from the slope of the line described by the equation $\ln([E]_t/[E]_0) = k_r t$. Using the oxime reactivation plots from the 2-PAM aging data, the aging rate (a) constant, k_a, was estimated from the slope of the line described by the equation $\ln(1-[E]_t/[E]_0) = k_a t$. Aging was determined by incubating a portion of the inhibited sample with a reactivator (concentration known to reactivate 100% of AChE(BChE)) at set time points and calculating if any AChE(BChE) was not reactivated. The percent not reactivated was considered the aged AChE(BChE). The difference between the reactivation and aging rate constant provided the true reactivation rate constant.

Bio 4 Spectrophotometric Plate Reader Setup

The kinetics program was preset prior to all testing. Measurement mode was set for absorbance with a measurement wavelength set at 412 nm with a reference wavelength of 0 nm. The read mode was set at normal with a kinetic cycle of 25 with

minimum reading time intervals (approximate run time was 8 minutes). The testing temperature range was set at 35 to 38 °C. The plate volume was set at 300 µl for blood specimens and 200 µl for solid tissue specimens. A shake was set before each measurement at a 3-second duration, conducted internally, and at normal intensity. Shaking was conducted between cycles at a 2-second duration, performed internally, and at normal intensity.

Modified Lowry Protein Determination Procedure

This experiment was utilized to determine the relative protein concentration within the solid tissue or blood components analyzed and determined the consistency of the testing solutions. Bovine serum albumin (BSA) was used to set up the standard curve with concentrations of 0 mg/ml, 50 mg/ml, and 200 mg/ml. All standards and specimens were analyzed with three individual replicates. The amount of sample needed for blood assays was 50 µl for each replicate tube. Samples were taken prior to plating and batched for testing and stored at -20 ºC. The standard curve was created by adding 3 ml of deionized (DI) water to each standard curve tube. Volumes were removed from respective standards and replaced with BSA. 50 µl and 200 µl of DI water was removed and replaced with 50 µl and 200 µl of BSA respectively. All tissue and blood samples received 3 ml of DI water. All tubes were vortexed. Reagent A was made by dissolving 4 g NaOH and 20 g Na_2CO_3 in 1 L or DI water. Reagent C was created using Reagent A and NaK tartrate and copper sulfate. The amount of reagent A was calculated based on number of tubes x 2.5 ml + 50 ml. For every 100 mls of reagent A, 1 ml of NaK tartrate and 1 ml of copper sulfate was added to reagent C. 2.5 mls of reagent C was added to every test tube and vortexed. Tubes were left to stand for 10 minutes at room

temperature. Reagent E was calculated based on the number of tubes x 0.250 mls + 2 mls. Based on this volume the amount of reagent E was created with 50% DI water and 50% Folin reagent. 250 µl of reagent E was added to each test tube and vortexed. Tubes were left to stand for 30 minutes at room temperature. They were read at 500 nm on a Thermo Scientific Biomate 3 spectrophotometer. Consistent detection of protein levels for each type of specimen provided confirmation that analyzed specimens contained proteins.